

Targeting ErbB receptors in a three-dimensional cell culture model of K-Ras mutant colorectal cancer

Von der Fakultät Energie-, Verfahrens- und Biotechnik
der Universität Stuttgart zur Erlangung der Würde eines
Doktors der Naturwissenschaften (Dr. rer. nat.)
genehmigte Abhandlung

Vorgelegt von
Yvonne Möller
aus Bad Hersfeld

Hauptberichter: Prof. Dr. Monilola Olayioye

Mitberichter: Prof. Dr. Nisar Malek

Tag der mündlichen Prüfung: 07. April 2017

Institut für Zellbiologie und Immunologie der Universität Stuttgart

2017

Table of contents

Table of contents	II
Abbreviations.....	IV
Summary.....	VI
Zusammenfassung	VIII
I. Introduction	1
1. Cancer.....	1
1.1. Hallmarks of cancer	1
2. Colorectal cancer	2
2.1. Development of CRC.....	2
2.2. Growth factor signaling	4
2.3. Differentiation and Polarization	8
2.4. Apoptosis	10
3. Cancer Therapy.....	12
3.1. Systemic intervention.....	13
3.2. Target specific compounds.....	14
3.3. Exploiting the apoptotic machinery for treatment	15
3.4. CRC treatment	16
4. oncogenic Ras in CRC.....	16
4.1. The role of oncogenic Ras in targeted therapy	16
4.2. The role of oncogenic Ras in apoptosis induction.....	18
4.3. The role of oncogenic Ras in polarization	18
4.4. Beyond oncogenic Ras.....	19
5. Model systems for CRC research.....	19
5.1. Three-dimensional culture systems	19
5.2. Three-dimensional culture models for CRC	21
5.3. Culture model for K-Ras mutated CRC	23
II. Material and Methods	24
1. Buffers, Solutions and Reagents.....	24
1.1. Protein extraction, SDS-PAGE and Western blotting	24
1.2. Viability Assay	24
1.3. Immunofluorescence.....	25
1.4. Kits	25
2. Cell culturing.....	25
2.1. Cell lines.....	25
2.2. Cell culture media and reagents.....	26
3. Antibodies and fluorescent dyes	26
3.1. Immunoblotting.....	26
3.2. Immunofluorescence staining	27

4. small interfering RNA (siRNAs)	28
5. Methods.....	28
5.1. Cell culturing.....	28
5.2. MTT, cytotoxicity, and caspase 3/7 activity assays	29
5.3. Immunofluorescence microscopy	30
5.4. TUNEL staining	30
5.5. Western blotting.....	30
5.6. FACS analysis	31
5.7. Quantitative PCR.....	31
5.8. Statistical analysis.....	32
III. Results	33
1. Oncogenic Ras and ErbB3 signaling.....	33
2. Oncogenic Ras and ErbB1-Targeted TRAIL	47
IV. Discussion	60
V. References.....	69
VI. Appendix	81

Abbreviations

aPKC	Atypical Protein Kinase C
AKT	Protein Kinase B (PKB)
AJ	Adherens Junction
Cet	Cetuximab
CRC	Colorectal Cancer
CTX	Choleratoxin
DcR	Decoy Receptor
DAPI	4',6-diamidin-2-phenylindol
Db-scTRAIL	Diabody single-chain TRAIL
DNA	Deoxyribonucleic Acid
Dox	Doxycycline
ECM	Extracellular Matrix
EGF	Epidermal Growth Factor
ErbB	Family of receptor tyrosine kinases
ERK	Extracellular-signal Regulated Kinases
FACS	Fluorescence Activated CellSorting
F-actin	Filamentous actin
FCS	Fetal Calf Serum
FDA	Food and Drug Administration (US)
GAP	GTPase Activating Protein
GEF	Guanine nucleotide Exchange Factor
GFP	Green Fluorescent Protein
HB-EGF	Heparin-Binding EGF-like Growth Factor
HRG	Heregulin (a.k.a neuregulin (NRG)),
IAP	Inhibitors of Apoptosis Protein
mAB	monoclonal Antibody
MAPK	Mitogen-Activated Protein Kinase
MTT	3-(4,5-dimethylthiazol-2yl)-2,5-diphenyl tetrazolium
n	Number of samples per experiment

N	Number of independent experiments
NF κ B	Nuclear Factor 'kappa-light-chain-enhancer' of activated B-cells
ns	Not significant
PI3K	Phosphatidylinositol 3-Kinase
Ras	Rat sarcoma
RNA	Ribonucleic Acid
RT	Room Temperature
RTK	Receptor Tyrosine Kinase
siRNA	Small Interfering RNA
SM	Smac Mimetic
tetON	Tetracycline (Tet)-inducible expression system
TGF- α	Transforming Growth Factor alpha
TKI	Tyrosine Kinase Inhibitor
TJ	Tight Junction
TRAIL	TNF-related apoptosis-inducing ligand
TRAILR	TRAIL Receptor
ut	Untreated
ZO-1	Zona Occuldens protein 1

Summary

K-Ras is a key signaling molecule regulating central biological processes like proliferation, polarization and survival, and is essential in the control of tissue homeostasis. Constitutive active K-Ras mutations are found in 40% of all colorectal cancers (CRC) contributing to tumor development, progression and therapy resistance. Despite constant efforts there are no targeted therapies available for K-Ras mutated CRC thus far.

To develop new, mechanism-based treatment strategies the contribution of oncogenic Ras to transformation and therapy resistance has to be understood in detail. For this purpose, the human epithelial colorectal adenocarcinoma cell line Caco-2 was used as a model in this thesis. Cultured Caco-2 cells represent an early stage of CRC. They express wild-type K-Ras and have no further mutations in downstream Ras signaling pathways. Seeded into a three-dimensional culture system, Caco-2 cells are able to polarize, partly recapitulating the morphological features of the normal colorectal epithelium. By introducing an oncogenic K-Ras variant (G12V) in this organotypic model system, using an inducible expression system, two new aspects of oncogenic Ras signaling could be described for the first time:

Firstly, the acute expression of K-Ras^{G12V} disrupted polarized morphogenesis of Caco-2 grown in 3D culture. I was able to identify a novel autocrine signaling loop that mediated the hyperproliferation and loss of cell polarity induced by K-Ras^{G12V} expression, which involved the receptor tyrosine kinase ErbB3 and transcriptional upregulation of its ligand heregulin (HRG).

Secondly, in Caco-2 3D cultures, K-Ras^{G12V} expression led to resistance against a targeted single-chain TRAIL molecule (Db-scTRAIL) comprising an ErbB1 blocking moiety derived from cetuximab and three TRAIL monomers. Here, I identified a resistance mechanism triggered by K-Ras^{G12V} involving the upregulation of the anti-apoptotic proteins cIAP1/2. The combination of Db-scTRAIL with a new Smac mimetic (SM83) was able to override this resistance not only in the Caco-2 model but also in additional Ras-mutated CRC cell lines.

Taken together these findings provide the basis for a new rational approach: combining ErbB3 blockade in Ras mutant CRC with an apoptosis inducing TRAIL molecule plus a

sensitizing Smac mimetic. This combination might efficiently block the autocrine Ras-HRG-ErbB3 loop and therefore suppress transformation whilst simultaneously inducing apoptosis.

Zusammenfassung

K-Ras ist ein Schlüsselmolekül in zentralen biologischen Prozessen wie Proliferation, Polarisation und Überleben und trägt essentiell zur Gewebekomöostase bei. Dauerhaft aktives Ras ist in 40 % der Kolorektalkarzinome nachweisbar und führt zu Tumorentstehung, Progression und Therapieresistenz. Trotz stetiger Forschung gibt es bis heute keine zielgerichtete Therapie für K-Ras mutierten Darmkrebs. Für die Entwicklung neuer Ansätze muss die Rolle von Ras in der Krebsentstehung und Therapieresistenz besser verstanden werden. Zu diesem Zweck wurde in der vorliegenden Arbeit die Zelllinie Caco-2, eine aus humanen Epithelzellen des Kolons gewonnene Adenokarzinomlinie, als Modell verwendet. Diese Zellen exprimieren natives K-Ras und weisen keine weiteren Mutationen in Ras assoziierten Signalwegen auf. Eine Besonderheit der Caco-2 Zellen ist ihr polares Wachstum in 3D Zellkulturen, wodurch sie den normalen Aufbau des Darmepithels nachbilden. Durch die induzierbare Expression einer K-Ras Variante (G12V) in diesem Zellsystem konnten in meiner Arbeit zwei neue Aspekte von onkogenem K-Ras beschrieben werden:

Erstens, störte die Expression von K-Ras^{G12V} das polare Wachstum der Caco-2 Zellen in der 3D-Kultur. Ich konnte einen hierfür verantwortlichen autokrinen Regelkreis identifizieren, welcher die Rezeptortyrosinkinase ErbB3 und die Hochregulierung des Liganden Heregulin (HRG) beinhaltet. Dieser Regelkreis ist für die durch K-Ras^{G12V} vermittelte, gesteigerte Proliferation sowie den Verlust der Zellpolarität verantwortlich.

Zweitens, induzierte die Expression von K-Ras^{G12V} in 3D-Kulturen Resistenz gegenüber einem zielgerichteten TRAIL-Molekül, das eine ErbB1-inhibierende Einheit, abgeleitet von cetuximab, und eine Kette von drei TRAIL Monomeren beinhaltet (Db-scTRAIL). Für die durch K-Ras^{G12V} ausgelöste Resistenz konnte ich die transkriptionelle Hochregulierung der anti-apoptischen Proteine cIAP1/2 als verantwortlich identifizieren, deren Inhibition durch ein neues Smac-Mimetikum die Resistenz gegenüber Db-scTRAIL überwinden konnte.

Zusammenfassend schlage ich aufgrund dieser Ergebnisse einen neuen rationalen Therapieansatz für Ras-mutierten Darmkrebs vor, der aus der Kombination von ErbB3-Inhibition mit einem Apoptose-induzierenden TRAIL-Molekül plus eines sensitivierenden

Smac-Mimetikum besteht. Diese Kombination könnte effizient die autokrine Ras-HRG-ErbB3 Signalkette unterbrechen und somit die Tumorentstehung inhibieren und gleichzeitig Zelltod induzieren.

I. INTRODUCTION

1. CANCER

Cancer is the leading cause of death in the developed countries. Every year 14 million new cases of cancer are diagnosed and 8.2 million cancer related deaths are counted worldwide [1]. The most common cancerous disease is lung cancer (30%), followed by breast (15%) or prostate cancer (10%) and colorectal cancer (8%).

1.1. Hallmarks of cancer

The term “cancer” describes a very heterogeneous and complex disease with specific causes and treatment options for each cancer entity. There are more than 100 types of cancer that often can be divided into specific subtypes, showing the complexity and difficulty to understand this disease and to develop evidence based treatment strategies for each cancer type.

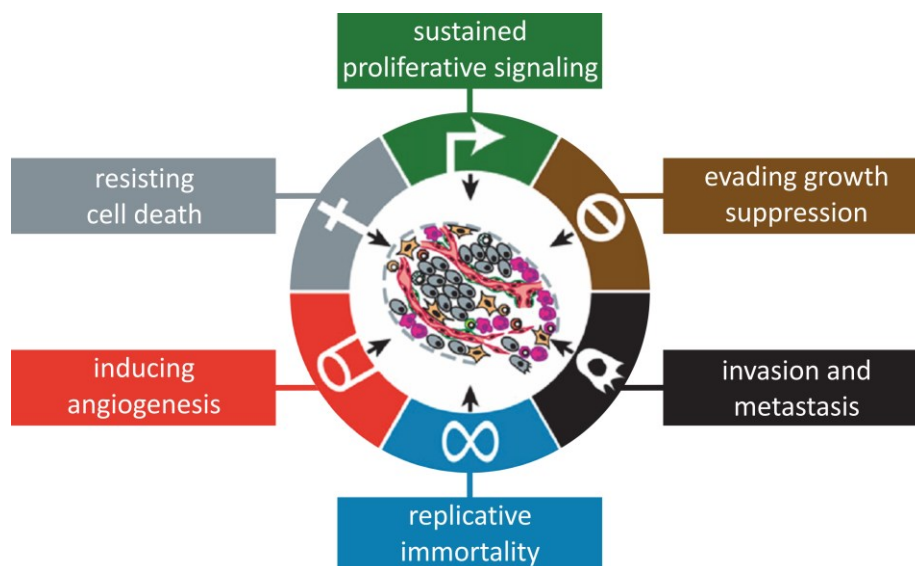


Figure I-1: Hallmarks of cancer. Illustration of the six hallmarks of cancer proposed by Hanahan and Weinberg in 2000. These hallmarks include deregulated cellular processes contributing to tumor development, progression and metastasis in almost all cancer types. [2]

But there are some common characteristics among all neoplastic diseases. Hanahan and Weinberg defined in the year 2000 the “hallmarks of cancer” [3].

They proposed that cancerous tissues are not only uncontrolled growing cell mass, but reflect a complex interplay between different types of cancer cells and non-transformed cells. These cells all contribute in different ways to sustained proliferative signaling, evasion of growth suppression, resistance to cell death, enabled replicative immortality, induction of angiogenesis, and activation of invasion. These mechanisms lead to uncontrolled growth, deterioration of adjacent tissue and organs, and finally spreading throughout the whole body and formation of distant metastasis (Fig. I-1). These characteristics are based on genetic mutations of the tumor cells and are supported by the surrounding tissue, the tumor stroma cells, together creating a favorable milieu known as the tumor micro-environment [2]. It has been realized that the tumor stroma not only plays an important role in cancer progression but also in the development of therapy resistance. Therefore, targeting the tumor stroma is now being considered as a new anti-cancer treatment strategy [4,5].

2. COLORECTAL CANCER

Colorectal cancer (CRC) is one of the most prevalent cancers worldwide. With approximately 1.36 million new cases diagnosed annually it is the second most common cancer type in the Western world and accounts for 694,000 related deaths per year recorded worldwide [6]. Beyond genetic mutations the dominant causative factors are still diet and lifestyle [7]. Especially in patients with advanced, metastatic CRC survival rates are low (11%) and recurrence rates high (up to 50%) [8,9]. Due to better screening programs and early removal of precancerous lesions (polyps) the incidence of CRC has declined in the last 10 years.

2.1. Development of CRC

Tumorigenesis in general can be described as a multistep process. In CRC a sequence of specific mutations leads to the transformation of the normal intestinal tissue into malignant neoplasms. In 1990 Fearon and Vogelstein specified the mutated genes in

essential pathways, responsible for the development of CRC [10]. This process is also known as the adenoma-carcinoma sequence (Fig. I-2).

Genomic instability is considered as the starting point of CRC development. The loss of DNA-repair functions by mutations in the mismatch repair genes (MMR) or alterations in the activation of MMR genes by changes in their methylation patterns can lead to microsatellite instability (MSI). Chromosomal instability (CIN) is the second origin of genomic instability and is caused by loss of cell cycle control genes like CDC4 [11]. Both – MSI or CIN – can result in the physical loss of tumor-suppressor genes during tumor progression, such as APC, TP53, and TGFBR2/SMAD [12].

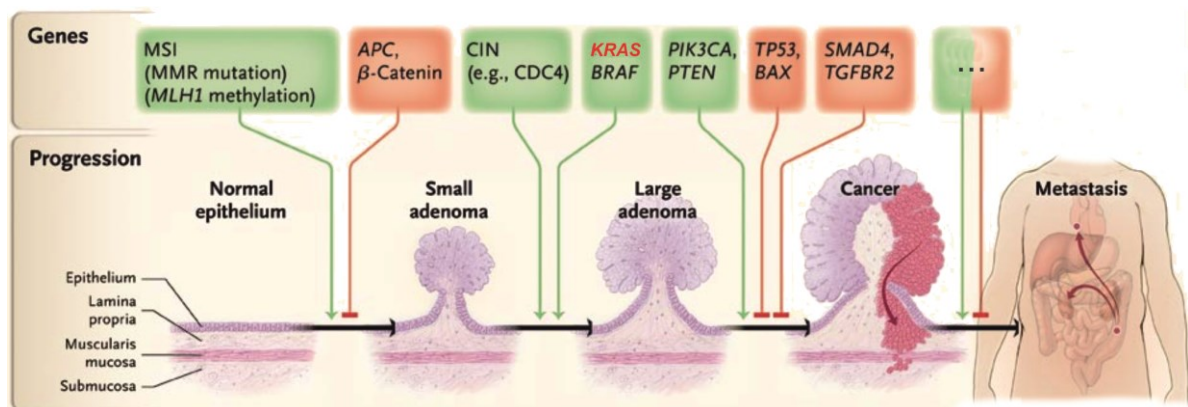


Figure I-2: Adenoma-carcinoma sequence. Genetic alterations in signaling pathways that are involved in the progression from the adenoma stage of CRC to advanced, metastatic CRC. Microsatellite instability (MSI) initiated by mismatch-repair (MMR) defects and chromosomal instability (CIN) lead to further loss-of-function (red) or gain-of-function (green) mutations within genes like APC, KRAS, PIK3CA, TP53, TGFBR2. See text for further details. [13]

The APC/Wnt/ β -catenin pathway for example regulates cell cycle progression and contributes to the differentiation and migration process of stem cells during tissue regeneration. Loss of APC is inevitable for tumor initiation and the development of benign polyps in the colon. p53, encoded by the TP53 gene, is a transcription factor that regulates the expression of several proteins important for cell cycle control. In cells with defect MMR p53 can induce apoptosis – the programmed cell death – by activation of the proapoptotic protein BAX in order to remove degenerated cells from the body. So p53 mutations lead to cell survival and tumor progression [13]. The mutational inhibition of growth factor signaling by TGF- β is induced by alterations in the TGF- β receptor 2

(TGFB2) or the downstream effector SMAD4, a third example for loss-of-function mutations in the subsequent progress of CRC [13]. TGF- β serves as a growth suppressor in the normal intestinal tissue and orchestrates processes like proliferation, differentiation, migration and apoptosis. In MSI positive CRC tumors mutations in the TGFB2 induce TGF- β resistance, resulting in hyperproliferation and the transition into an invasive and metastatic tumor state (mCRC) [14].

Beyond loss-of-function mutations, activation of oncogenic pathways plays a key role in the transition of adenomas to carcinomas. Activation of growth factor signaling pathways occur at several stages of the signaling cascade. Mutations within the mitogen-activated protein kinase (MAPK) signaling pathway by constitutive activation of the small GTPase Ras or the kinase Raf lead to growth factor independence and sustained cell proliferation. Activation of the phosphatidylinositol 3-kinase (PI3K) pathway can be observed by constitutive activation of the catalytic subunit of the PI3K (PIK3CA) or by inactivation of the phosphatase PTEN that negatively regulates PI3K (Fig. I-4) [12].

Taken together, the progression of CRC from benign polyps (adenomas) to invasive carcinomas is driven mainly by alterations in growth factor signaling, regulation of differentiation and induction of cell death.

2.2. Growth factor signaling

Inadequate activation of growth factor signaling pathways can be caused by constitutive activation or overexpression of oncogenes or depletion/inhibition of tumor-suppressors, resulting in uncontrolled and sustained cell growth and evasion of cell death [3].

Two important growth factor signaling pathways are the ERK/MAPK pathway and the AKT/PI3K pathway (Fig I-4) that are activated by mutations in most neoplasms [15]. Both are important for adequate proliferation. In addition the AKT/PI3K pathway negatively controls apoptosis and leads to enhanced survival.

ErbB receptor signaling

In non-transformed cells both growth factor signaling pathways are tightly controlled. Activation only occurs after binding of ligands (growth factors) to their specific receptor at

the cell surface. One important receptor family is the ErbB family of receptors, which comprises ErbB1/EGFR, ErbB2/HER2, ErbB3/HER3 and ErbB4/HER4. These receptor tyrosine kinases (RTK) possess an extracellular ligand-binding domain, a single membrane spanning region, and a cytoplasmic tyrosine kinase domain (Fig. I-3) [16,17]. Upon binding of the specific peptide ligand, the receptors homo- and heterodimerize. This leads to receptor activation and transphosphorylation of specific tyrosines within the cytoplasmic tail. These phosphotyrosines provide docking sites for intracellular signaling molecules that trigger the activation of the MAPK and PI3K pathways, which mediate biological responses such as proliferation, migration and survival (Fig. I-4) [17,18].

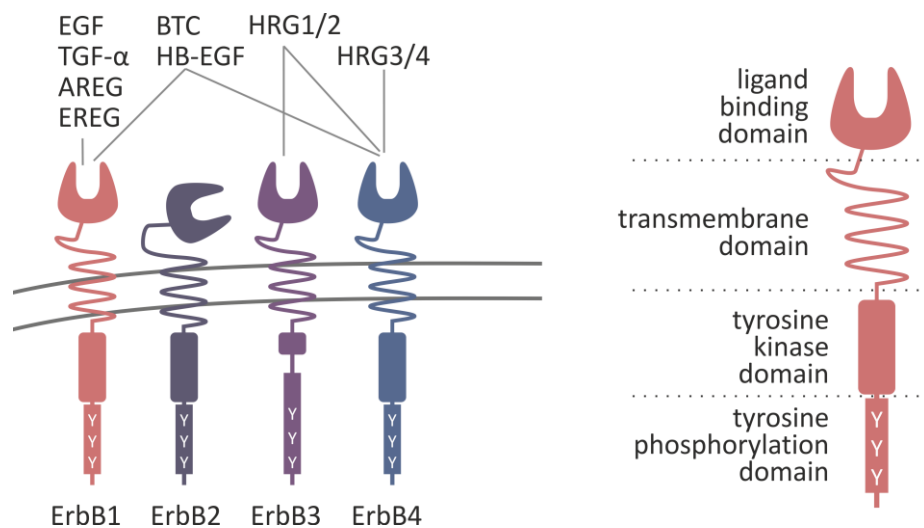


Figure I-3: ErbB receptor family. The ErbB receptor family comprises the four receptor tyrosine kinases ErbB1/EGFR, ErbB2/HER2, ErbB3/HER3 and ErbB4/HER4. Several peptide ligands can activate the receptors by binding to the extracellular domain of their corresponding receptors, resulting in homo- or heterodimerization and transphosphorylation of the intracellular tail and consequent downstream signaling. (Adapted from [17,19])

ErbB receptors are activated by a variety of different peptide ligands. ErbB1 is potently activated by the growth factors EGF and TGF- α . Although ErbB2 has no direct ligand, it readily dimerizes with the other ErbB receptors due to its constitutively active conformation [20]. ErbB3 is unique in that it has an impaired kinase domain, but in a heterodimer with a signaling competent ErbB family member ErbB3 becomes phosphorylated and can serve as a signaling platform [21,22]. The presence of several consensus sites for the p85 subunit of PI3K mediates the potent induction of AKT/PI3K signaling by phosphorylated ErbB3 [22,23]. The heregulins (HRGs; also known as

neuregulins (NRGs)), a family of peptide ligands comprising more than 20 different isoforms encoded by the genes NRG1-4, specifically bind ErbB3 and ErbB4 (Fig. I-3) [19,24]. Malignant activation of ErbB receptor signaling can be caused by mutations of the receptors or by changes in the expression level. Overexpression of ErbB1 is observable in head and neck cancer, esophageal cancer, and colorectal cancer. ERBB3 somatic mutations can be found in 11% of colon and gastric cancers [25]. The ligands are also found to be upregulated and contribute to hyperproliferation and treatment escape, either by autocrine mechanisms or paracrine signaling by the surrounding stroma cells [26,27]. In cancer different mechanisms can contribute to autocrine signals: firstly, cell polarity and therefore the separation between apical and basolateral membranes of epithelial cells can be compromised [28] and secondly, tumor-specific changes in gene expression can result in the complementation of cognate ligand-receptor pairs in the transformed tissue [29,30].

Downstream effector proteins of ErbB receptor signaling

RTK signaling converges at the level of the protein Ras, a master regulator of several crucial signaling pathways in the cell. Amongst these pathways are the MAPK and PI3K pathways, regulating not only proliferation and apoptosis but also tissue organization [31,32]. This makes Ras a major proto-oncogene. Ras proteins belong to the family of small GTPases and comprise three members, H-Ras, K-Ras and N-Ras. Ras proteins cycle between an active GTP-bound and an inactive GDP-bound state. The transition between these stages is regulated by guanine nucleotide exchange factors (GEFs) that facilitate the activation of Ras and GTPase activating proteins (GAPs) that enhance the intrinsic GTPase function of Ras and thus inactivate the protein. Activated RTKs serve as docking sites for the adaptor protein GRB2, that recruits the GEF SOS to the plasma membrane where it activates the membrane bound Ras protein by exchange of GDP to GTP. Activated Ras then binds to the serine/threonine kinase Raf. This relocation of Raf to the plasma membrane activates the kinase, which then phosphorylates and activates MEK, which in turn phosphorylates and activates ERK. ERK then phosphorylates and activates transcription factors that promote cell cycle progression and proliferation (Fig. I-4) [33]. Additionally active Ras can directly interact with the catalytic subunit of PI3K leading to

the activation of the serine/threonine kinase AKT, which has a strong anti-apoptotic function and is crucial for cell survival (Fig. I-4).

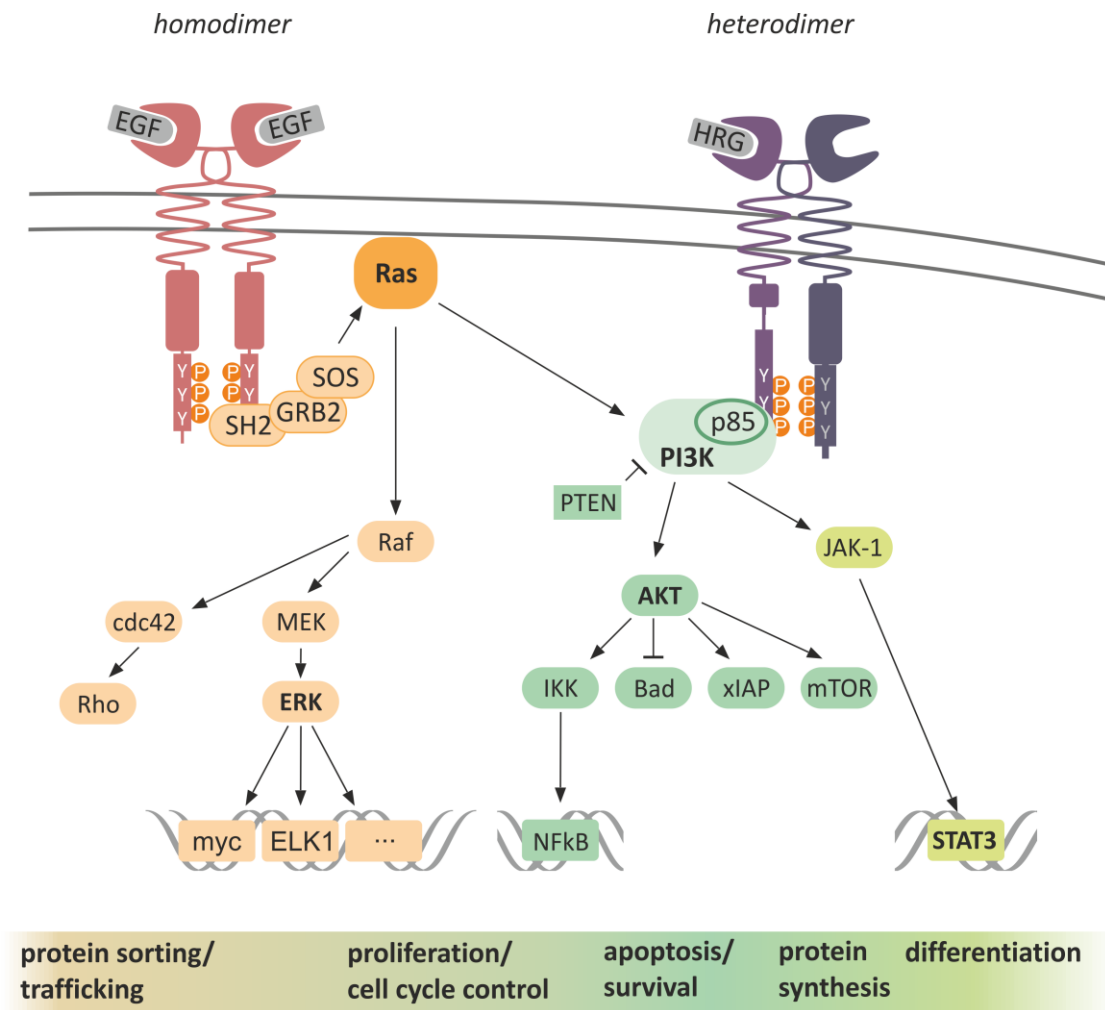


Figure I-4: ErbB receptor signaling and corresponding downstream signaling pathways. Homo- or heterodimerization upon ligand binding leads to receptor activation, followed by transphosphorylation (P) of tyrosines (Y) in the intracellular domain. These p-tyrosines serve as docking site for adaptor proteins like GRB2 or for the p85 regulatory subunit of PI3K. Subsequent activation of downstream signaling molecules activates the MAPK (sand) or PI3K (green) pathways. See text for further details. (Adapted from [18,33])

Mutated Ras is one of the main drivers of growth factor independent signaling and is constitutively active due to specific point mutations. The most frequent mutations in CRC occur at codon 12 or 13 (predominantly G12D and G12V or G13D conversion) [34]. Nearly 40% of all CRC cases harbor activating mutations in the KRAS gene [8,35,36]. Another common oncogene in the same pathway is B-Raf, mutated in 12% of all CRC patients.

Mutations in K-Ras and B-Raf are mutually exclusive, whereas mutations in K-Ras and PI3K can be detected in the same CRC cell [37].

2.3. Differentiation and Polarization

Polarization is a prerequisite for tissue homeostasis and normal function. Through the restriction of protein distribution within the cell, different compartments and cell poles are defined. This is achieved by a diffusion barrier built by tight junctions (TJ) comprising proteins like ZO-1 and Occludins. Furthermore, intercellular adhesion via adherens junctions (AJ) is important to maintain tissue organization and cell-cell communication. AJ comprise for instance the protein E-cadherin. The establishment of these junctions and the polarized phenotype is regulated by three polarity complexes called Crumbs, Par and the Scribble complex. All of them are regulated by a well-orchestrated interplay of different pathways [38]. The main regulators of the underlying cellular processes are small GTPases of the Ras and Rho families, the latter controlling cytoskeleton rearrangement and therefore cell shape and movement [32] as well as membrane trafficking [39].

In the normal intestinal epithelium the apical-basal polarity of the epithelial cells has an important barrier function. It distinguishes the inside, facing the basal membrane (basal side), and the outside (apical side), representing the outer surface of this exocrine tissues (Fig. I-5). The controlled excretion of digestive proteases into the gut lumen and the absorption of nutrients at the brush border into the cells and the transport towards adjacent tissues and the blood vessels is one example for the functional difference of the apical and basal side of the intestinal tissue (Fig. I-5). Spatially restricted protein and receptor distribution by site directed trafficking and excretion of ligands and the maintenance of this asymmetry are also important for proper signal transduction. In epithelia that express both, the ligands and receptors, the tight junctions separate the different subcellular membranes, the receptors and cognate ligands are directed to, thereby preventing unwanted autocrine stimulation [40].

Loss of polarity is a hallmark and precondition of cancer [38]. 80% of all malignancies arise from epithelial tissues like the intestine. Several alterations are known to interfere with proper polarization and tissue architecture. Activation of ErbB2 together with oncogenic

expression of mutated Ras is known to induce tissue disorganization and loss of polarity in cancer cell lines [41,42]. Mutated Ras in combination with loss of polarity proteins like Scribble also shows the necessity of cooperation between two oncogenic events like loss of tumor-suppressors and constitutive activation of Ras to induce tissue depolarization in CRC models [43,44].

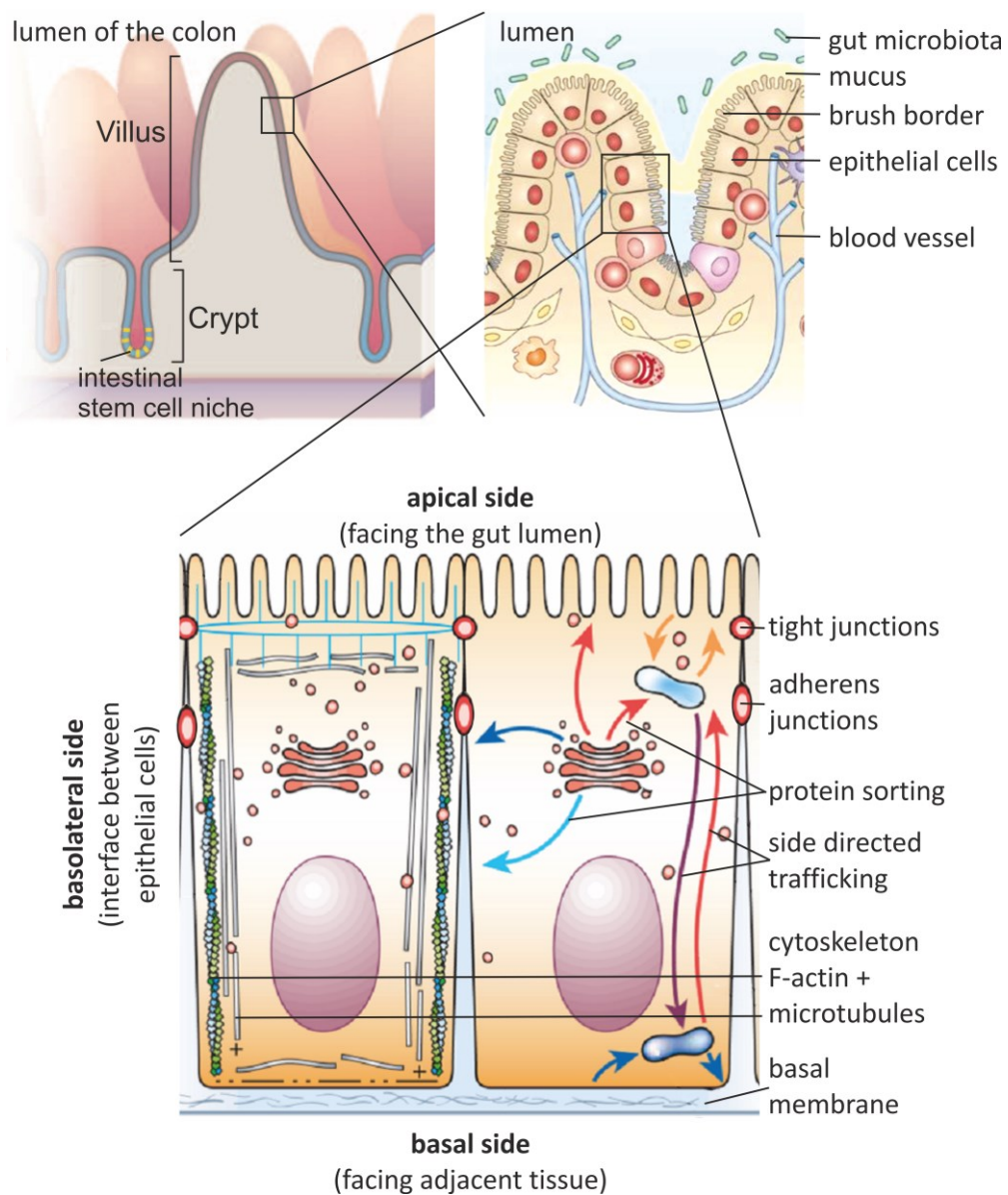


Figure I-5: The intestinal epithelium. The barrier between the lumen of the colon and the adjacent tissue is built by a layer of epithelial cells. At the macro level this tissue is organized in finger-like projections that extend into the lumen, the villi, and the crypts with different types of cells like goblet cells, which produce mucus, or stem cells responsible for renewal of the tissue. The intercellular barrier between the epithelial cells is maintained by tight junctions (TJ). Side-directed trafficking generates further functional differences between the apical and basal side of the cells. See text for further details. (Adapted from [32,45,46])

2.4. Apoptosis

Programmed cell death, also known as apoptosis, ensures tissue homeostasis by depletion of damaged or unnecessary cells and protects the organism against malignant transformation by eliminating the affected cells, if repair is not possible. Dysregulation of apoptosis often leads to cancer development or therapy resistance. Once activated, the apoptotic program leads to morphological changes like chromatin condensation, nuclear fragmentation and formation of so-called apoptotic bodies that can be engulfed by phagocytic cells [47]. There are two major pathways controlling the apoptotic machinery: the extrinsic and the intrinsic (Fig. I-7), both converge in the activation of caspases (cysteine aspartyl-specific proteases) that cleave key cellular proteins, degrade the cellular structure and irrevocably induce cell death [47].

The extrinsic pathway can be triggered by binding of death ligands to their receptor, activating the downstream apoptotic signaling cascade. One of these ligands is TRAIL (TNF-related apoptosis-inducing ligand), a member of the TNF superfamily (tumor necrosis factor). It forms active homotrimers that crosslink TRAIL receptors on the cell surface (Fig. I-6) [48]. Oligomerization of the TRAIL receptors initiates the recruitment of adaptor proteins like FADD (Fas-associated death domain protein) and the formation of the death-inducing signaling complex-II. This ultimately leads to the activation of initiator caspase 8 and 10 and consecutive activation of effector caspase 3, 6 and 7, resulting in apoptotic cell death (Fig. I-7) [49]. There are four known TRAIL receptors, the death receptors TRAILR1 (DR4) and TRAILR2 (DR5) and two decoy receptors TRAILR3 (DcR1) and TRAILR4 (DcR3) that are not signaling competent and are considered as antagonistic receptors [50].

The intrinsic apoptotic pathway can be triggered by DNA damage or growth factor deprivation. These internal stimuli activate the pro-apoptotic proteins BAX and BAK that form pores in the outer mitochondrial wall and release cytochrome-c from the intermembrane space of mitochondria [47]. Cytochrome-c release activates APAF-1, which forms together with caspase 9 the so-called apoptosome. Within this structure caspase 9 autoactivates and further activates the effector caspase 3 and 7 by proteolytic cleavage.

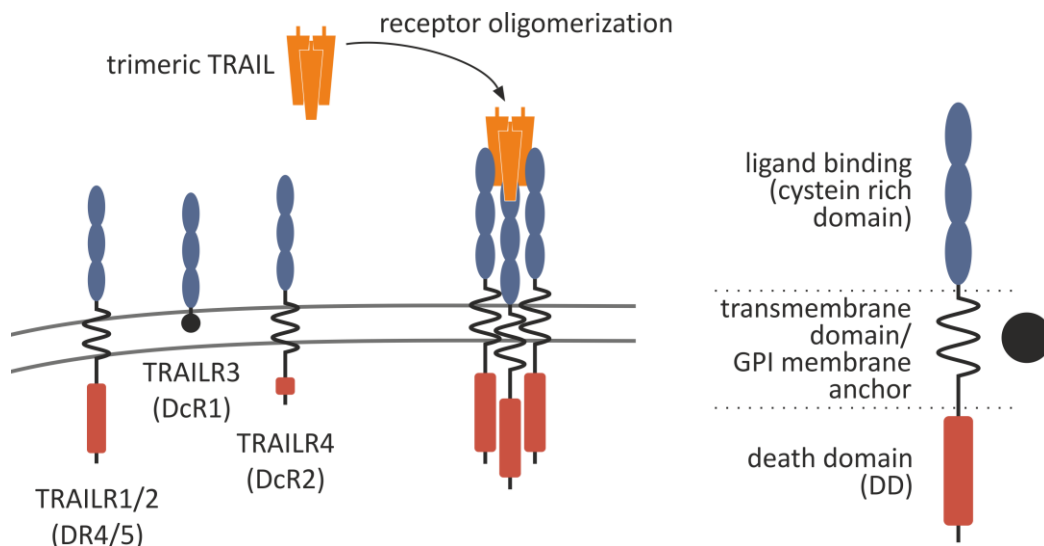


Figure I-6: TRAIL and its receptors. TRAIL is a homotrimeric ligand binding to the death receptors (DR) leading to receptor trimerization an essential step in receptor activation. The TRAIL receptors TRAILR1 (DR4) and TRAILR2 (DR5) contain an intracellular death domain (DD), which is essential for apoptosis signaling. The decoy receptors TRAILR3 (DcR1) and TRAILR4 (DcR3) compete with DR4 and DR5 for binding to TRAIL and therefore counteract apoptosis induction. (Adapted from [51])

Both pathways are tightly regulated by the balance of pro- and anti-apoptotic proteins. Misregulation of this balance is a common escape mechanism of cancer cells to avoid clearance [47]. Inactivating mutations in the TRAIL receptors were described for lung cancer and gastric cancers [52]. Overexpression of the anti-apoptotic Bcl-2 protein, which inhibits the activation of BAX/BAK, is correlated with poor survival and therapy resistance in several cancers [53].

Amplification of the inhibitors of apoptosis proteins (IAP) is also a common motif in cell death evasion by cancer cells. cIAP1 and cIAP2 are amplified in many carcinomas and considered as proto-oncogenes. They inhibit caspase activation by direct binding and thus block apoptosis [54]. Depletion of these IAPs can also result in anti-apoptotic signaling via activation of the NF κ B pathway, which initiates the expression of several anti-apoptotic proteins like Bcl-2 or XIAP, showing the importance of a balanced level of these apoptosis modulating proteins [47].

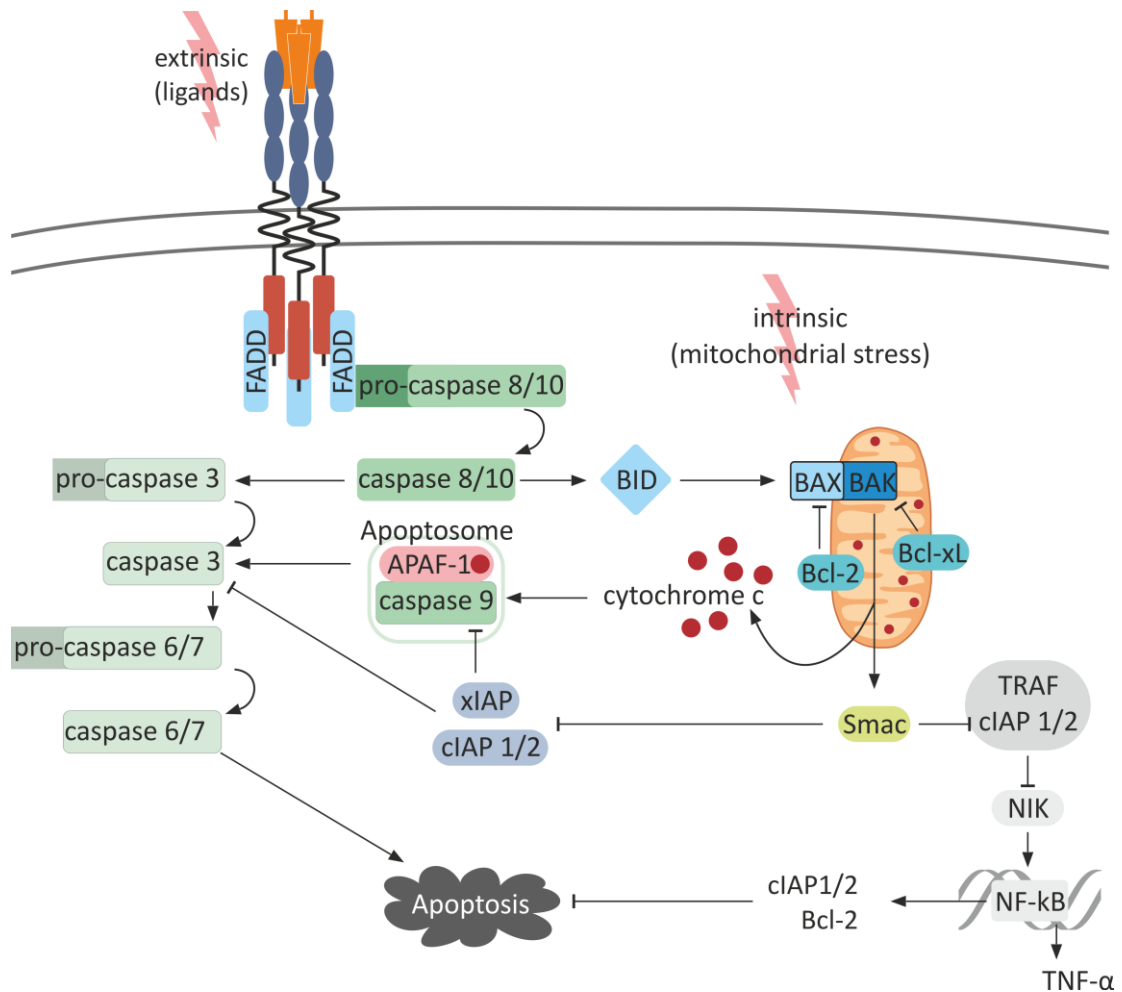


Figure I-7: Apoptotic signaling. There are two apoptosis inducing pathways, the extrinsic, activated by death inducing ligands like TRAIL, and the intrinsic, triggered by intracellular stress signals. Both pathways converge in the activation of caspases and the induction of cell death. See text for further details. (Adapted from [47,48])

3. CANCER THERAPY

Treatment of cancerous diseases is as diverse and complex as the different cancer types and subtypes are. With growing knowledge of the underlying mechanisms of cancer development and progression new treatment options emerge. In 2011 Hanahan and Weinberg adapted their model of the “hallmarks of cancer” according to the development in cancer research (Fig. I-8) [2]. Besides new origins of cancer they also summarized how these processes can be exploited for treatment, for example by specific inhibition of growth factor signaling pathways or the activation of apoptosis in cancer cells or the activation of an anti-cancer immune response.

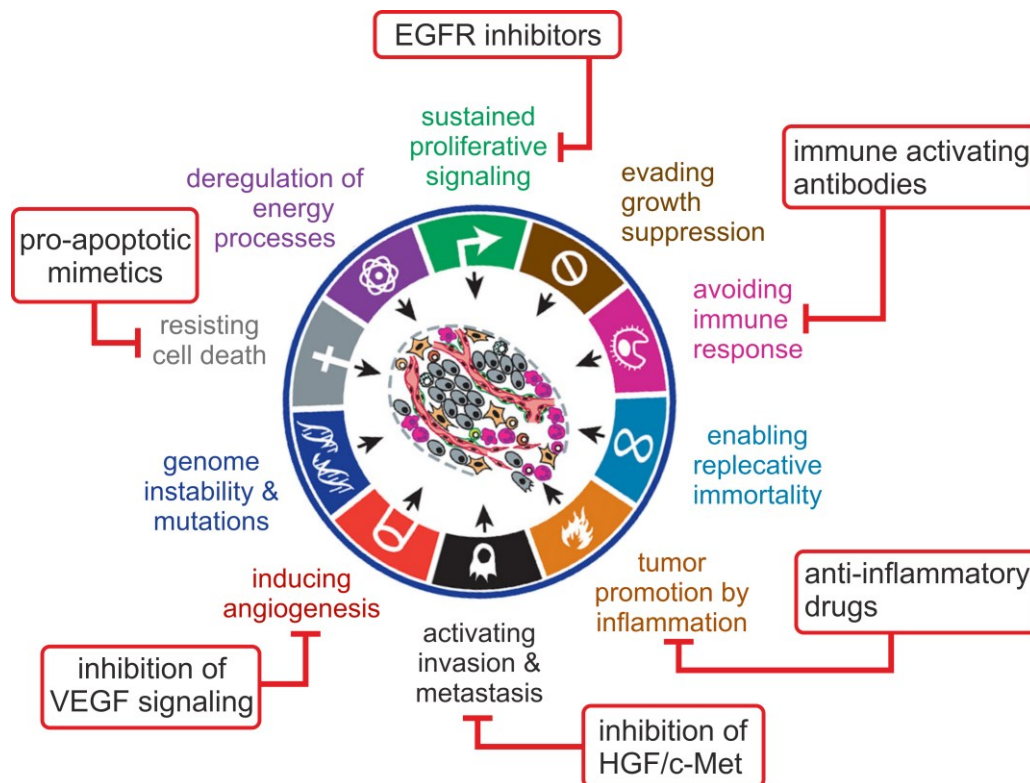


Figure I-8: Targeting the hallmarks of cancer. Drugs that interfere with each of the traditionally defined and new emerging hallmarks have been developed and are under clinical investigation or already have been approved for clinical use in treating certain forms of human cancer. The treatment options listed depict selected examples of target mechanisms and the related anti-cancer agents. [2]

3.1. Systemic intervention

Because of the high proliferative capacity of most of the malignant neoplasms anti-proliferative strategies are common treatment options. These involve chemotherapeutics that inhibit proliferation and kill hyperproliferative tissues. Another option is radiation, leading to DNA strand breaks that cannot be repaired by the tumor cells, as these have often lost their DNA repair capability - another hallmark of cancer [2,55].

But the first option with the greatest chance for cure in cancer treatment is still the surgical removal of the tumor mass. Systemic therapies, like chemotherapy or radiation, are often used as neoadjuvant or concomitant therapies to reduce tumor mass beforehand or kill remaining and circulating tumor cells after surgery.

3.2. Target specific compounds

An important concept in modern tumor therapy is based on oncogene addiction. This means that tumor growth is dependent on one single mutated gene or a specific pathway. Blocking of this pathway or gene can lead to rapid response and tumor cell death. This knowledge led to a paradigm shift in treating cancer within the last two decades - from relative non-specific cytotoxic agents towards selective, mechanism-based targeted therapies [56]. There are specific inhibitors that attack each of the hallmarks of cancer proposed by Hanahan in 2011, including those that block receptor activation, restore cell cycle control, inhibit proliferation and invasion or induce apoptosis (Fig. I-8) [2]. Furthermore unleashing the immune system from inhibitory factors produced by the tumor or tumor stroma cells to support the innate anti-tumor response has evolved as a promising new approach, especially when combined with targeted therapies [57].

Targeting the activation of proliferative pathways can be achieved by small molecules that interfere with RTK signaling by blocking the intrinsic tyrosine kinase activity [58]. A major problem in the treatment with these tyrosine kinase inhibitors (TKI) is the development of resistance during treatment either by evading the inhibitory effect by using another pathway or by acquired resistance against the TKIs due to secondary mutations in the tyrosine kinase domain [59].

Antibody-based therapy

Higher specificity is achieved by targeting the RTKs on cancer cells with antibodies that are highly specific for their target antigen. The variable domains of the antibody can be designed to bind the extracellular ligand binding domain of a receptor (Fig. I-9, left). Such antibodies interfere with ligand induced receptor activation by allosteric or competitive inhibition. They can further trigger cytotoxic cellular responses upon recognition of the targeted cell by the immune system. But they can also serve as a delivery platform for cytotoxic agents that are coupled to the targeting moiety whereby the therapeutic accumulates at the tumor site [60].

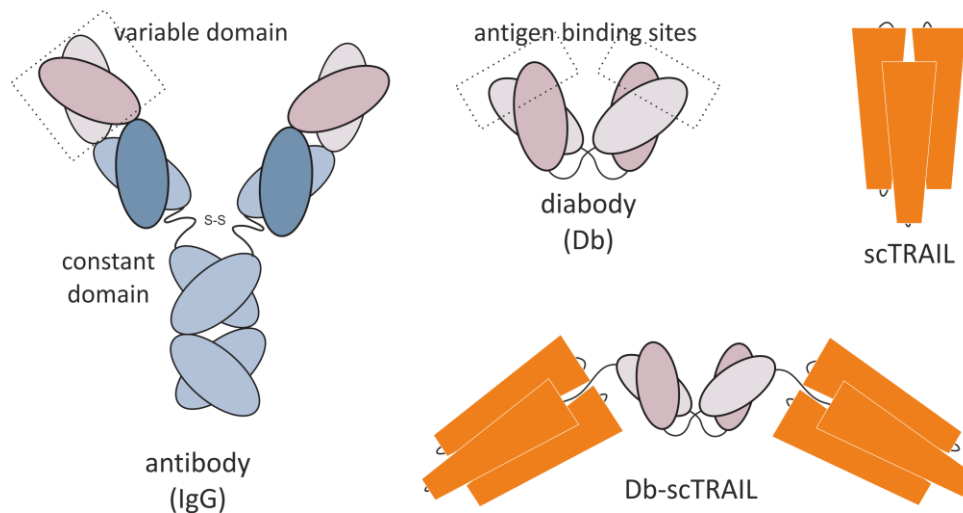


Figure I-9: Targeting agents for cancer therapy. Antibodies like Immunoglobulin G (IgG) comprise a constant region and a variable domain, that itself contains hypervariable sequences, specific for its antigen. Diabody (Db) formats only contain the variable domains connected via short linker domains (black lines). ScTrail is a single polypeptide chain comprising three TRAIL monomers. Combining the diabody format with scTRAIL by genetic engineering lead to the targeted Db-scTRAIL molecule used in this thesis.

One of the best studied antibody targets is the ErbB receptor family. Antibodies against the extracellular domain of ErbB1 are for instance cetuximab or panitumumab. Cetuximab is a chimeric human-murine immunoglobulin (IgG1); this means that the constant domain of a human IgG is fused to the variable domains of a murine antibody targeting the extracellular domain of human ErbB1. Thereby the immune response against the murine part is alleviated, reducing cellular cytotoxicity [61]. Cetuximab competes with ErbB1 ligands such as EGF or TGF- α for receptor binding, thereby repressing receptor phosphorylation and the activation of downstream signaling [8].

3.3. Exploiting the apoptotic machinery for treatment

Inducing apoptosis is an elegant way to kill tumor cells by exploiting the cell death machinery. TRAIL is a death ligand that induces apoptosis via the extrinsic pathway preferentially in tumor cells via the death receptors TRAILR1 and TRAILR2 [62]. Clinical trials using recombinant TRAIL confirmed the low toxicity to normal tissue, but therapeutic effects were insufficient compared to the results obtained in mouse models [48,63]. Additionally to the limited effects observed in clinical trials, several resistance mechanisms against TRAIL induced apoptosis have been described in tumor cell lines. Activation of pro-

survival pathways via AKT and myc signaling or the expression of anti-apoptotic proteins like XIAP, cFlipL or Bcl-2 have been shown to block the induction of apoptosis [62,64].

To improve the antitumor activity of the recombinant TRAIL molecules a trimeric TRAIL was engineered at the institute [65]. It is well known that correct trimerization and zinc coordination of recombinant TRAIL is crucial for its biological activity [63]. Accordingly, the design of a single polypeptide chain comprising three TRAIL monomers (scTRAIL) enhanced the bioactivity of the recombinant molecule significantly [65]. Such molecules can further be fused to antibodies directed against tumor markers. It was previously shown that the fusion of scTRAIL to a single-chain antibody fragment (scFv) functionally mimicked natural membrane-bound TRAIL and that it was more effective than scTRAIL alone [65]. The introduction of a diabody configuration, based on the humanized variable regions of cetuximab (Db-scTRAIL) (Fig. I-9, right), resulted in an even higher bioactivity of recombinant TRAIL, both in vitro and in vivo [66].

Apart from its tumor targeting effect, the ErbB1-directed antibody moiety contained within the Db-scTRAIL molecule might actively interfere with ErbB1 signaling.

3.4. CRC treatment

The current treatment of CRC is based on the stage of the diagnosed tumor. Early stage tumors can be removed by surgery alone and survival rates are high (75-95%). Once the tumor has spread and entered a metastatic stage, survival rates dramatically drop below 10%. Here, systemic therapies are used like chemotherapy with fluorouracil, capecitabine or oxaliplatin. In addition to chemotherapy, targeted therapies have entered the clinic. Currently, the ErbB1 blocking antibodies cetuximab and panitumumab are approved for the treatment of metastatic CRC with wild-type K-Ras status in combination with chemotherapy or as a maintenance therapy in chemo-refractory tumors [67–70].

4. ONCOGENIC RAS IN CRC

4.1. The role of oncogenic Ras in targeted therapy

The proto-oncogene Ras plays a central role in uncoupling the activation of the MAPK and PI3K pathway from extracellular signaling cues such as growth factor binding to RTKs,

thereby conferring growth factor independence to mutant cells (Fig. I-4). Therefore, tumors with mutated K-Ras fail to respond to cetuximab and panitumumab. Thus, the use of anti-ErbB1 mAbs in CRC therapy is restricted to patients with no detectable K-Ras mutation [70,71]. Interestingly, compared to other K-Ras mutations DeBrook and colleagues could show a clear overall survival benefit of patients carrying a G13D mutation when treated with cetuximab [72].

Despite constant efforts in pharmaceutical and academic research, direct targeting and inhibition of Ras is still a problem [73,74]. There are no targeted therapies currently available for patients with K-Ras mutant CRC [75,76]. In recent years, several small molecules that target Ras have been designed, which are now under clinical evaluation. There are four main strategies: Firstly, inhibition of the initial activation of Ras by GEF inhibitors. Unfortunately, these inhibitors most predominantly affect wild-type Ras. Secondly, an oncogene specific strategy to inhibit Ras activation is to covalently link a modified GDP to the thiol group of the newly introduced cysteine of K-Ras^{G12C}. Thus, the inactive GDP-bound form cannot be transposed into the active GTP-bound form. In cell culture models such covalent inhibitors showed high specificity for oncogenic Ras but also varying efficiency between different cell lines. Thirdly, the interaction of Ras and its effector proteins can be blocked by small molecules that bind to the surface of Ras. Inhibitors for Ras-PI3K or Ras-Raf interaction are currently under development [74]. Finally, the most promising approach is the inhibition of the farnesylation of Ras, which is crucial for the recruitment of Ras to the plasma membrane and thus for downstream signaling [73]. Up to now the clinical evaluation of these farnesyltransferase inhibitors could not recapitulate the effects observed in pre-clinical experiments. An important factor are resistance mechanisms by alternative membrane recruitment options of the cells, e.g. by palmitoylation [74].

Instead of directly targeting Ras, inhibition of the downstream effectors has been investigated as well. The MAPK pathway is active in 50% of all CRC [33], due to aberrant activation of Ras or Raf. Several MEK inhibitors are in clinical trials and are effective in Ras/Raf-mutated tumors. B-Raf inhibition showed promising results especially in melanoma, for the treatment of which two MEK inhibitors were approved by the FDA

[77,78]. Despite the promising results in pre-clinical studies MEK inhibitors were not successful in K-Ras mutated CRC patients. Acquired resistance during MEK inhibitor treatment seems to be inevitable and involves the upregulation of the oncogene Ras itself and hyperactivation of ErbB3/PI3K/AKT signaling [76,79]. Additionally, the coexistence of PI3K mutations counteracts MEK inhibition. To combat these resistance mechanisms dual targeting of the MAPK and PI3K pathways entered clinical trials, including combinations of MEK/PI3K, MEK/mTOR or MEK/AKT inhibition (summarized in [76]). The results of these studies hopefully will result in new treatment options for K-Ras mutated CRC patients.

4.2. The role of oncogenic Ras in apoptosis induction

Beyond the clear contribution of Ras to oncogenesis and its capacity to potently activate proliferation, K-Ras mutations play a paradoxical role in apoptosis. Activation of the PI3K pathway by mutated Ras leads to phosphorylated AKT that inhibits the pro-apoptotic protein Bad. Furthermore, Ras can activate the transcription factor NFκB that promotes transcriptional upregulation of the anti-apoptotic proteins XIAP, cIAP2 and Bcl-2 [47,80]. Activation of the MAPK pathway was reported to play an anti- or pro-apoptotic role, depending on the cellular context [81,82]. Accordingly, the contribution of oncogenic Ras signaling to the sensitivity of tumor cells toward apoptosis-inducing ligands such as TRAIL is unclear. Drosopoulos et al. reported that the CRC cell line Caco-2, stably transfected with K-Ras^{G12V}, was sensitized to TRAIL induced apoptosis via a MEK dependent mechanism [83]. Similar results were obtained in lung cancer cell lines in vitro and in tumor xenografts in mice [84]. Additionally to its direct influence on PI3K and MAPK pathway, oncogenic Ras also leads to increased levels of growth factors, either by the elevated transcription of ErbB1 ligands [30,85] or release of membrane bound ligands by shedding in CRC cell lines [86]. This autocrine activation loop is associated with hyperproliferation and resistance to ErbB receptor targeting therapies as well as TRAIL mediated apoptosis [87].

4.3. The role of oncogenic Ras in polarization

Besides its role in hyperproliferation, evasion of growth suppression and resistance to apoptosis, mutant K-Ras plays an important role in another cancer hallmark: loss of

polarization. In a 3D cell culture model of colonic cyst formation, Magudia et al. described a role for K-Ras^{G12V} in basolateral polarity aberrations independent of its hyperproliferative effect. K-Ras^{G12V} expression in Caco-2 cells lead to unpolarized cysts with no lumen and the lack of tight junctions at the apical surface [88]. This defect in polarization could be observed already at the two cell stage, suggesting that uncontrolled Ras signaling can contribute to early stages of cancer development, showing the importance of oncogenic Ras in tumor initiation.

4.4. Beyond oncogenic Ras

Besides oncogenic Ras, several other genes within the RTK signaling pathways are found to be mutated, contributing to therapy resistance and tumor development. The overexpression of ErbB2/ErbB3 correlates with resistance to targeted therapies as well [89,90]. ErbB3, the unappreciated ErbB receptor, gained more and more attention regarding tumor development and therapy resistance in the last years [91–93]. Additionally, the receptor c-Met, a RTK that can also form dimers with the ErbB receptor family members, was reported to interfere with ErbB receptor blockade in CRC adding to the complex interplay of the different pathways [94,95]. Elevated levels of growth factors, derived from tumor cells or the microenvironment, such as NRG, contribute to tumor progression and resistance as well [96,97].

5. MODEL SYSTEMS FOR CRC RESEARCH

5.1. Three-dimensional culture systems

Studies in cell culture have been instrumental in delineating tumor-associated signaling pathways and genetic alterations on cellular behavior. Some cells, like the intestinal cell line Caco-2, show a certain level of polarization in 2D culture when grown in long-term cultures. The 2D cultures, however, lack the complex signaling processes initiated by interactions of the cells with the extracellular matrix (ECM). Cultivation of epithelial cells in a three-dimensional (3D) environment containing ECM components recapitulates better the conditions found in vivo [98,99]. There are several culture techniques ranging from scaffold-free hanging drop systems to matrix dependent cell cultures and even more

complex co-culturing systems, including ex vivo techniques like tissue organoids or slice cultures (Fig. I-10) (reviewed in [100,101]).

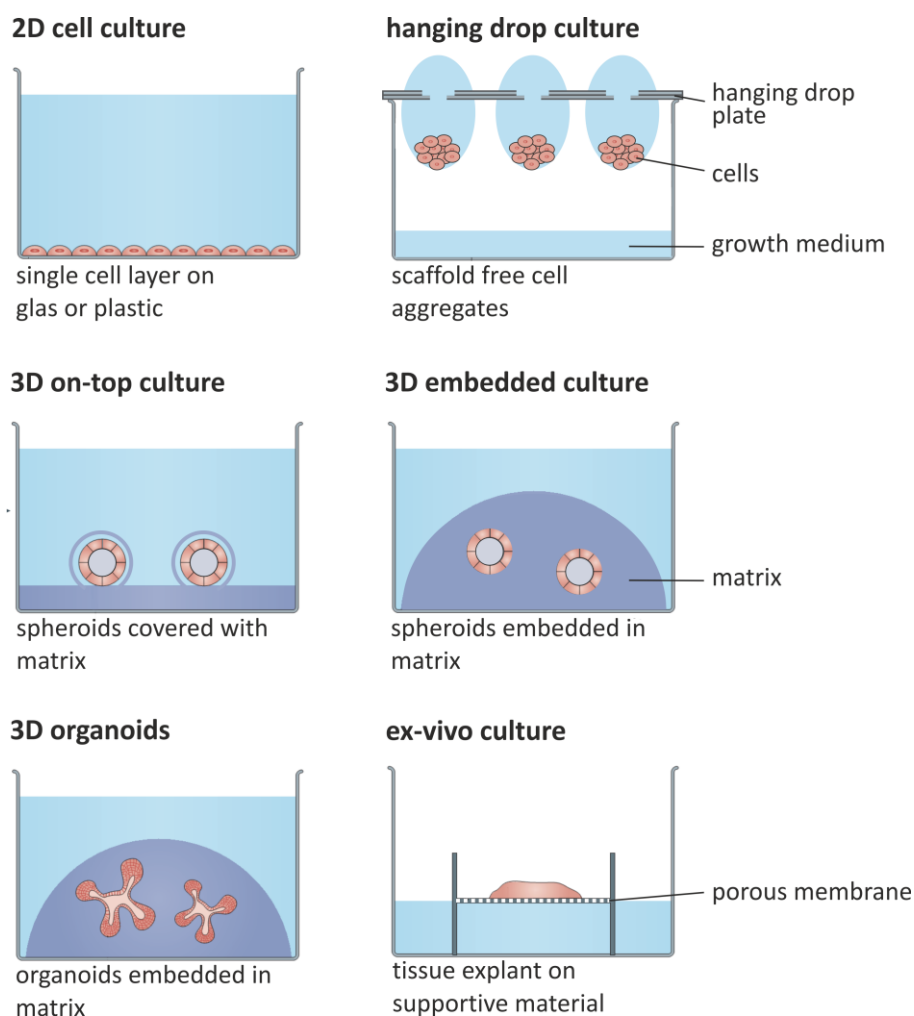


Figure I-10: Cell culture models used in cancer research. Current cell culturing methods range from unstratified 2D cultures over scaffold dependent 3D cultures, where cells form fully polarized spheroids, to highly complex ex vivo organoid cultures or explant cultures of whole tissue slices. (for further details see reviews [100,101])

In advanced 3D culture systems the establishment and maintenance of polarized morphology and the cell-matrix interaction can recapitulate the different steps of tumor initiation, progression and treatment response more precisely. Indeed several publications show the pivotal impact of the growth conditions on central cancer related pathways including cell cycle control [102], proliferation [98,99], apoptosis [103,104] or drug response [105]. That is why three-dimensional culture systems are also used for cancer

drug discovery [106] and should be considered as an important tool for translational cancer research and as an alternative for animal experiments.

5.2. Three-dimensional culture models for CRC

A common cellular model system for CRC is the Caco-2 cell line grown in a 3D matrix culture [101]. Caco-2 cells harbor mutations in APC, p53, and SMAD4, but are wild-type for the MAPK and PI3K pathways [88]. They furthermore express low levels of the receptors ErbB1, ErbB2 and ErbB3. Thus, Caco-2 cells are an ideal model for studying the effects of mutated K-Ras on transformation and treatment with ErbB receptor targeting agents in this setting. The 3D culture of Caco-2 cells mimics the *in vivo* situation of the intestinal epithelium more closely than 2D culture techniques and is comparably easy to handle [107]. Caco-2 cells grown under 3D conditions form fully differentiated polarized cysts with a basolateral side, contacting the surrounding ECM, and an apical side facing a fluid-filled lumen (Fig. I-11). To culture Caco-2 cells in a 3D environment Lee et al. established a method called “on-top-culture” (Fig. I-10).

Here, Caco-2 cells are seeded on top of a thin layer of matrix proteins, mimicking the basal membrane (e.g. composed of laminin, collagen IV, nidogen/enactin and proteoglycan) [98]. After 12 days of growth a distinct apical side forms, marked by F-actin accumulation, and a central fluid-filled lumen starts to develop. In contrast to the acini formation in the breast cancer cell line MCF10A lumen formation does not involve apoptosis, but rather requires cAMP signaling and activation of apical chloride channels accompanied by fluid efflux [107]. The maturation of the cysts can be facilitated by addition of cholera toxin (CTX) leading to faster water efflux into the lumen and thus shortened cell culture time.

These early 3D cultures of Caco-2 cells already show apical formation of tight junctions (e.g. marked by ZO-1), important for lumen formation and spheroid maintenance. The basolateral side can be distinguished by the adherens junction protein E-cadherin. The polarity complex PAR, comprising the protein aPKC (atypical protein kinase C) further accumulates at the apical pole of polarized cells.

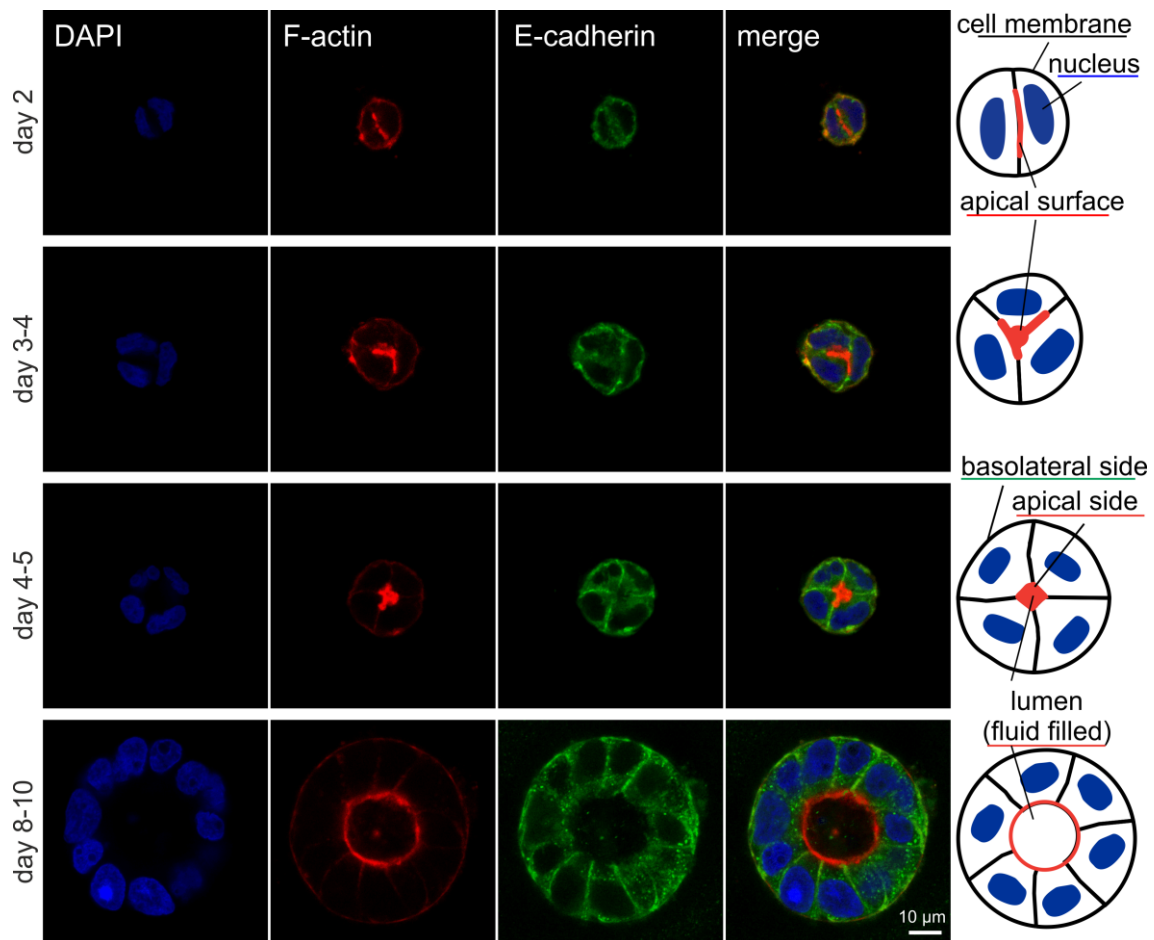


Figure I-11: 3D cell culture of Caco-2 cells. Seeded in 3D Caco-2 cells start to differentiate already on the 2-cell stage (apical F-actin accumulation). After approximately 10 days of culture they form fully polarized cysts with a fluid filled lumen. The cysts show clear apical-basolateral differentiation by apical F-actin and basolateral E-cadherin accumulation (scale: 10 μ m).

In recent years the development of more advanced 3D intestinal organoid cultures derived from primary tissues has enabled the study of differentiation programs and epithelial tissue organization in a colorectal cancer setting *ex vivo* in even more detail [45]. The intestinal organoids resemble the natural assembly of the intestinal epithelium including the crypt/villus structure and therefore the intestinal stem cell niche (Fig. I-5), enabling not only research on self-renewal processes but also the role of cancer stem cells in these organoid cultures [108]. The organoids can be isolated from genetically engineered mice, carrying the genotype of this mouse lineage or can be directly modified by transfection or precise genome editing methods. Thereby new model systems developed. Today human intestinal organoids from healthy donors can be precisely manipulated to resemble specific cancer genotypes [109]. Whole libraries of organoids from different tumor

subtypes are used to study tumorigenesis and drug sensitivity in the heterogeneous setting of CRC [110,111]. As this organoid culture technique is much more complex and requires still donor animals I used the 3D model of Caco-2 cells as a surrogate model in this study and organoid experiments were performed for validation by our partners [112].

5.3. Culture model for K-Ras mutated CRC

To study the early stages of transformation of CRC from adenoma to carcinoma, the Caco-2 cells inducibly expressing oncogenic K-Ras^{G12V} were utilized [113]. The tetracycline (Tet)-inducible expression system (tetON system) enables the timely expression of the oncogene by addition of doxycycline (dox) to the cell culture. The bi-cistronic K-Ras-IRES-GFP transcriptional cassette gets activated [114] leading to the acute expression of K-Ras^{G12V} and free GFP that can be easily detected by fluorescence microscopy and serves as a surrogate marker for oncogene expression.

II. MATERIAL AND METHODS

1. BUFFERS, SOLUTIONS AND REAGENTS

1.1. Protein extraction, SDS-PAGE and Western blotting

Blocking solution: 0.5% (v/v) blocking solution (Roche Diagnostics, Basel, Switzerland), 0.05% (v/v) Tween-20, 0.01% (v/v) thimerosal in PBS

Blotting buffer: 200 mM glycine, 25 mM Tris base, 20% (v/v) methanol in ddH₂O

Laemmli protein sample buffer (5x): 400 mM Tris pH 6.8, 500 mM dithiothreitol, 50% (v/v) glycerol, 10% (w/v) SDS, 0.2% (w/v) bromophenol blue in ddH₂O

PBS: 140 mM NaCl, 2.7 mM KCl, 8 mM Na₂HPO₄, 1.5 mM KH₂PO₄ in ddH₂O, pH 7.4

PBS-Tween: 0.05% (v/v) Tween-20 in PBS

RIPA buffer: 50 mM Tris (pH 7.5), 150 mM NaCl, 1% Triton-X 100, 0.5 sodium deoxycholate, 0.1% SDS, 1 mM sodium orthovanadate, 10 mM sodium fluoride and 20 mM β-glycerophosphate plus Complete protease inhibitors in ddH₂O (Roche)

SDS-PAGE running buffer: 25 mM Tris pH 8.8, 192 mM glycine, 0.1% (v/v) SDS in ddH₂O

SDS-PAGE running gel solution: 8%/10%/12% (v/v) acrylamide, 375 mM Tris pH 8.8, 0.1% (w/v) SDS, 0.1% APS, 0.06% TEMED in ddH₂O

SDS-PAGE stacking solution: 5% (v/v) acrylamide, 130 mM Tris pH 6.8, 0.1% (w/v) SDS, 0.1% APS, 0.1% TEMED in ddH₂O

1.2. Viability Assay

MTT solution: 5 mg/ml 3-(4,5-dimethylthiazol-2-yl)-2,5-diphenyl tetrazolium (MTT; Roth, Karlsruhe, Germany) in PBS

MTT-Stop solution: 10% SDS in ddH₂O, 50% N,N-Dimethylformamid

1.3. Immunofluorescence

Blocking solution: 5% (v/v) goat serum (Invitrogen, Karlsruhe, Germany), 0.1% (v/v) Tween-20

PFA fixing solution: 4% (v/v) PFA in PBS

Permeabilizing solution: 0.2% (v/v) Triton X-100 in PBS

Mounting solution: Fluoromount G (Southern Biotechnology, Birmingham, AL, USA)

1.4. Kits

Protein concentration: DC Protein Assay (Bio-Rad, Hercules, USA)

Western Blot Detection: HRP SuperSignal®West substrate pico (Pierce/Thermo, Rockford, USA); HRP SuperSignal®West substrate dura (Pierce/Thermo)

Cell Viability: CytoTox-Glo™ Cytotoxicity Assay (Promega, Madison, WI, USA); Caspase-Glo®3/7 Assay (Promega); in situ cell death detection kit (TMR) (Roche)

Western Blotting: NuPAGE® Novex Bis-Tris Gel; iBlot®Gel Transfer Stacks (both Invitrogen)

RNA Isolation: RNeasy® Plus Mini Kit (Qiagen, Foster City, CA, USA)

qPCR: QuantiTect Primer Assays® for SYBR® Green-based expression analysis (Qiagen)

2. CELL CULTURING

2.1. Cell lines

Fresh cultures of the human cell lines were established every three months from frozen stocks stored in liquid nitrogen. Caco-2, HCT-116, and LoVo cells were obtained from Interlab Cell Line Collection (Genova, Italy) in 2012 and Caco-2 cells were reauthenticated by SNP analysis in 2016 (Multiplexion, Immenstadt, Germany).

Caco-2tet cells, stably expressing the doxycycline-inducible system components rtTA and rtTS [113] and Caco-2tet B-Raf^{V600E}, Caco-2tet K-Ras^{G12V} and Caco-2tet vector cells were described previously [104,113]. The corresponding parental cells were authenticated in 2014 (Multiplexion). All Caco-2tet cell lines were kindly provided by Prof. Tilman Brummer, University Freiburg.

2.2. Cell culture media and reagents

Medium: RPMI 1640 (Invitrogen); DMEM (Invitrogen)

Matrix: PureCol®-S collagen (Advanced Biomatrix, San Diego, CA, USA); Growth factor reduced matrigel (BD)

Supplements: Fetal calf serum (FCS) (PAA Laboratories, Pasching, Austria); Cholera toxin (CTX; Sigma Aldrich); Doxycycline (dox; Merck, Darmstadt, Germany)

Reagents: Trypsin/EDTA (10x) (Invitrogen); Cell Recovery Solution (BD)

Growth factors: EGF (Sigma-Aldrich); TGF- α , HB-EGF, HRG (PeproTech, Hamburg, Germany); AREG, EREG, BTC (ImmunoTools, Friesoythe, Germany)

Small molecules / Inhibitors: pan-ErbB inhibitor AZD8931 (Sapitinib) (Absource Diagnostics, Munich, Germany); Z-VAD-FMK (Bachem AG, Bubendorf, Switzerland); SM83 (synthesis and purification of was described previously [115,116])

Antibodies / Inhibitors: Cetuximab from Merck (Darmstadt, Germany); Db-scTRAIL (was produced in HEK293 cells and purified from cell culture supernatants [66])

3. ANTIBODIES AND FLUORESCENT DYES

3.1. Immunoblotting

All antibodies were diluted in blocking solution; for primary antibodies 0.01% (v/v) azide was added for storage at 4°C.

List of primary and secondary antibodies with the used dilution for immunoblotting, sorted by name of antigen:

primary antibodies

monoclonal mouse anti-**alpha-tubulin** (1:5000) (Sigma-Aldrich, St Louis, MO, USA)

monoclonal rabbit anti-**pAKT** (T308) (1:1000) (Cell Signaling, Danvers, MA, USA)

monoclonal mouse anti-**pAKT** (S473) (1:1000) (Cell Signaling, Danvers, MA, USA)

monoclonal mouse anti-**AKT** (pan) (1:1000) (Cell Signaling, Danvers, MA, USA)

polyclonal rabbit anti-**Bcl-2** (1:1000) (Cell Signaling, Danvers, MA, USA)

monoclonal rabbit anti-**Bcl-xL** (1:400) (Cell Signaling, Danvers, MA, USA)

monoclonal rabbit anti-**caspase 3** (1:1000) (Cell Signaling, Danvers, MA, USA)

polyclonal rabbit anti-**clAP1** (1:1000) (Cell Signaling, Danvers, MA, USA)
monoclonal rabbit anti-**clAP2** (1:1000) (Cell Signaling, Danvers, MA, USA)
monoclonal rabbit anti-**pEGFR/ErbB1** (Y1068) (1:1000) (Cell Signaling, MA, USA)
monoclonal mouse anti-**EGFR/ErbB1** (1:500) (Thermo Scientific, Fremont, MA, USA)
monoclonal rabbit anti-**pErbB2** (Y1221/1222) (1:500) (Cell Signaling, Danvers, MA, USA)
polyclonal rabbit anti-**ErbB2** (1:1000) (Santa Cruz Biotechnology, Dallas, TX, USA)
monoclonal rabbit anti-**pErbB3** (Y1289) (1:500) (Cell Signaling, Danvers, MA, USA)
polyclonal rabbit anti-**ErbB3** (1:1000) (Santa Cruz Biotechnology, Dallas, TX, USA)
polyclonal rabbit anti-**pERK** (T202/Y204) (1:1000) (Cell Signaling, Danvers, MA, USA)
monoclonal mouse anti-**ERK** (1:1000) (Cell Signaling, Danvers, MA, USA)
monoclonal mouse anti-**FlipS/L** (1:400) (Santa Cruz Biotechnology, Dallas, TX, USA)
monoclonal mouse anti-**GFP** (1:1000) (Roche Applied Science, Mannheim, Germany)
monoclonal mouse anti-**Ras** (1:200) (BD, CA, San Jose, USA)
monoclonal mouse anti-**Smac** (1:1000) (Cell Signaling, Danvers, MA, USA)
monoclonal rabbit anti-**survivin** (1:1000) (Cell Signaling, Danvers, MA, USA)
polyclonal rabbit anti-**TRAILR1** (1:1000) (Santa Cruz Biotechnology, Dallas, TX, USA)
polyclonal rabbit anti-**TRAILR2** (1:500) (Cell Signaling, Danvers, MA, USA)
monoclonal mouse anti-**xiAP** (1:400) (BD, CA, San Jose, USA)

secondary antibodies

HRP-labeled secondary anti-mouse and anti-rabbit IgG antibodies (1:10000) were from GE Healthcare (Buckinghamshire, UK).

3.2. Immunofluorescence staining

All antibodies were diluted freshly in blocking buffer.

List of primary and secondary antibodies and fluorescent dyes that were used for immunofluorescence with corresponding dilution, sorted by name of antigen:

primary antibodies

polyclonal rabbit anti-**aPKC** (zeta) (1:200) (Santa Cruz Biotechnology, Dallas, TX, USA)
monoclonal mouse anti-**E-cadherin** (1:250) (BD, CA, San Jose, USA)
polyclonal rabbit anti-**ZO-1** (1:200) (Invitrogen)

secondary antibodies

Alexa Fluor 488- and 546- labeled secondary anti-mouse and anti-rabbit IgG antibodies (1:500) and Alexa Fluor 633-labeled phalloidin (1:100) (Invitrogen) were used.

fluorescence dyes

nuclear staining: **DAPI** (1:1000) (Sigma-Aldrich, St. Louis, USA)

F-actin staining: Alexa Fluor® 633 **phalloidin** (1:100) (Invitrogen)

4. SMALL INTERFERING RNA (SIRNAS)

All siRNAs were diluted in 1x siRNA buffer (MWG Biotech) to a final concentration of 20 µM. As non-targeting negative controls (siNT) ON-TARGETplus® non-targeting control pool (Dharmacon) or Silencer®Select Negative Control#2 (Invitrogen) were used. In all cases, two independent siRNAs were used: siErbB1 refers to siGenome SMARTpool EGFR (M-003114-03-0005) from Dharmacon; siErbB1#2 refers to Silencer®Select ErbB1 (s565) (Invitrogen); siErbB2 refers to a single duplex with the sense sequence: 5'-GGACGAAUUCUGCACAAUG-3', from Eurofins MWG Operon; siErbB2#2 refers to Silencer®Select ErbB2 (s612) from Invitrogen; siErbB3 refers to siGenome SMARTpool ErbB3 (M-003127-03-0005) from Dharmacon; siErbB3#2 refers to Silencer®Select ErbB3 (s4779) from Invitrogen); siHRG1#1 refers to Silencer®Select NRG1 (s230508), siHRG1#2 refers to Silencer®Select NRG1 (s230507), siHRG2#1 refers to Silencer®Select NRG2 (s18322) and siHRG2#2 refers to Silencer®Select NRG2 (s18321) (all from Invitrogen).

5. METHODS

5.1. Cell culturing

Caco-2, HCT-116, and LoVo cell lines were cultured in RPMI 1640 and Caco-2tet cells in DMEM, both supplemented with 10% FCS without antibiotics. Cell lines were incubated in a humidified atmosphere of 5% CO₂ at 37 °C. When cells reached 70-80% confluence, they were transferred to a new cell culture vessel; detachment was achieved by using 1x trypsin/EDTA. For growth factor dependent assays cells were grown in medium containing 2% FCS plus 10 ng/ml growth factor.

3D cell culture

For growth in 3D, cells were seeded on a bed of growth factor reduced matrigel and PureCol®-S collagen (1:1) and overlaid with growth medium containing 2% matrigel. Lumen expansion was induced by addition of 100 ng/ml Cholera toxin (CTX) at day 3 post seeding. Transgene expression in the Caco-2tet cells was induced by 2 µg/ml doxycycline (dox).

Transient transfection with siRNAs

Cells were transiently transfected with siRNA using DharmaFECT1 (Dharmacon, Lafayette, CO, USA) according to manufacturer's instructions. For transient transfections of Caco-2 or Caco-2tet cells 1.8×10^5 cells/well in 1 ml medium were seeded in 12-well dishes. The next day medium was exchanged with 800 µl fresh growth medium and 200 µl transfection mix was added, prepared according to manufacturer's protocol. One day later cells were replated for further experiments. All steps described were performed with RNase-free solutions, reaction tubes and pipette tips to avoid RNase contamination.

5.2. MTT, cytotoxicity, and caspase 3/7 activity assays

For 2D cultures, 2.5×10^3 cells/well in 100 µl medium were plated into uncoated 96-well plates. For 3D cultures, 5×10^3 cells/well were seeded into matrigel/collagen-coated 96-well plates in 100 µl medium containing 2% matrigel. Viability was determined by addition of 10 µl MTT solution (5 mg/ml) followed by incubation for 3 h. Cells were lysed by addition of 100 µl MTT-stop solution and absorbance was measured at 570 nm using the multimode reader Infinite® 200 PRO (Fa. Tecan, Männedorf, Switzerland). Cytotoxicity was measured using the CytoTox-Glo™ Cytotoxicity Assay (Promega). The activity of dead-cell protease in the culture was determined by addition of 50 µl luminogenic substrate. After 15 min incubation at RT, luminescence was measured using the multimode reader Infinite® 200 PRO (Fa. Tecan), followed by cell lysis and measurement of total luminescence for normalization. Caspase 3/7 activity was determined using the Caspase-Glo®3/7 Assay (Promega) by addition of 70 µl luminogenic substrate containing the DEVD sequence. After 30 min incubation at RT, luminescence was measured using the multimode reader Infinite® 200 PRO (Fa. Tecan).

5.3. Immunofluorescence microscopy

Cells grown in 3D on matrigel/collagen coated 8-well glass chamber slides (BD) were fixed with 4% PFA for 15 min, permeabilized 10 min and blocked with 5% goat serum in PBS-Tween. Cells were then incubated with primary antibodies in blocking buffer (2 h at RT), washed with PBS-Tween and incubated with secondary antibody in blocking buffer (2 h at RT). F-actin and nuclei were counterstained with Alexa Fluor 633-labeled phalloidin and DAPI. Slides were mounted in Fluoromount G and analyzed on a confocal laser scanning microscope. To determine the number of polarized cysts with a 'predominant single apical lumen' (PSAL) [42], spheroids were analyzed in terms of roundness, cell-free lumen formation and F-actin staining of the apical surface. Round spheroids with a single-cell layer around a hollow lumen and distinct F-actin staining were scored as normal/polarized, cysts lacking at least two of these features were scored as abnormal/unpolarized.

5.4. Tunel staining

DNA strand breaks were analyzed with the in situ cell death detection kit (TMR red; Roche). Cells grown in 3D culture were fixed with 4% PFA for 1 h at RT and permeabilized with 0.1% Triton-X 100 in 0.1% sodium citrate for 2 min at RT. Labeling was performed according to the manufacturer's protocol for 1 h at 37°C. Nuclei were counterstained with DAPI. Slides were mounted in Fluoromount G and analyzed on a confocal laser scanning microscope (LSM 700; Zeiss, Oberkochen, Germany). Images were processed with the ZEN software (Zeiss). Tunel-positive cells were counted using ImageJ (W Rasband, National Institute of Health, USA; V 1.48).

5.5. Western blotting

Cells were lysed in RIPA buffer. For lysates from 3D cultures, cells were cultured on pure matrigel without collagen. Spheroids were isolated after 4 days by dissolving the matrigel in ice cold Cell Recovery Solution (BD). After centrifugation for 4 min at 200*g and 4 °C, supernatant was discharged and the remaining spheroids were lysed in RIPA buffer. Lysates were clarified by centrifugation for 10 min at 13,000 rpm and 4°C. Supernatant was transferred to a new tube and either directly separated by SDS polyacrylamide gel

electrophoresis (SDS-PAGE) or stored at -20 °C. To determine total protein concentration, the DC Protein Assay was utilized according to the manufacturer's instructions. Proteins were denatured in 1x Laemmli sample buffer for 5 min at 100 °C. Equal amounts of protein were separated by SDS-PAGE (NuPAGE® Novex Bis-Tris Gel; Invitrogen) and transferred to nitrocellulose membrane (iBlot®Gel Transfer Stacks; Invitrogen). Alternatively lysates were loaded on 8%/10%/12% polyacrylamide gels, depending on the molecular weight of the analyzed proteins, and transferred to polyvinylidene difluoride membranes (Roth). Membranes were blocked with 0.5% blocking reagent (Roche) and incubated with primary antibodies, followed by HRP-conjugated secondary antibodies. Visualization was done with ECL detection system (Pierce).

5.6. FACS analysis

Analysis of transgene expression of the Caco-2tet cells was performed after 72 h dox treatment. Cells were detached with Trypsin, washed, re-suspended in PBS containing 2% FCS and 0.01% sodium azide, and analyzed using an EPICS FC500 flow cytometer (Beckman Coulter, Krefeld, Germany). Post-acquisition data analysis was performed using FlowJo software (Tree Star; Ashland, OR, USA).

5.7. Quantitative PCR

Total RNA was isolated from cells using the RNeasy® Plus Mini Kit (Qiagen) according to the manufacturer's protocol. For 2D cell cultures, 2×10^5 to 1×10^6 cells were lysed with RLT buffer. For 3D culture, 4×10^5 cells were seeded in 12-well plates on matrigel, as described for protein extraction. Pelleted spheroids were lysed in 350 µl RLT buffer. RNA samples were quantified using a Nanophotometer (Implen, Munich, Germany) at OD 260/280 nm. q-PCR was performed with QuantiTect Primer Assays® for SYBR® Green-based expression analysis (Qiagen) using a Cfx96 device (Biorad) according to the manufacture's protocol for one-step RT-PCR. Changes in the relative expression level were calculated using the $2^{-\Delta\Delta Ct}$ method (CFX manager software 3.1, Biorad). GAPDH was used as the endogenous control gene for normalization. Used primers were Hs_NRG1_1_SG QuantiTect Primer Assay, Hs_NRG2_1_SG QuantiTect Primer Assay and Hs_GAPDH_2_SG QuantiTect Primer Assay (all Qiagen).

5.8. Statistical analysis

Data are expressed as mean \pm S.E.M.; 'n' refers to the number of samples/experiment, 'N' to the number of independent experiments. Statistical significance was evaluated by t-test and one-way ANOVA followed by Tukey's post-test (GraphPad Prism version 4.03; GraphPad Software Inc., La Jolla, CA, USA). p-values below 0.05 were considered as significant (*p < 0.05; **p < 0.01; ***p < 0.001; ns, p > 0.05).

III. RESULTS

1. ONCOGENIC RAS AND ERBB3 SIGNALING

- IN HYPERPROLIFERATION AND POLARIZATION DEFECTS-

The human CRC cell line Caco-2 forms polarized cysts when grown in 3D matrigel cultures, recapitulating morphological features of the intestinal epithelium. These cysts are characterized by a single epithelial cell layer with apical-basolateral polarity that surrounds a hollow lumen [107]. In this study I used parental Caco-2 cells and a Caco-2tet cell line that inducibly express oncogenic K-Ras^{G12V}. Thus this cell lines are well suited to investigate the influence of acute expression of oncogenic Ras on proliferation and differentiation in the context of CRC.

K-Ras^{G12V} expression impede Caco-2 polarization in 3D

In the Caco-2tet K-Ras^{G12V} cells addition of doxycycline induces the bi-cistronic expression of the oncogene K-Ras^{G12V} and GFP, whereas vector control cells express GFP only. Three days after dox addition, more than 85% of the cells were GFP positive by FACS analysis (Fig. III-1a). Immunoblotting of Caco-2tet K-Ras^{G12V} cell lysates confirmed Ras overexpression along with that of GFP, concomitant with strong ERK phosphorylation, whereas vector control cells expressed only GFP (Fig. III-1b).

When these cells were seeded into 3D cultures in the absence of doxycycline, both Caco-2tet vector and K-Ras^{G12V} cells formed well-differentiated and polarized spheroids with basolateral adherens junctions (E-cadherin staining) and apical F-actin accumulation around a cell-free lumen. Addition of doxycycline had no effect on the morphology of the control cells, expressing GFP only, whereas the K-Ras^{G12V} expressing cells formed multi-luminal spheroids that lacked distinct polarization (Fig. III-2). These differentiation defects caused by K-Ras^{G12V} are in accordance with a recent report by Magudia et al. [88].

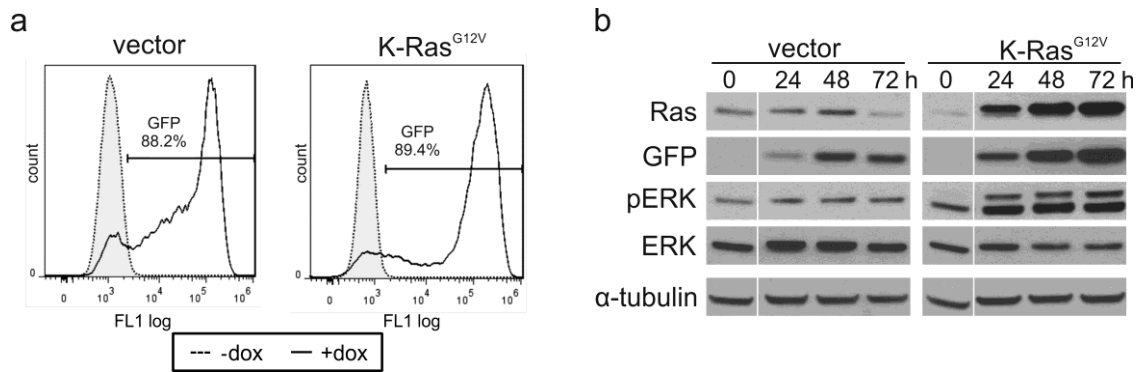


Figure III-1: Inducible expression of oncogenic K-Ras^{G12V} in Caco-2tet cells. (a) Caco-2tet vector control and K-Ras^{G12V} cells were treated with 2 μg/ml dox for 72 h (+ dox). Cells were harvested and GFP fluorescence was analyzed by flow cytometry. Non-induced cells were used as a control (- dox). (b) Caco-2tet vector control and K-Ras^{G12V} cells were grown in 2D treated with dox for the indicated times prior to lysis. Lysates were analyzed by immunoblotting using the indicated antibodies. Tubulin was detected as loading control. All panels shown are from the same blot.

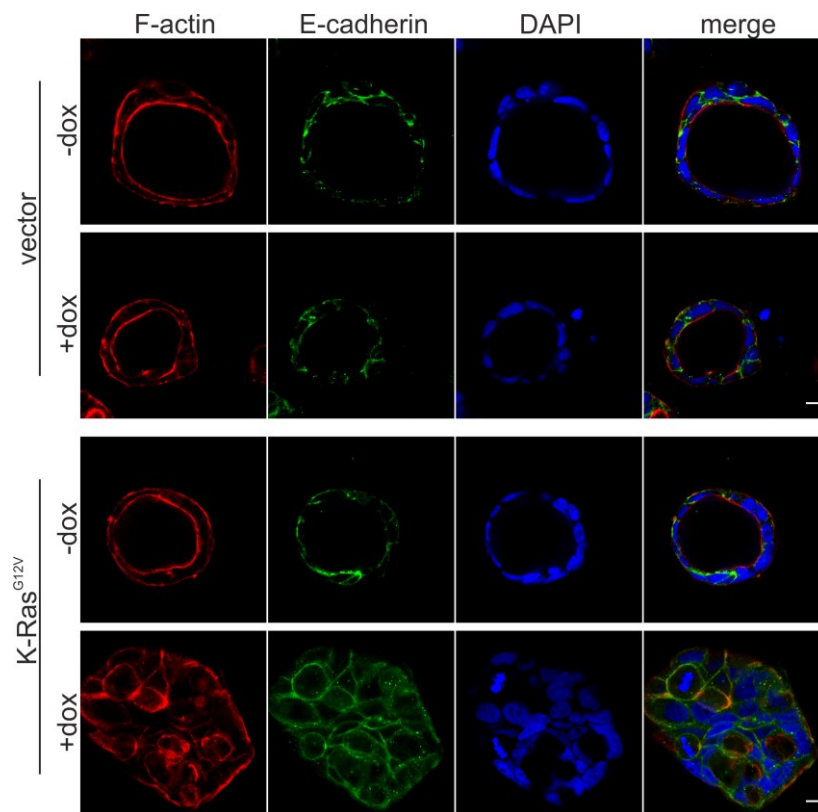


Figure III-2: Expression of oncogenic K-Ras^{G12V} in Caco-2tet cells interferes with normal morphogenesis. Caco-2tet vector control and K-Ras^{G12V} cells were seeded into 3D cultures in the absence or presence of dox. Three days post seeding lumen expansion was induced by addition of CTX. Cultures were fixed three days later and stained with E-cadherin-specific antibody (green), phalloidin (F-actin; red) and DAPI (nuclei; blue). Shown are confocal sections of representative cysts (scale: 10 μm).

Quantification of the effects of K-Ras^{G12V} expression, visualized by the bi-cistronic GFP expression, showed that the average number of cells in the midplane of the cysts doubled compared to the non-induced control and only 15% of the cysts were scored as normally differentiated, based on morphological criteria (see methods for details) including well-defined apical F-actin accumulation (Fig. III-3a-c).

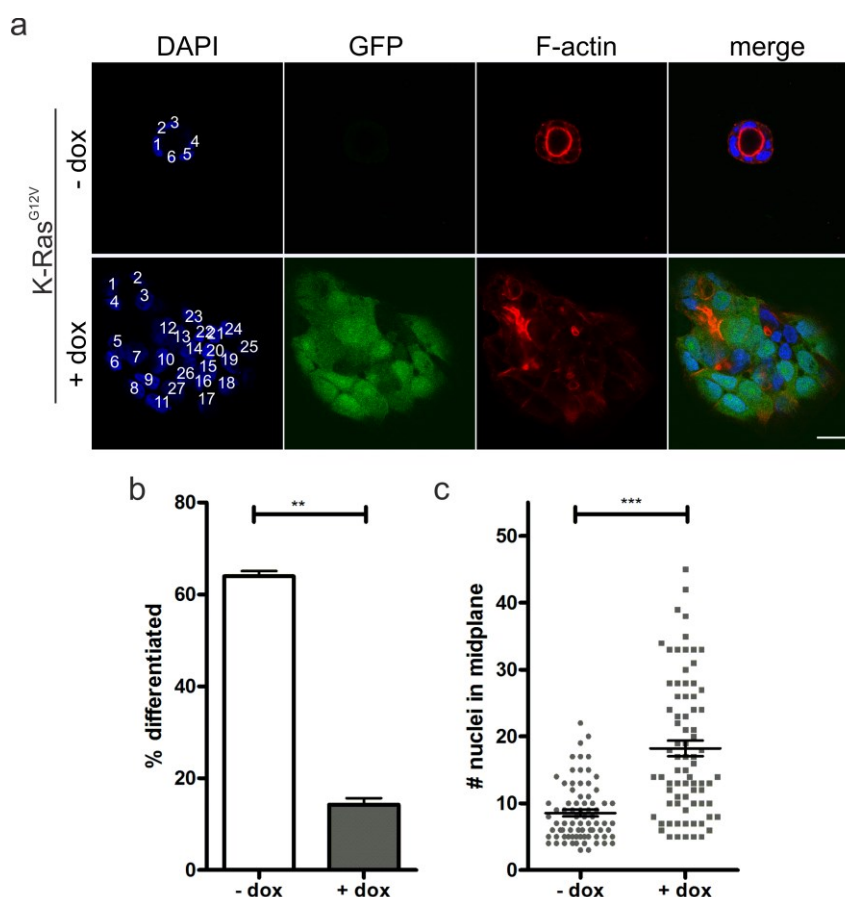


Figure III-3: Quantification of aberrant morphogenesis of Caco-2tet K-Ras^{G12V} cells in 3D culture.

(a) Caco-2tet K-Ras^{G12V} cells were seeded into 3D in the absence or presence of dox. Three days post seeding lumen expansion was induced by addition of CTX. Cultures were fixed two days later and stained with DAPI (nuclei; blue) and phalloidin (F-actin; red). GFP is co-expressed with K-Ras^{G12V} (green). Shown are confocal sections of the midplane of representative cysts, nuclei are numbered in white (scale: 20 μ m). (b) The percentage of differentiated cysts from (a) was determined (n>70; N=3). (c) The number of nuclei in the midplane of cysts was counted as depicted in (a) (n=25; N=3).

ErbB receptor inhibition restores Caco-2tet K-Ras^{G12V} polarization

To investigate the potential contribution of the ErbB receptors to the aberrant morphogenesis and hyperproliferation induced by K-Ras^{G12V} expression, the doxycycline-containing 3D cultures were treated with the pan-ErbB inhibitor AZD8931.

Interestingly, the abnormal morphology of K-Ras^{G12V}-expressing Caco-2 cysts was partially restored, with almost 40% of cysts displaying polarized structures with a predominant single apical lumen (Fig. III-4a,b) and a significant reduction of cyst size (Fig. III-4c), comparable to that of K-Ras^{G12V} cells without dox (Fig. III-3c).

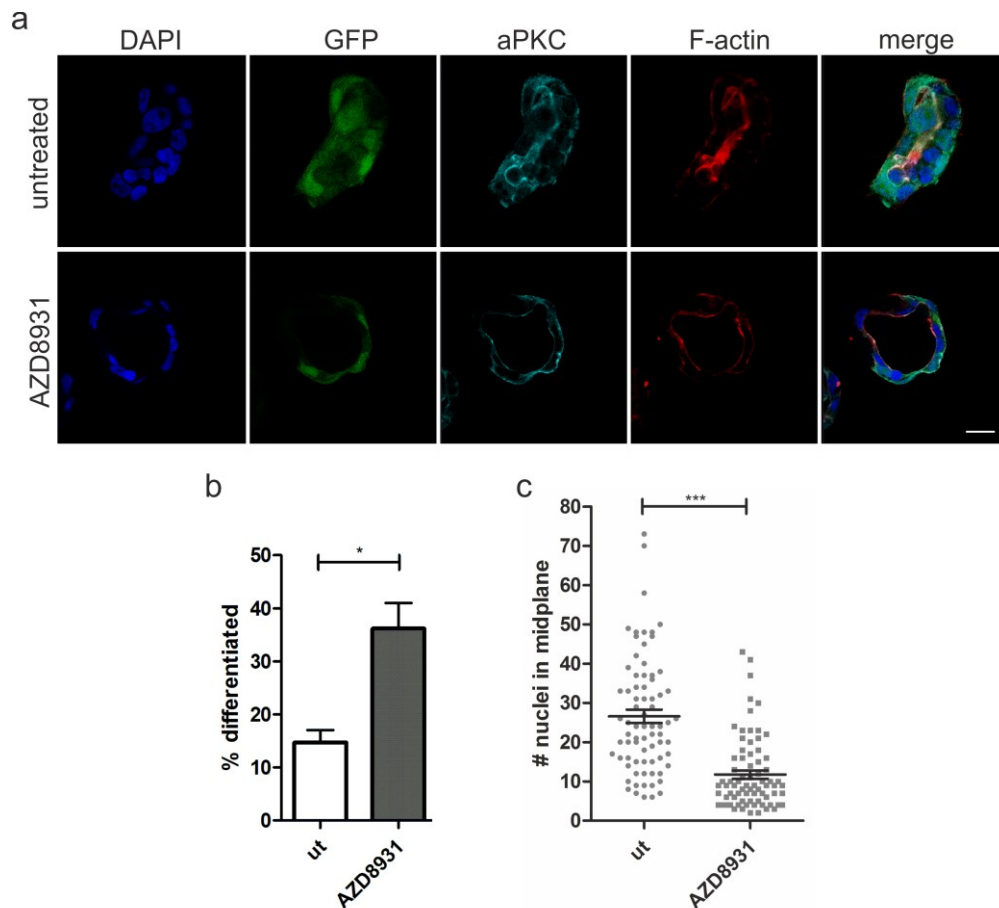


Figure III-4: ErbB receptor inhibition restores morphogenesis of Caco-2tet K-Ras^{G12V} cells in 3D. (a) Caco-2tet K-Ras^{G12V} cells were seeded into 3D cultures. One day post seeding K-Ras^{G12V} expression was induced with dox and cultures were left untreated (ut) or treated with 200 nM AZD8931. Two days later CTX was added to the culture. Cultures were fixed the next day and stained with DAPI (nuclei; blue), anti-aPKC antibody (cyan) and phalloidin (F-actin; red). GFP is co-expressed with K-Ras^{G12V} (green). Shown are confocal sections of the midplane of representative cysts (scale: 20 μ m). (b) The percentage of differentiated cysts of (a) was determined (n>60; N=3). (c) The number of nuclei in the midplane of cysts of (a) was counted (n=25; N=3).

Analysis of inhibitor treatment affecting ErbB receptor signaling showed low basal phosphorylation of AKT and ERK in the non-induced cells (-dox). K-Ras^{G12V} expression (+dox) revealed hyperactivation of MAPK and PI3K pathways. ErbB1 phosphorylation was readily detectable in both control and K-Ras^{G12V}-expressing cells, whereas no

phosphorylation was visible for ErbB2 and ErbB3. Expression of ErbB4 was below the detection limit in this cell line (data shown in [112]).

AZD8931 potently suppressed ErbB1 phosphorylation in control (-dox) and oncogenic Ras-expressing cells. Comparable results were obtained with a second inhibitor (ErbB2-II), which also restored the morphogenetic defects in Caco-2tet Ras^{G12V} cells. This inhibitor blocked HRG-induced ErbB2 and ErbB3 activation, but had no effect on EGF-induced ErbB1 phosphorylation (data shown in [112]).

ErbB3 is required for the K-Ras^{G12V} induced polarization defect

To identify the ErbB receptors that cooperate with K-Ras^{G12V} signaling, gene silencing experiments were performed. Caco-2tet K-Ras^{G12V} cells were transfected with control siRNA (siNT) or ErbB receptor-specific siRNAs (siErbB1/2/3) and then seeded into 3D culture, followed by the induction of K-Ras^{G12V} expression the next day.

Morphological analysis revealed that the cysts formed by oncogenic Ras-expressing cells depleted of ErbB1 or ErbB2 were comparable to those transfected with the siRNA control. By contrast, upon ErbB3 depletion, the K-Ras^{G12V}-induced defect in polarized morphogenesis was rescued, as seen by the apical accumulation of the apical markers atypical PKC (aPKC) and F-actin (Fig. III-5a,b). Note that K-Ras^{G12V} expression was not affected by the siRNA transfection as judged by the GFP signal. Additionally, in the absence of ErbB3, the hyperproliferation triggered by K-Ras^{G12V} was abrogated (Fig. III-5c) with average cell numbers in the midplane of cysts comparable to those observed in non-induced control cultures (see Fig. III-3c). This was specific to the 3D cultures, as ErbB3 depletion did not affect the proliferation of Ras^{G12V}-expressing cells grown in 2D monolayers (data not shown). ErbB receptor knockdown was verified by immunoblotting (Fig. III-5d) and similar results were obtained by independent siRNAs (data not shown).

Taken together, these findings uncover a role for ErbB3 signaling in oncogenic Ras-induced hyperproliferation and polarity loss, which were partially rescued by pharmacologic pan-ErbB inhibition or specific siRNA-mediated knockdown.

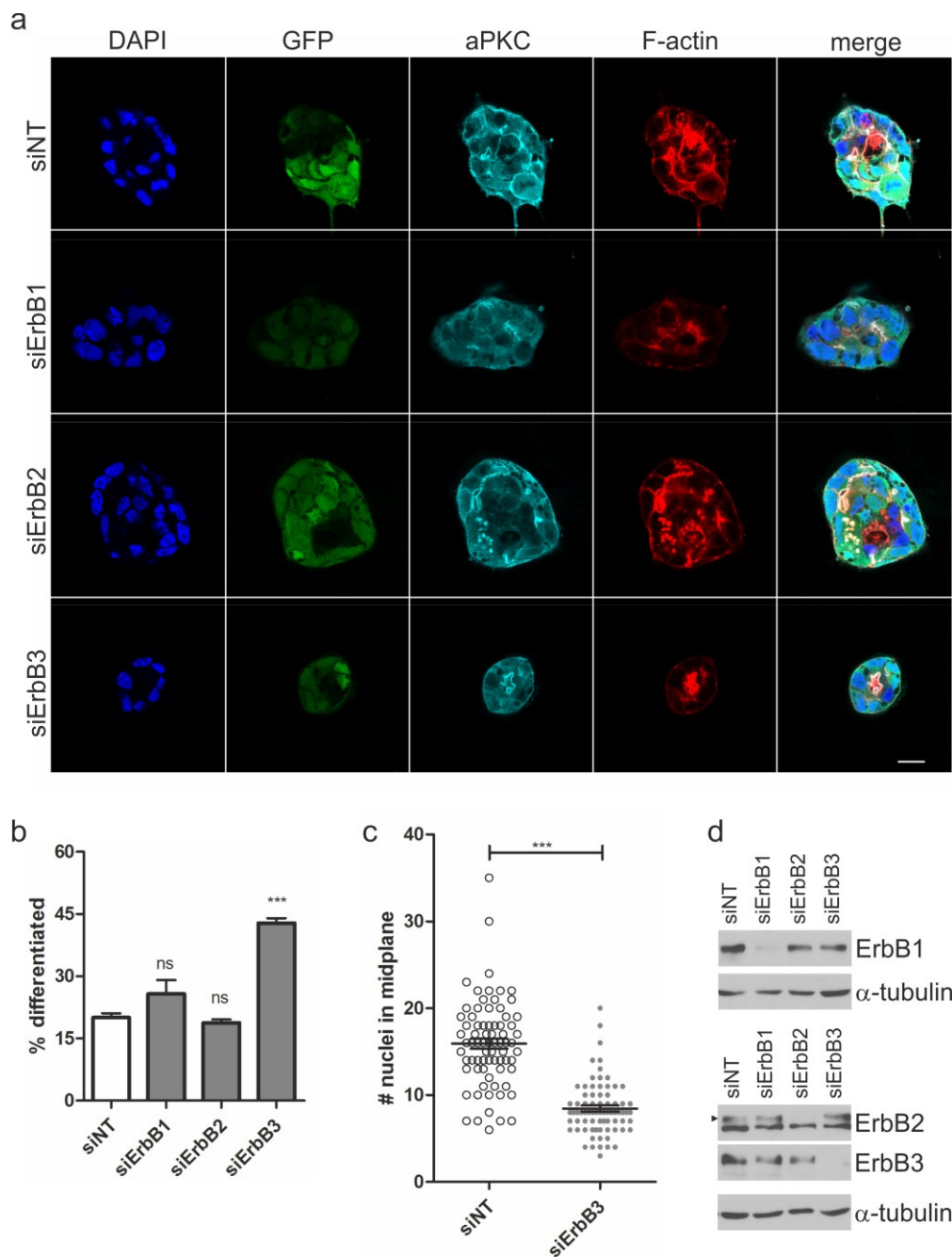


Figure III-5: ErbB3 knockdown rescues hyperproliferation and polarized morphogenesis of Caco-2 cells expressing oncogenic K-Ras. (a) Caco-2tet K-Ras^{G12V} cells were transfected with non-targeting (siNT) and ErbB receptor-specific siRNAs, respectively. The next day cells were seeded into 3D. One day post seeding K-Ras^{G12V} expression was induced with dox. Two days later CTX was added. Cultures were fixed the next day and stained with DAPI (nuclei; blue), anti-aPKC antibody (cyan) and phalloidin (F-actin; red). GFP is co-expressed with K-Ras^{G12V} (green). Shown are confocal sections of the midplane of representative cysts (scale: 20 μm). (b) The percentage of differentiated cysts of (a) was determined (n>70; N=3). (c) The number of nuclei in the midplane of cysts of (a) was counted (n=25; N=3). (d) Two days after gene silencing, lysates were generated and analyzed by immunoblotting using the indicated antibodies. Tubulin was detected as a loading control. Specific bands are marked by arrowheads.

ErbB3 activation by HRG disrupts Caco-2 cyst formation

To analyze the impact of specific activation of the different ErbB receptors by their ligands concerning Caco-2 3D proliferation and morphogenesis, parental cells were seeded in growth factor-reduced matrigel with low serum (2%) in the presence of the different ErbB ligands. Stimulating effects on proliferation were detected following EGF, TGF- α , and HB-EGF addition and strongest stimulation was induced by HRG (Fig. III-6a).

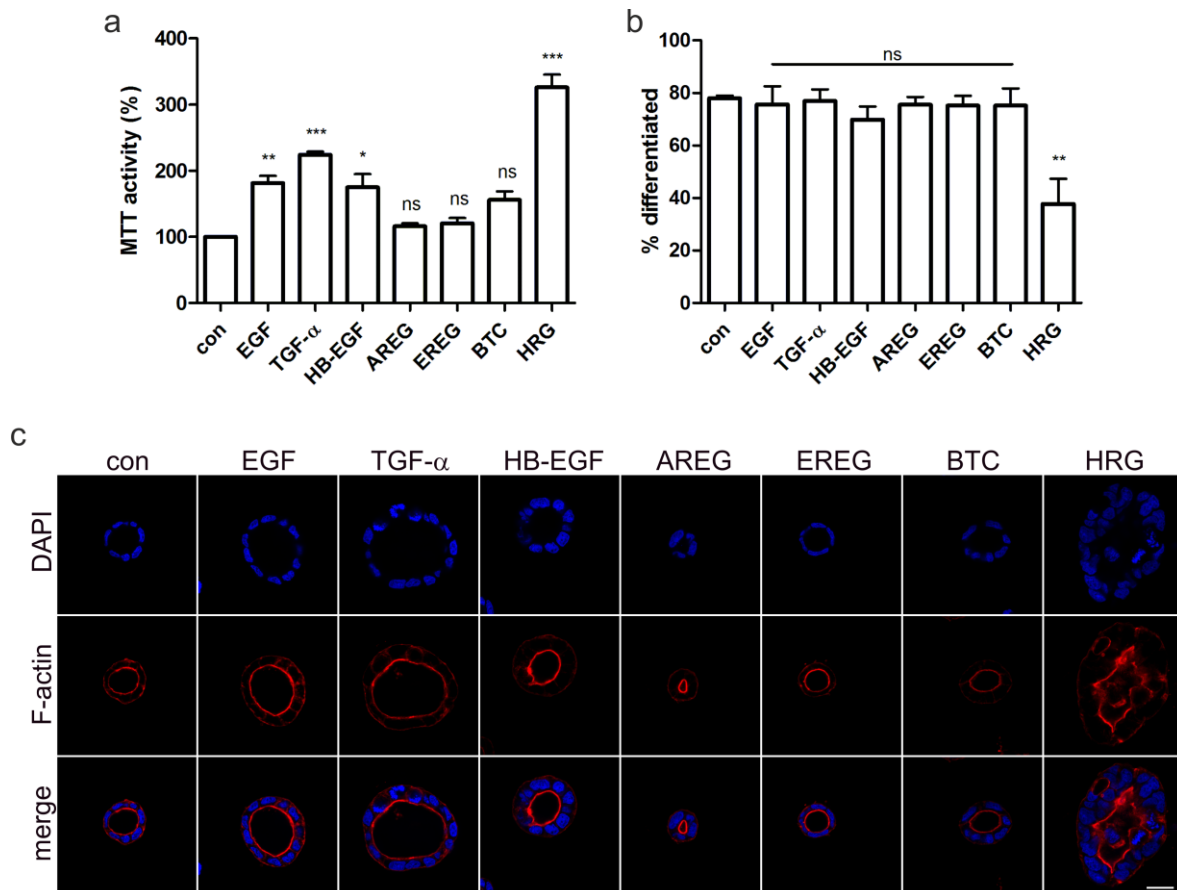


Figure III-6: Heregulin induces hyperproliferation and impairs polarized morphogenesis of Caco-2 cysts. (a) Caco-2 cells were grown in 3D containing 2% FCS in the presence of the indicated growth factors (10 ng/ml) or in 2% FCS only as a control (con). Cultures were analyzed by MTT assay at day 6 (N=3). (b,c) Cells were grown as described in (a). Three days after seeding CTX was added. Cultures were fixed the next day and stained with DAPI (nuclei; blue) and phalloidin (F-actin; red). (b) The percentage of differentiated cysts was determined (n>70; N=3). (c) Shown are confocal sections of the midplane of representative cysts (scale: 20 μ m).

Importantly, despite effects on proliferation as seen by the increased sizes of cysts (Fig. III-6c), apart from HRG, none of the ErbB ligands interfered with polarized cyst morphology and lumenogenesis (Fig. III-6b). In the presence of HRG, a significant drop in

the percentage of polarized cysts was noted (Fig. III-6b,c), similar to the phenotype induced by K-Ras^{G12V}. Expression of aPKC and E-cadherin, which demarcate the apical and basolateral membranes, respectively, were retained in the presence of HRG, but aPKC was mislocalized (Fig. III-7a). To prove that HRG signaling was disrupting apical-basolateral polarity and not simply inducing hyperproliferation leading to luminal filling, cyst development was analyzed in more detail. Already at the two-cell stage, apical-basolateral polarization is observed, with F-actin accumulating at the cell-cell interface, associated with the formation of tight junctions that are positive for ZO-1 (Fig. III-7b; day 2, -HRG). This apical surface is maintained as the cyst develops, specifying the position of the lumen. HRG interfered with correct F-actin localization and ZO-1 recruitment, indicating that the initial establishment of polarity and tight junctions were impaired (Fig. III-7b,c).

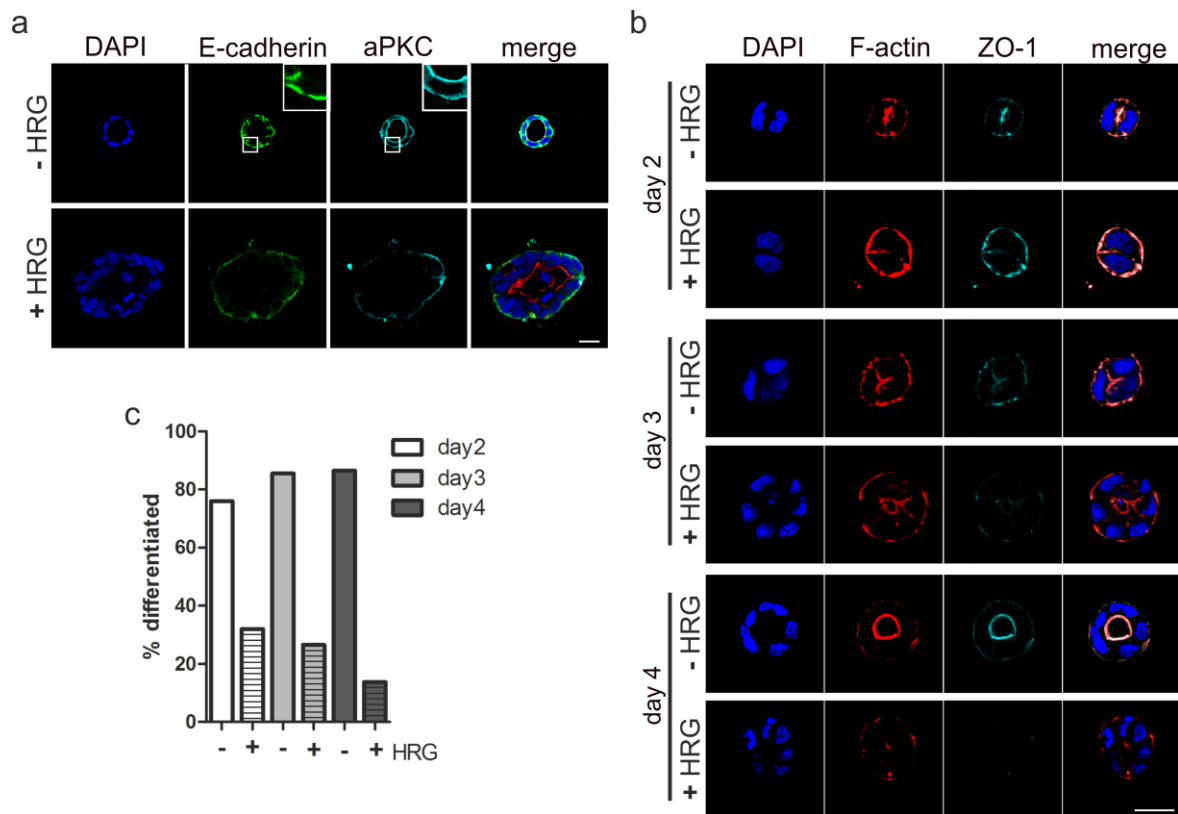


Figure III-7: Heregulin impairs apical-basolateral polarity and lumenogenesis of Caco-2 3D cultures. Caco-2 cells were grown in 3D containing 10% FCS in the presence or absence of HRG (10 ng/ml) (a) Cells were fixed at day 5 one day after addition of CTX and stained with anti-E-cadherin antibody (green), anti-aPKC antibody (cyan) and DAPI (nuclei; blue). (b,c) Cultures were fixed at the indicated days after seeding, and stained with DAPI and phalloidin (F-actin; red). At day three CTX was added. (b) Shown are confocal sections of the midplane of representative cysts (scale: 20 μ m). (c) The percentage of differentiated cysts was determined (n>25; N=2).

To address the qualitative differences in receptor activation and downstream signaling Caco-2 2D monolayers were stimulated for 15 min with the different ErbB ligands. Phosphorylation levels of ErbB1, ERK and AKT induced by EGF, TGF- α and HB-EGF closely mirrored the growth stimulation observed. HRG is the only exception. It stimulated ErbB3 phosphorylation associated with strong PI3K pathway activation, as judged by AKT phosphorylation (Fig. III-8a). ErbB2 phosphorylation at Tyrosine 1222/1221 was barely detectable following application of any ligand. Phosphorylation after EGF, TGF- α and HB-EGF and HRG stimulation was observed at Tyrosine 1248 only (data not shown).

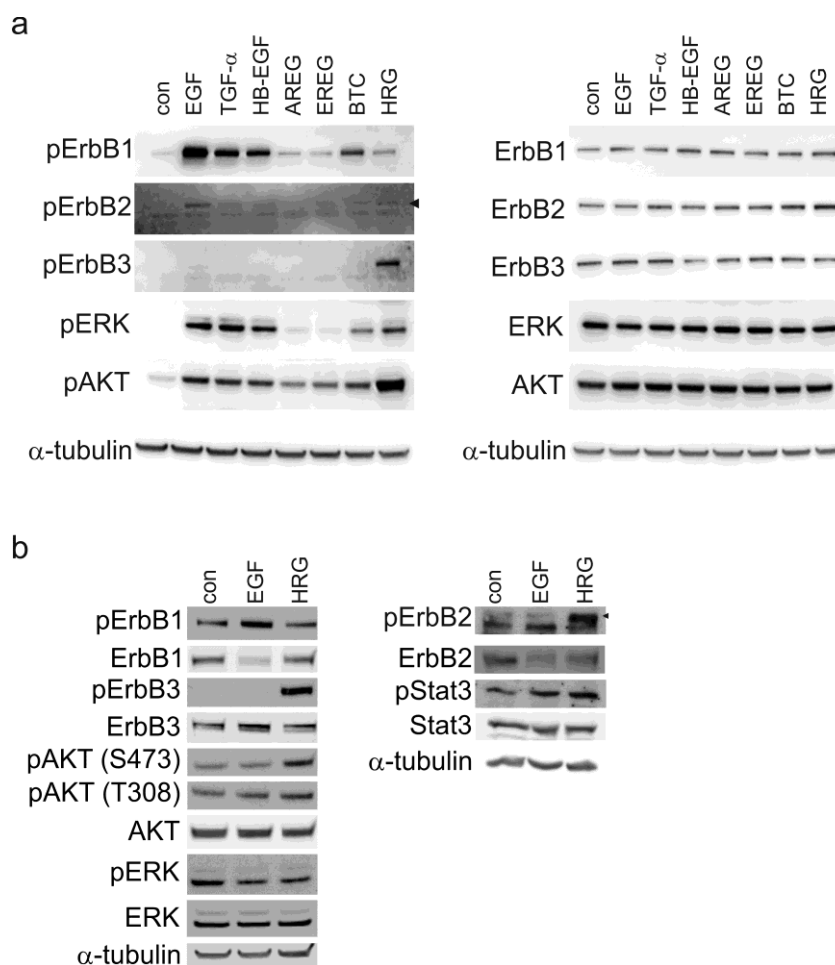


Figure III-8: HRG activates ErbB3 signaling and PI3K pathway. (a) Caco-2 cells were seeded in 2D, serum-starved overnight (2% FCS) and, prior to lysis, stimulated with the indicated growth factors (10 ng/ml) for 15 min or left untreated (con). Lysates were analyzed by immunoblotting. Tubulin as a loading control was detected. Shown is a representative blot (N=2). (b) Caco-2 cells grown in 3D containing 2% FCS in the presence of the indicated growth factors (10 ng/ml) or in 2% FCS (con). Three days post seeding cysts were lysed and analyzed by immunoblotting using the indicated antibodies (pErbB2(Tyr1248)). Tubulin was detected as loading control. Shown is a representative blot (N=2) [experiment (b) performed by S. Schmid [112]].

A comparison of the activation of the signaling molecules after incubation of 3D cultures for four days, focusing on EGF or HRG showed that ErbB receptor phosphorylation was still enhanced compared to the 2% serum control, but ERK phosphorylation was downregulated after prolonged ligand stimulation, whereas Stat3 phosphorylation was slightly elevated in the presence of the ligands. Compared to EGF, HRG led to sustained AKT phosphorylation in this experiments (3-fold) at serine 473 (Fig. III-8b), which was comparable to the extent of AKT phosphorylation induced by K-Ras^{G12V}. Long-term stimulation with EGF or HRG suppressed ERK activation, probably owing to compensatory feedback mechanisms. Finally, to prove that ErbB3 was mediating the HRG effect, knockdown of ErbB3 and also ErbB2, as ErbB3 preferentially heterodimerizes with ErbB2, was performed. In the absence of HRG, the receptor knockdowns had little effect on the polarized morphogenesis of the control cultures (siNT) (Fig. III-9a, left). However, in the presence of HRG, ErbB3 depletion fully restored polarized cyst structure and lumen formation to the level seen in the control. Knockdown of ErbB2, however, failed to do so (Fig. III-9a, right). Knockdown efficiency was comparable for both receptors (Fig. III-9b).

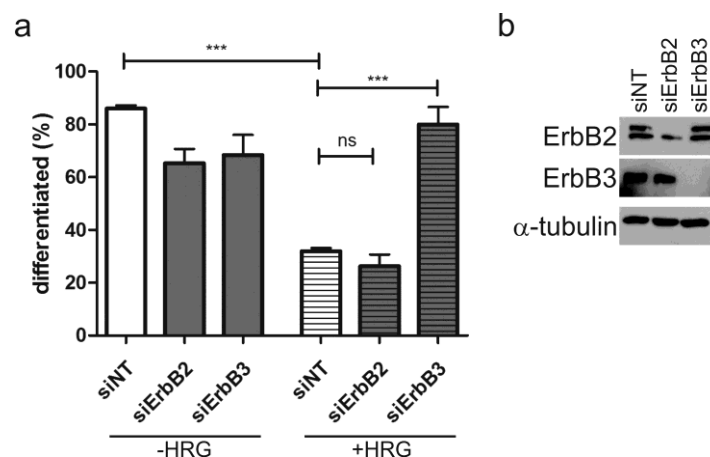


Figure III-9: HRG-induced ErbB3 signaling impairs polarized morphogenesis of Caco-2 cells. (a) Caco-2 cells were transfected with non-targeting (siNT) and ErbB-receptor specific siRNAs, respectively. The next day, cells were seeded into 3D in the presence or absence of HRG (10 ng/ml). Three days post seeding lumen expansion was induced by addition of CTX. The percentage of differentiated cysts was determined (n>50; N=3). (b) Two days after gene silencing, lysates were generated and analyzed by immunoblotting. Tubulin was detected as a loading control. Specific bands are marked by arrowheads.

Experiments in 3D murine intestinal organoid cultures, as an organotypic model for normal intestinal epithelium, confirmed the morphological phenotypes found after EGF

and HRG stimulation [112]. Here the outgrowth of single intestinal crypts into organoids with a crypt-villus axis was stalled in the absence of ErbB1 ligands. EGF supported the outgrowth of organoids, as reported previously [45]. However the substitution of EGF by HRG lead to hyperproliferative organoids with multiple irregularly shaped crypts and mislocalized F-actin.

Taken together, the analysis of normal tissue is consistent with the here described data obtained from Caco-2 cells and provides support that activation of a HRG-ErbB3-AKT signaling axis can contribute to hyperproliferation and tissue disorganization in the intestinal epithelium.

K-Ras^{G12V} induced HRG2 expression is responsible for the observed polarization defect

Based on these findings, I hypothesized that K-Ras^{G12V} expression in Caco-2 3D cultures may lead to enhanced HRG production. Indeed, real-time qPCR analysis revealed that oncogene expression induced HRG1/2 transcript levels, which was significant for HRG2 in 2D and 3D cultures (Fig. III-10a,b).

It is particularly noteworthy that only active K-Ras^{G12V} but not active B-Raf^{V600E} led to HRG expression (Fig. III-10a), indicating that oncogenic K-Ras triggers a distinct transcriptional program. Comparison of human CRC cell lines with wild-type K-Ras genes and those carrying an active Ras-mutation revealed strongly increased HRG2 transcript levels in three out of four cases as well (SW480, LoVo, HCT116; Fig. III-10c). This indicates that the upregulation of HRG expression by oncogenic Ras signaling is not restricted to the Caco-2 model system.

Next, silencing of HRG expression prior to the induction of oncogenic Ras was performed. In full support of my hypothesis, the combined depletion of HRG1 and HRG2 reduced spheroid size and significantly increased the number of polarized cysts with apical lumen (Fig. III-11a-c). This rescue was also observed by independent siRNAs (Fig. III-11; #2) and was comparable to the rescue obtained by pharmacological ErbB inhibition (Fig. III-4b) or ErbB3 silencing (Fig. III-9a). HRG1/2 knockdown was confirmed by qPCR analysis (Fig. III-11c).

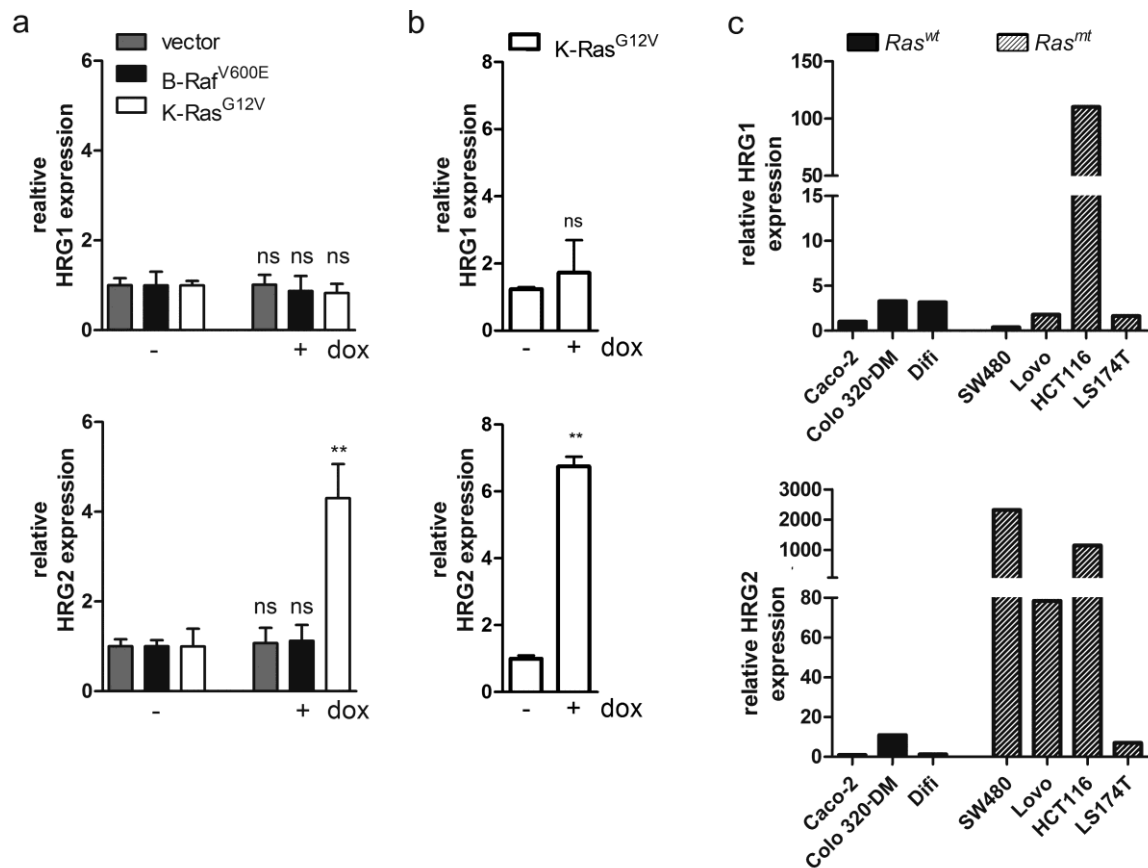


Figure III-10: Oncogenic K-Ras but not B-Raf induces HRG Expression. (a) Caco-2tet vector, B-Raf^{V600E} and K-Ras^{G12V} cells were seeded into 2D in the presence of dox for 72 h. RNA was isolated and analyzed by qPCR for the expression of HRG1 or HRG2, normalized to GAPDH expression (N=3). (b) Caco-2tet K-Ras^{G12V} cells were seeded into 3D in the presence of dox for 72 h. Cysts were isolated and lysed. RNA was analyzed by qPCR for the expression of HRG1 or HRG2, normalized to GAPDH expression (N=3). (c) The indicated human CRC cell lines were seeded into 3D culture. Three days later, cysts were isolated, RNA was extracted and HRG1 or HRG2 expression was determined by qPCR, normalized to GAPDH (N=2) [experiment (c) performed by J. Hendrick [112]]

To prove that HRG was acting through extracellular ErbB3 binding, treatment of the K-Ras^{G12V} expressing cells with an ErbB3-specific antibody that competes with HRG was performed (Fig. III-12a,b). Importantly, this treatment suppressed proliferation and significantly restored the number of cysts with a normal polarized morphology. In conclusion, the hyperproliferation and polarity loss induced by K-Ras^{G12V} expression in the 3D Caco-2 model can be ascribed to autocrine HRG-ErbB3 signaling. Interestingly, it was shown that several ErbB ligands including HRG1 were upregulated in mouse adenoma compared to normal intestinal tissue [112], pointing at the existence of additional mechanisms activating ErbB receptor signaling during tumor initiation and progression.

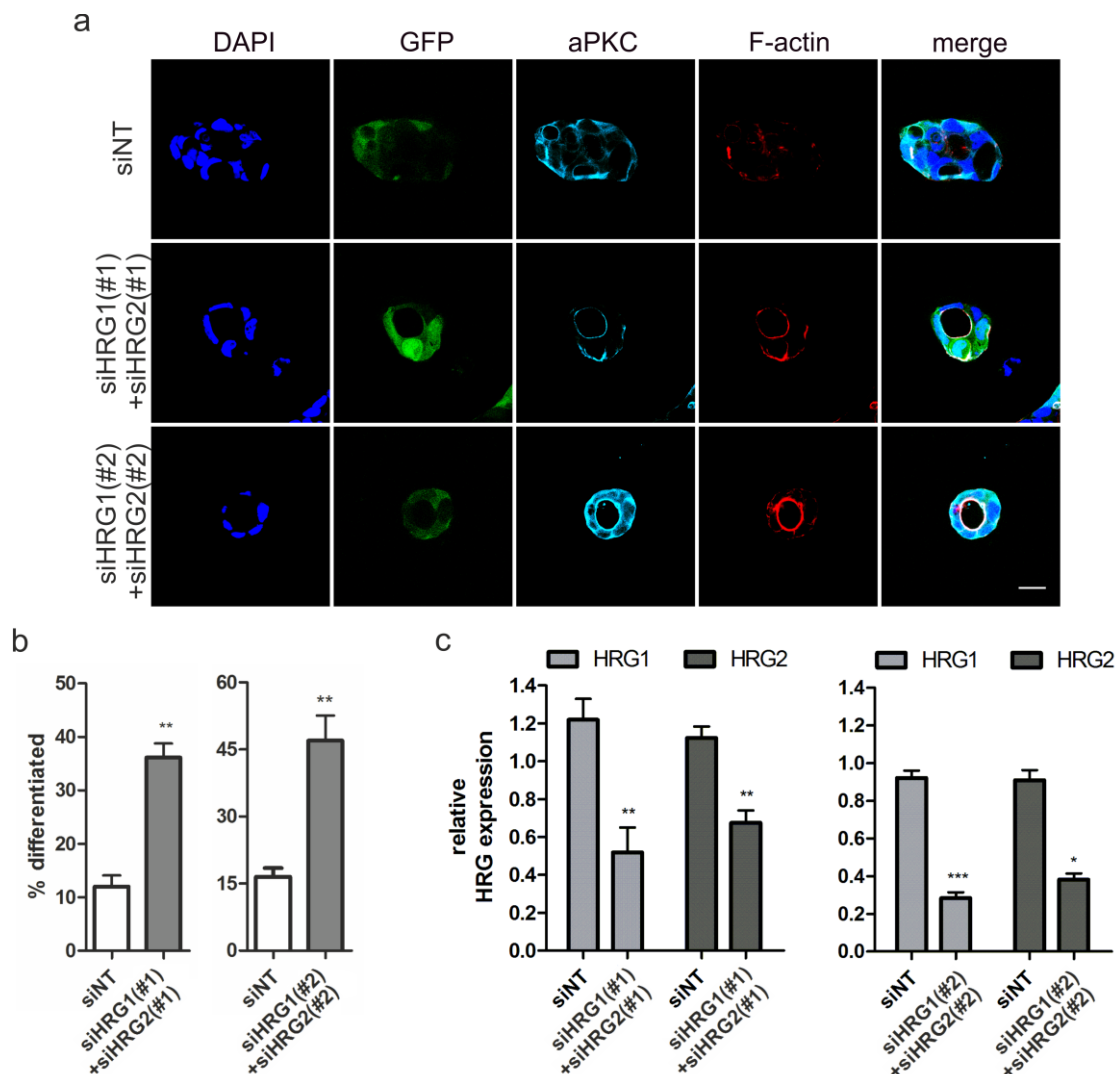


Figure III-11: HRG depletion restores lumen formation in oncogenic K-Ras^{G12V} expressing Caco-2 cells. (a) Caco-2tet K-Ras^{G12V} cells were transfected with non-targeting (siNT) and a mix of HRG1- and HRG2-specific siRNAs, respectively. Two independent siRNA sets were used (#1 and #2). The next day cells were seeded into 3D and K-Ras^{G12V} expression was induced with dox one day later. Two days later CTX was added. Cultures were fixed the next day and stained with DAPI (nuclei; blue), anti-aPKC antibody (cyan) and phalloidin (F-actin; red). GFP is co-expressed with K-Ras^{G12V} (green). Shown are confocal sections of the midplane of representative cysts (scale: 20 μ m). (b) The percentage of differentiated cysts of (a) was determined (n>70; N=3). (c) Two days after gene silencing (independent siRNA sets #1 and #2) RNA of the transfected cells was extracted. HRG levels were determined by qPCR, normalized to GAPDH (N=3).

Together with the increased ErbB3 positivity, detected in human high-grade primary CRC specimens [112], my findings provide support for an autocrine signaling loop engaged by oncogenic K-Ras involving ErbB3 that contributes to the dedifferentiation of the intestinal epithelium during tumor initiation and progression.

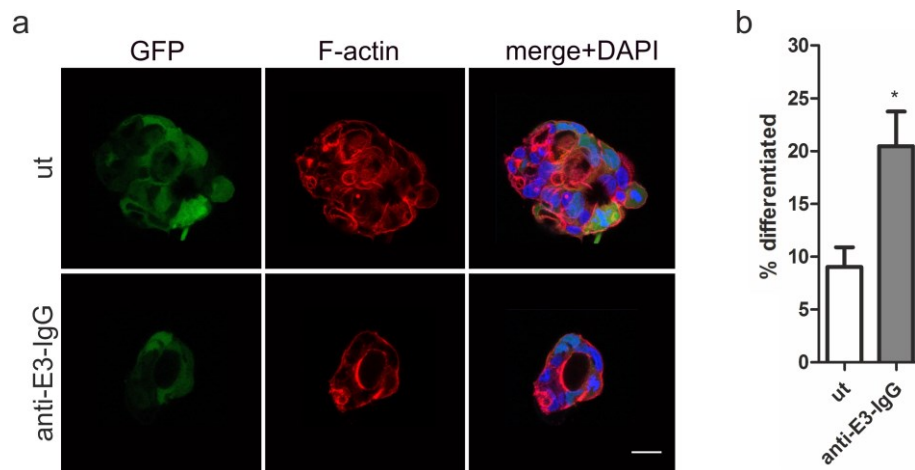


Figure III-12: ErbB3 specific inhibition by an antibody overcomes Ras^{G12V} induced polarization defects. (a) Cells were seeded into 3D culture in the presence of dox and were treated with 100 nM anti-E3-IgG or left untreated (ut). Three days later CTX was added. Cultures were fixed the next day and stained with DAPI (nuclei; blue), anti-aPKC antibody (cyan) and phalloidin (F-actin; red). GFP is coexpressed with K-Ras^{G12V} (green). Shown are confocal sections of the midplane of representative cysts (scale: 20 μ m). (b) The percentage of differentiated cysts of (a) was determined (n>70; N=3). [experiment (a) performed by L. Schmitt and J. Hendrick [112]]

2. ONCOGENIC RAS AND ERBB1-TARGETED TRAIL - OVERCOMING APOPTOSIS RESITANCE BY A SMAC MIMETIC -

Targeting of ErbB1 has become standard therapy in advanced CRC. Cetuximab, a monoclonal antibody against the extracellular domain of the ErbB1 receptor, interferes with ligand binding and thus activation of the receptor [117]. Retrospective analysis showed that ErbB1 targeting antibodies are only efficient in K-Ras wild-type tumors. Thus, the use of cetuximab was limited to K-Ras wild-type, ErbB1-expressing metastatic CRC in the year 2012 by the FDA. This restricts the application of the antibody dramatically, because one third of CRC patients harbor an activating mutation of Ras [75]. However, Ras/Raf mutated tumors often express high levels of ErbB1 and so the receptor could be used for the targeting of cytotoxic agents that for example induce apoptosis, independently of the mutational status of downstream signaling molecules. Here a single-chain TRAIL molecule, fused to a diabody that contains the antigen-binding domains of cetuximab, was used to target the apoptosis inducing moiety to ErbB1-positive cells (Db-scTRAIL, see Fig. I-9). This format previously showed efficient induction of apoptosis due to its hexameric configuration [66]. Furthermore Db-scTRAIL competes with ErbB1 ligand binding and receptor activation. To analyze the contribution of ErbB1 targeting to the Db-scTRAIL-induced apoptosis in the setting of Ras wild-type and Ras mutant CRC cells I applied the Caco-2tet K-Ras^{G12V} model system. The parental cell line Caco-2 is ErbB1-positive and therefore represents an ideal model system for studying the combined effect of ErbB1 inhibition and apoptosis induction in the context of oncogenic Ras. In addition to the effects induced by Ras^{G12V} expression, the contribution of cell culture conditions and ECM interaction to Db-scTRAIL sensitivity was investigated in the following part of my thesis.

Cetuximab efficiently blocks ligand induced ErbB1 activation

As shown in the previous experiments the different ErbB ligands differ in their capacity to drive the proliferation of Caco-2 cells (Fig. III-6). Firstly the presence of the most potent ErbB1 ligands, EGF and TGF- α and how these ligands affected ErbB1 inhibition by

cetuximab was investigated. Cells were seeded in matrigel cultures containing low serum (2%) in the presence of EGF or TGF- α , ensuring that proliferation was mainly driven via ErbB1 signaling. MTT activity measurements after six days of cultivation indicated that EGF and TGF- α enhanced the proliferation of Caco-2 cells compared with control cells grown in low serum only (Fig. III-13a). Microscopic analysis revealed that in the presence of EGF and TGF- α Caco-2 cysts were larger and contained more cells (Fig. III-13b). In agreement with the previous results, the ErbB1 ligands did not interfere with polarized morphogenesis, as judged by the typical apical distribution of F-actin and the formation of a cell-free lumen (Fig. III-13b and III-6c).

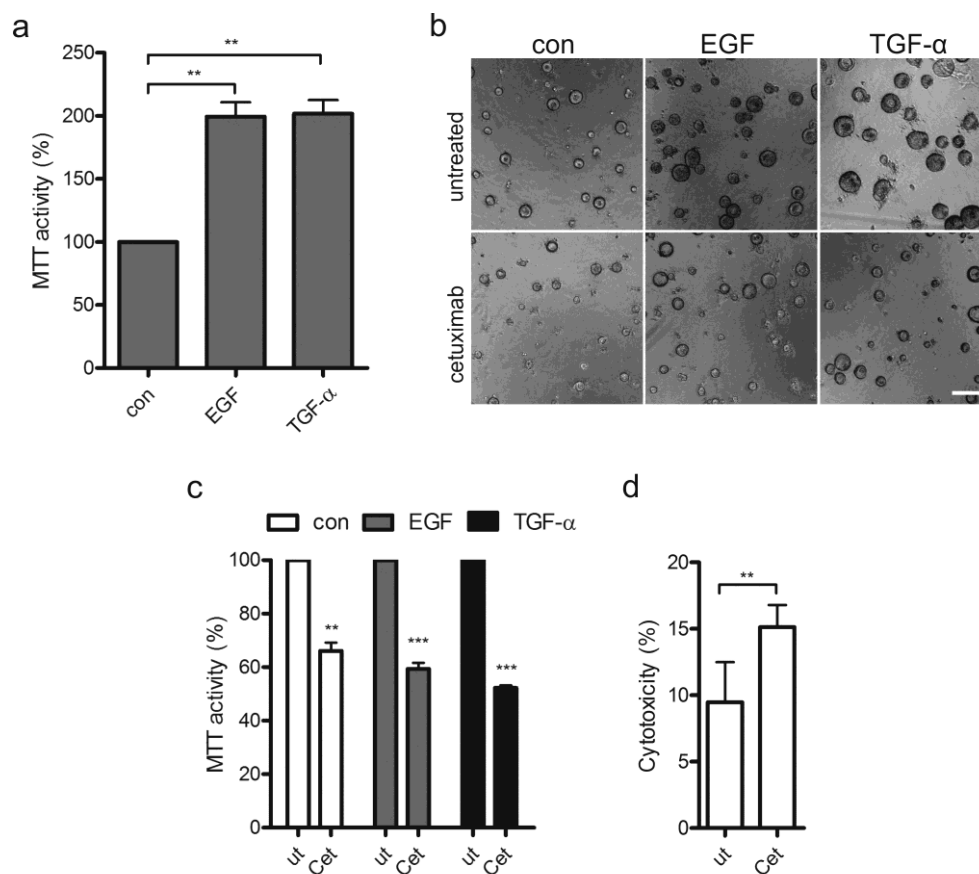


Figure III-13: Caco-2 3D cultures are sensitive to pharmacological ErbB1 inhibition. Caco-2 cells were grown in 3D culture containing 2% FCS in the presence of growth factors (10 ng/ml) or in 2% FCS only (con). (a) Cultures were analyzed by MTT assay at day 6 and normalized to the control (N=5). (b) Caco-2 3D cultures were left untreated or treated with 0.5 μ M cetuximab for 72 h and analyzed by phase microscopy (scale: 50 μ m). (c,d) Three days post seeding, 3D cultures were left untreated or treated with 0.5 μ M cetuximab (cet) for 72 h. (c) Viability was determined by MTT assay and normalized to the untreated control (ut) (N=4). (d) Cytotoxicity was determined using the CytoTox-Glo Cytotoxicity Assay (N=3).

To address how ErbB1 blockade affected basal and ErbB1 ligand-induced proliferation of established Caco-2 cysts the cells were treated three days after seeding with cetuximab (0.5 μ M) and analyzed three days later. Compared with the control, in these cultures the MTT activity was significantly reduced by 35-50%, but cells were still viable, did not show any signs of apoptosis and only negligibly increased cytotoxicity (Fig. III-13c,d).

This indicates that ErbB1 activation contributes to basal proliferation, but is not required for survival. Cetuximab also potently inhibited proliferation in the presence of EGF and TGF- α as seen by the reduction of MTT activity and the reduced size of the cysts (Fig. III-13b,c). Together these experiments demonstrate that proliferation of Caco-2 cells in 3D cultures is sensitive to pharmacological ErbB1 inhibition and can thus potentially be suppressed by targeted compounds as Db-scTRAIL.

3D culturing renders Caco-2 cells sensitive to Db-scTRAIL induced apoptosis

To first test the efficacy of the targeting agent Db-scTRAIL, Caco-2 cells were cultured for three days in 3D in medium containing 10% FCS before addition of Db-scTRAIL followed by MTT measurements three days later. In these cultures, relatively low doses of Db-scTRAIL caused a significant reduction of cell viability which was associated with the disruption of cysts and the formation of apoptotic bodies (Fig. III-14a,b) and induction of apoptosis (Fig. III-15a).

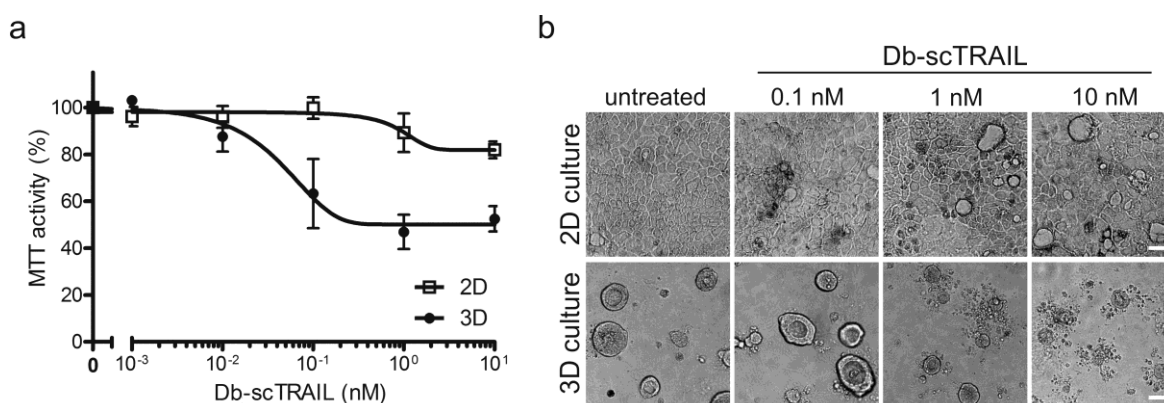


Figure III-14: Caco-2 3D cultures are sensitive to Db-scTRAIL. Cells were grown in 3D or 2D in medium containing 10% FCS. (a) Three days post seeding, cultures were treated with Db-scTRAIL. Viability was measured 72 h later by MTT assay and normalized to the untreated control (N=3). (b) Phase contrast images of the 3D and 2D cultures described in (a) treated with the indicated concentrations of Db-scTRAIL for 72 h (scale: 50 μ m).

Interestingly, in conventional 2D cell cultures on plastic, Caco-2 cells were highly resistant to Db-scTRAIL treatment (Fig. III-14a,b), in line with a previous report using recombinant human TRAIL [118].

Pretreatment of the Caco-2 3D cultures with Z-VAD, a pan-caspase inhibitor, significantly reduced the cytotoxic effect of Db-scTRAIL (Fig. III-15b). The induction of apoptosis by Db-scTRAIL was confirmed by the analysis of DNA fragmentation by TUNEL staining (Fig. III-15c,d). Compared with 2D cultures, the dose-dependent activation of caspase 3/7 in response to Db-scTRAIL was significantly increased in 3D cultures (Fig. III-15a).

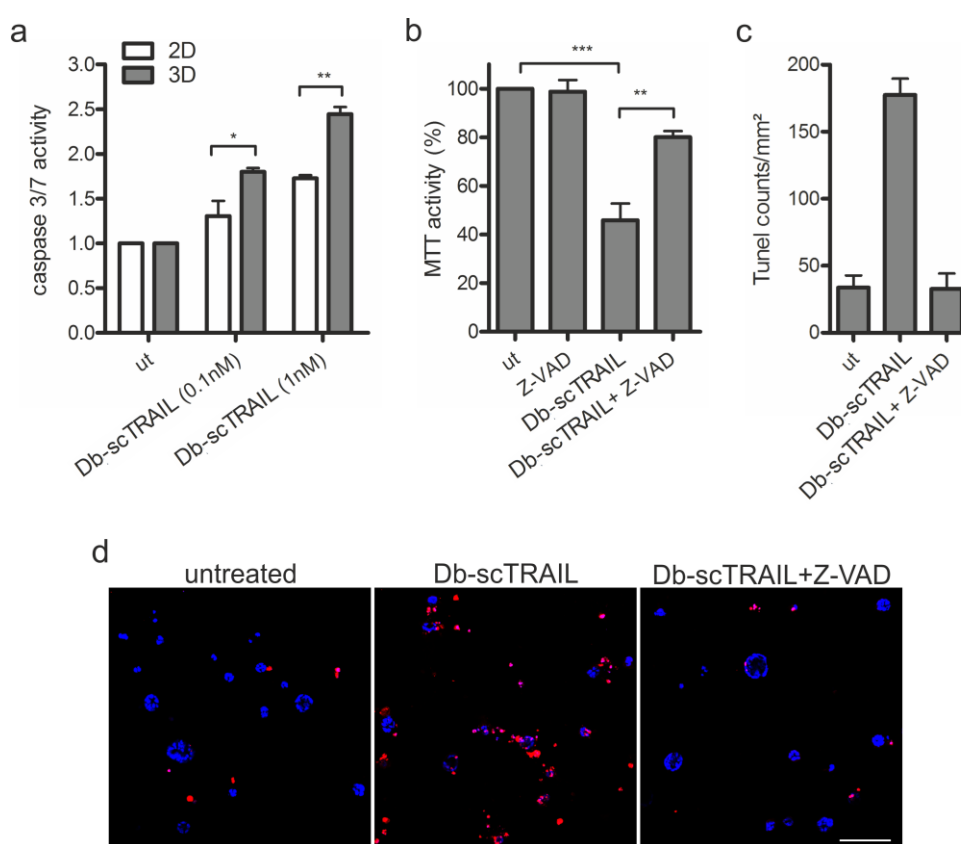


Figure III-15: Db-scTRAIL induces apoptosis in Caco-2 3D culture. Cells were grown in 3D or 2D in medium containing 10% FCS. (a) Three days post seeding, cultures were treated with 0.1 nM or 1 nM Db-scTRAIL for 24 h. Caspase 3/7 activity was measured and normalized to the respective untreated control (ut) (N=3). (b) Three days post seeding, 3D cultures were pretreated with 20 μ M Z-VAD as indicated before addition of 1 nM Db-scTRAIL. Viability was measured 72 h later by MTT assay and normalized to the untreated control (ut) (N=3). (c) 24 h after treatment cells were fixed and stained for DNA strand breaks. TUNEL-positive cells were counted (N=2). (d) Representative pictures of the TUNEL stainings described in (c), TUNEL-positive cells (red), DAPI (nuclei; blue). Shown are confocal sections (scale: 100 μ m).

This difference in sensitivity toward Db-scTRAIL in 3D versus 2D cultures could not be attributed to changes in ErbB1 or TRAILR1/2 expression (Fig. III-16). Unfortunately, because the decoy receptors DcR1/DcR2 could not be detected by immunoblotting with the antibodies available, expression changes in these receptors could not be ruled out. Analysis of key signaling pathways revealed that, in 3D cultures, the activity of the PI3K pathway was suppressed compared with cells grown in 2D as measured by phospho-AKT levels whereas the ERK/MAPK pathway was upregulated as seen by increased ERK1/2 phosphorylation (Fig. III-16). Additionally reduced expression levels of the anti-apoptotic protein cIAP2 were observable in Caco-2 cells grown in 3D cultures (Fig. III-16).

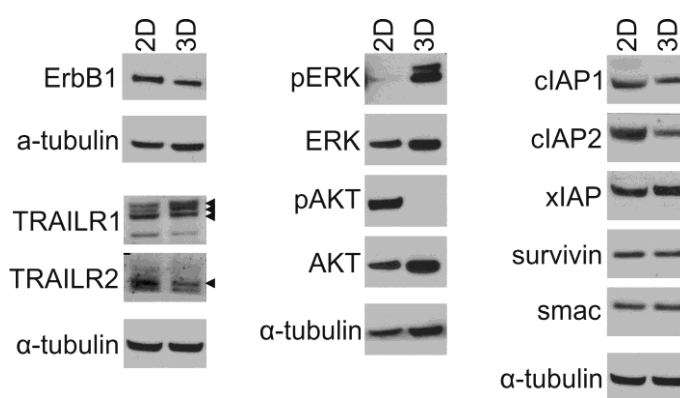


Figure III-16: 3D culturing alters pro- and anti-apoptotic protein expression. Caco-2 cells were grown in 3D or 2D in medium containing 10% FCS. Four days post seeding, lysates were generated and analyzed by immunoblotting. Shown is one representative blot of three independent experiments. Tubulin was detected as a loading control. Specific bands are marked by arrowheads.

However, inhibition of PI3K by LY294002 in 2D cultures was not sufficient to sensitize cells to Db-scTRAIL (data not shown), indicating a more complex scenario in 3D cultures. Together, these results underscore the impact of the culture conditions on the cellular response toward apoptosis-inducing agents.

Db-scTRAIL activity is not limited by ErbB1 ligands

ErbB1 activation not only stimulates cell proliferation but can also protect from TRAIL-induced apoptosis [119]. Therefore, the efficacy of Db-scTRAIL was explored in the presence of ErbB1 ligands. Immunoblotting of lysates of EGF- and TGF- α -stimulated cells revealed a similar degree of suppression of ligand-induced ErbB1 phosphorylation by either cetuximab or Db-scTRAIL pretreatment (Fig. III-17a,c), indicating the efficient

competition of the diabody moiety with the ErbB1 ligands. This could also be confirmed in 3D cultured Caco-2 cells stimulated with EGF (Fig. III-17b,d). Accordingly, EGF and TGF- α had no protective effect on viability in 3D (Fig. III-17e) nor were these ligands able to interfere with caspase activation (Fig. III-17f), demonstrating that Db-scTRAIL activity is not limited by the presence of ErbB1 ligands.

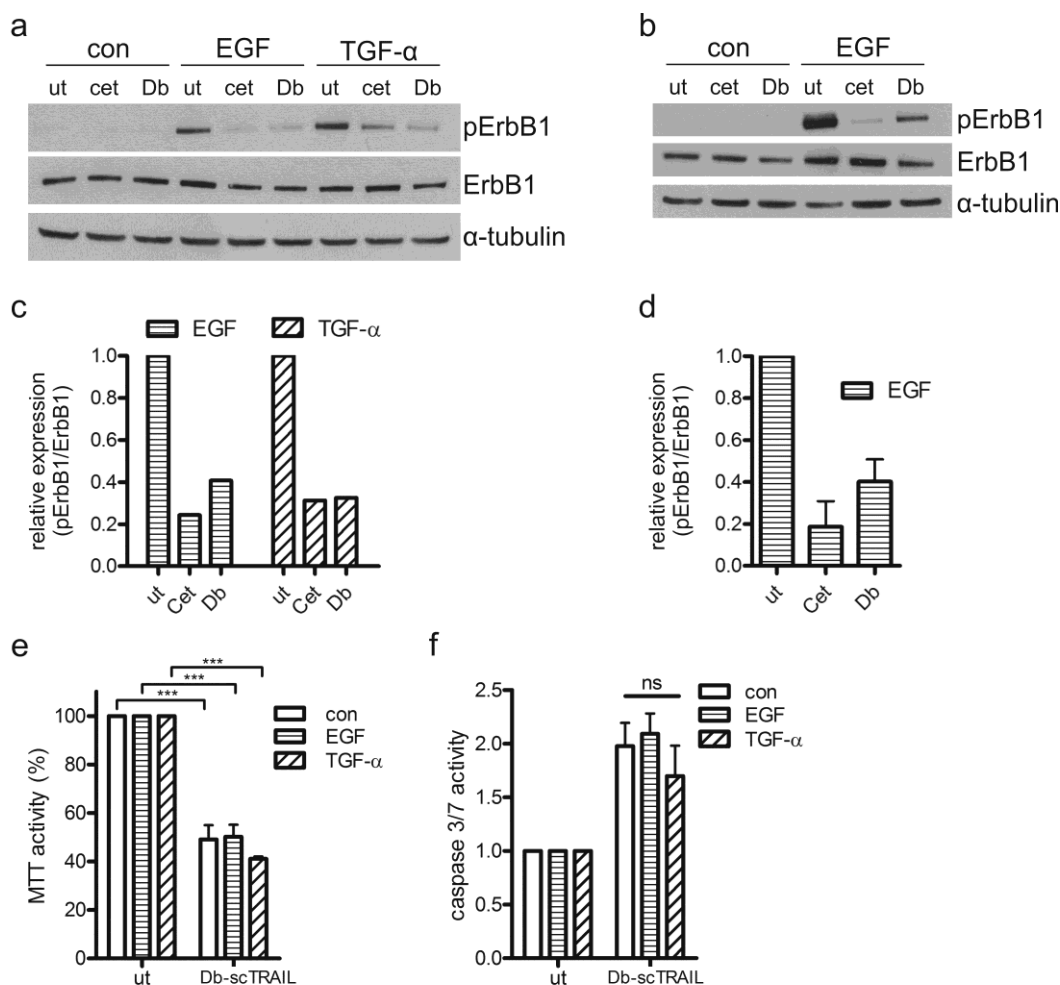


Figure III-17: ErbB1 activation does not impair Db-scTRAIL activity. (a) Caco-2 cells grown in 2D were left untreated or treated with 4 nM Db-scTRAIL or 4 nM cetuximab for 15 min prior to stimulation with EGF or TGF- α (10 ng/ml) for 10 min. Phosphorylated and total proteins were detected by immunoblotting. Shown is one representative blot (N=3). Tubulin was detected as a loading control. (b) Immunoblotting of Caco-2 cells grown in 3D treated as in (a), shown is one representative blot (N=2). (c) Quantification of Western blots from (a). Phospho-ErbB1 levels were normalized to the corresponding total protein levels; levels in the untreated control were set as 1 (N=3). (d) Quantification of Western blots from (b) (N=2). (e,f) Three days post seeding, Caco-2 3D cultures grown in the absence or presence of growth factors were treated with 1 nM Db-scTRAIL. (e) Viability was determined by MTT assay after 72 h and normalized to the respective untreated control (ut). (N=3) (f) Caspase 3/7 activity was measured after 24 h. Values were normalized to the corresponding untreated control (ut) (N=3).

Importantly scTRAIL alone or in combination with cetuximab failed to elicit a cytotoxic response in Caco-2 3D cultures at all (Fig. III-18), supporting the previous data that the diabody-mediated dimeric structure of Db-scTRAIL confers superior bioactivity over scTRAIL [66].

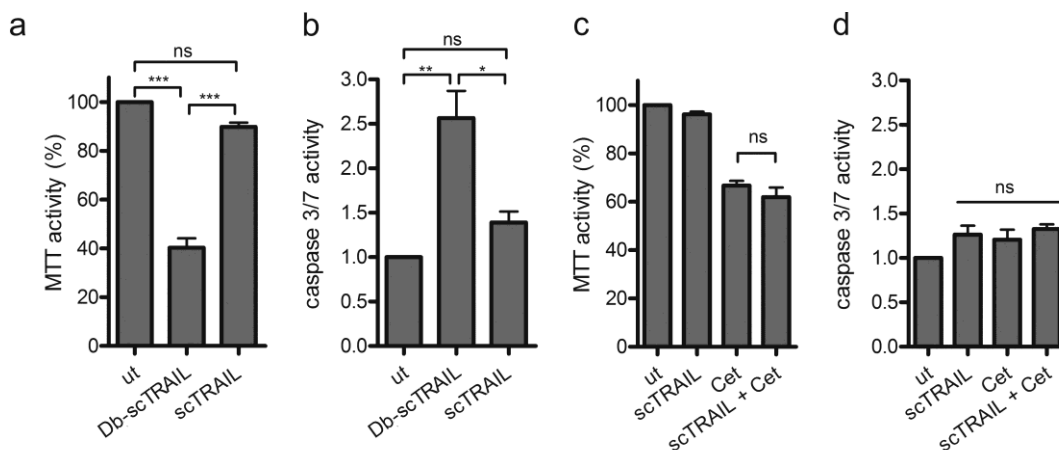


Figure III-18: Db-scTRAIL bioactivity is superior to scTRAIL plus cetuximab. Caco-2 cells were grown in 3D cultures in medium containing 10% FCS. (a,b) Three days post seeding, cultures were left untreated (ut) or treated with 1 nM Db-scTRAIL or 1 nM scTRAIL. (a) Cell viability was determined by MTT assay after 72 h and normalized to the untreated control (ut) (N=3). (b) Caspase 3/7 activity was measured after 24 h. The values shown were normalized to the untreated control (ut) (N=3). (c,d) Three days post seeding, cultures were left untreated (ut) or treated with 1 nM scTRAIL, 1 nM cetuximab or the combination of both. (c) Cell viability was determined by MTT assay after 72 h and normalized to the untreated control (ut) (N=3). (d) Caspase 3/7 activity was measured after 24 h. The values shown were normalized to the untreated control (ut) (N=3).

To understand in more detail the resistance mechanisms toward Db-scTRAIL, re-isolated cysts from untreated and Db-scTRAIL-treated 3D matrigel cultures were analyzed by immunoblotting of cell lysates (Fig. III-19).

Interestingly, lysates derived from surviving cysts (Fig. III-19a, arrows) revealed that these Db-scTRAIL-insensitive cells contained especially low ErbB1 levels. Of note, TRAIL receptor levels in these cells were similar to those in untreated cells, suggesting that the distribution of ErbB1 expression in the cell population strongly impacts Db-scTRAIL sensitivity (Fig. III-19b,c).

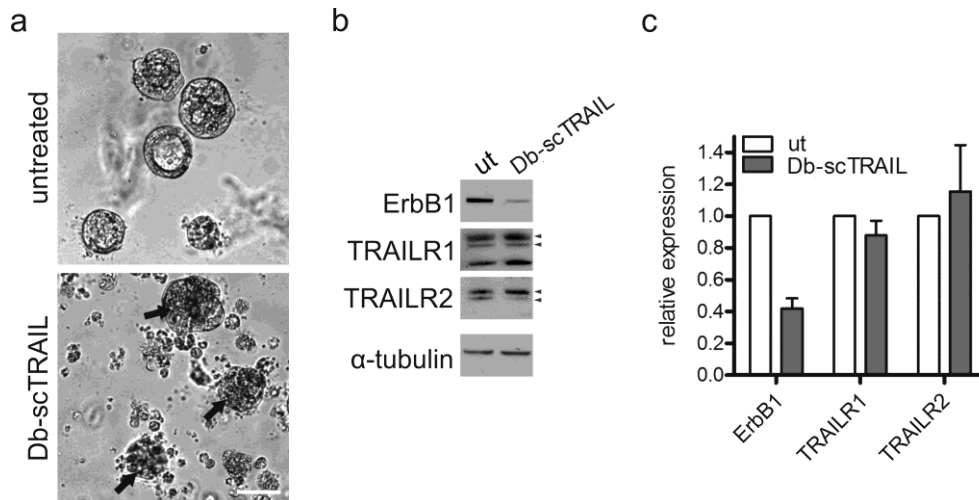


Figure III-19: ErbB1-directed targeting determines the bioactivity of Db-scTRAIL. (a) Three days post seeding Caco-2 3D cultures were either left untreated or treated with 5 nM Db-scTRAIL for 72 h. Surviving cysts in the phase contrast images are indicated by arrows (scale: 50 μ m). (b) Lysates derived from the 3D cultures shown in (a) were analyzed by immunoblotting. Shown is one representative blot of three independent experiments. Tubulin was detected as a loading control. Specific bands are marked by arrowheads. (c) Quantification of Western blots from (b). Protein levels were normalized to the corresponding tubulin control; levels in the untreated cultures were set as 1 (N=3).

K-Ras^{G12V} expression induces Db-scTRAIL resistance in Caco-2 spheroids

As mutated Ras renders cells insensitive to ErbB1 inhibition [70] and could impact TRAIL-sensitivity [83], the effects of K-Ras^{G12V} expression on Db-scTRAIL induced cytotoxicity were determined. Therefore, 3D cultures of Caco-2tet K-Ras^{G12V} were treated with doxycycline for three days. Compared with the control cells, viability measurements revealed decreased sensitivity of oncogenic Ras expressing cells to Db-scTRAIL (Fig. III-20a). To confirm that this partial resistance was due to reduced apoptosis, TUNEL stainings were performed and caspase 3/7 activation measured. Indeed, K-Ras^{G12V} cells showed strongly reduced DNA fragmentation after treatment with 1 nM Db-scTRAIL (Fig. III-20b) and only a weak induction of caspase activity (Fig. III-20c).

This resistance was not due to ErbB1 or TRAILR1/2 downregulation (Fig. III-21). In fact, immunoblotting of 3D cell lysates of the vector and K-Ras^{G12V} cells revealed increased TRAILR2 protein levels (Fig. III-21a,b), in agreement with previous reports [83,84]. Oncogenic Ras can interfere with apoptosis at multiple levels, for example, by the activation of PI3K survival signaling pathway and changes in transcriptional programs

[81,82]. Indeed, in 2D cultures, increased AKT phosphorylation in K-Ras^{G12V} expressing cells was observable.

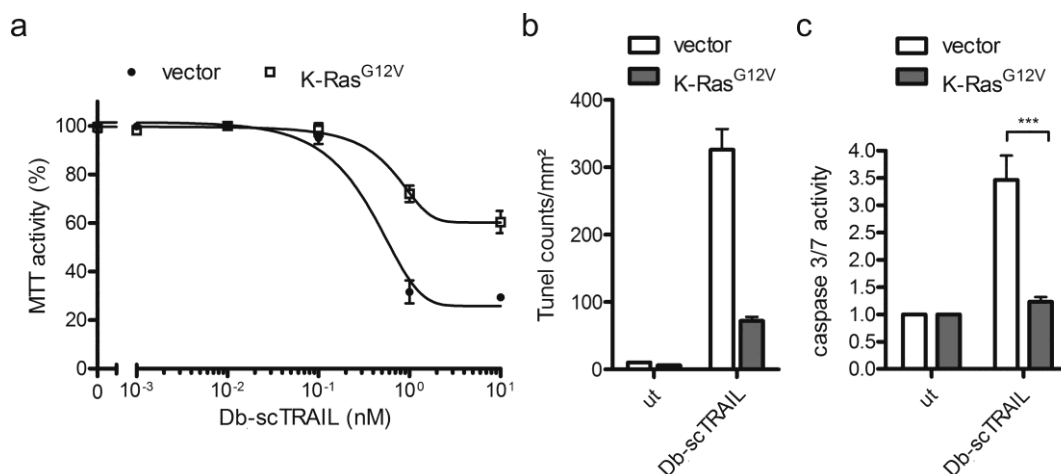


Figure III-20: Oncogenic K-Ras protects Caco-2tet cells from Db-scTRAIL induced apoptosis. (a-c) Caco-2tet vector control and K-Ras^{G12V} cells were seeded into 3D cultures in the presence of dox. Three days later, cultures were treated with Db-scTRAIL. (a) Viability was measured 72 h later by MTT assay and normalized to the untreated control (N=3). (b) 24 h after treatment with 1 nM Db-scTRAIL, cells were fixed and stained for DNA strand breaks. TUNEL-positive cells were counted (N=2). (c) Caspase 3/7 activity was measured after 24 h treatment with 1 nM Db-scTRAIL. Values shown were normalized to the corresponding untreated control (ut) (N=3).

In 3D cultures, however, the suppression of the PI3K/AKT pathway appears to be dominant (see Fig. III-16), with K-Ras^{G12V} expression leading to marginally elevated AKT phosphorylation only (data not shown). Interestingly, expression analysis of selected key regulators of the apoptotic machinery revealed significantly elevated levels of the anti-apoptotic proteins cIAP2, Flip_s, and Bcl-xL (Fig. III-21b).

The upregulation of the anti-apoptotic protein cIAP2 was specific for the K-Ras mutation and could not be detected by active B-Raf^{V600E} mutation, providing evidence for an independent mechanism (Fig. III-21c).

A smac mimetic sensitizes K-Ras mutated CRC cells to Db-scTRAIL treatment

Because molecular changes occurred at different levels of the apoptotic pathway, blocking of K-Ras^{G12V} induced anti-apoptotic signaling as far downstream as possible seemed promising. Inhibitors of apoptosis (IAP) proteins, such as cIAP2, interfere with apoptosis by the direct binding, inhibition and/or degradation of caspases and components of the Ripoptosome, and by antagonizing non-canonical NFκB signaling [120]. The activity of IAP

proteins is balanced by Smac/Diablo, a protein released from mitochondria in cells primed for apoptosis. Peptides that mimic the aminoterminal IAP-binding sequence of Smac, so-called Smac mimetics, were found to enhance the cytotoxicity of chemotherapeutic agents and death ligands such as TRAIL [121,122].

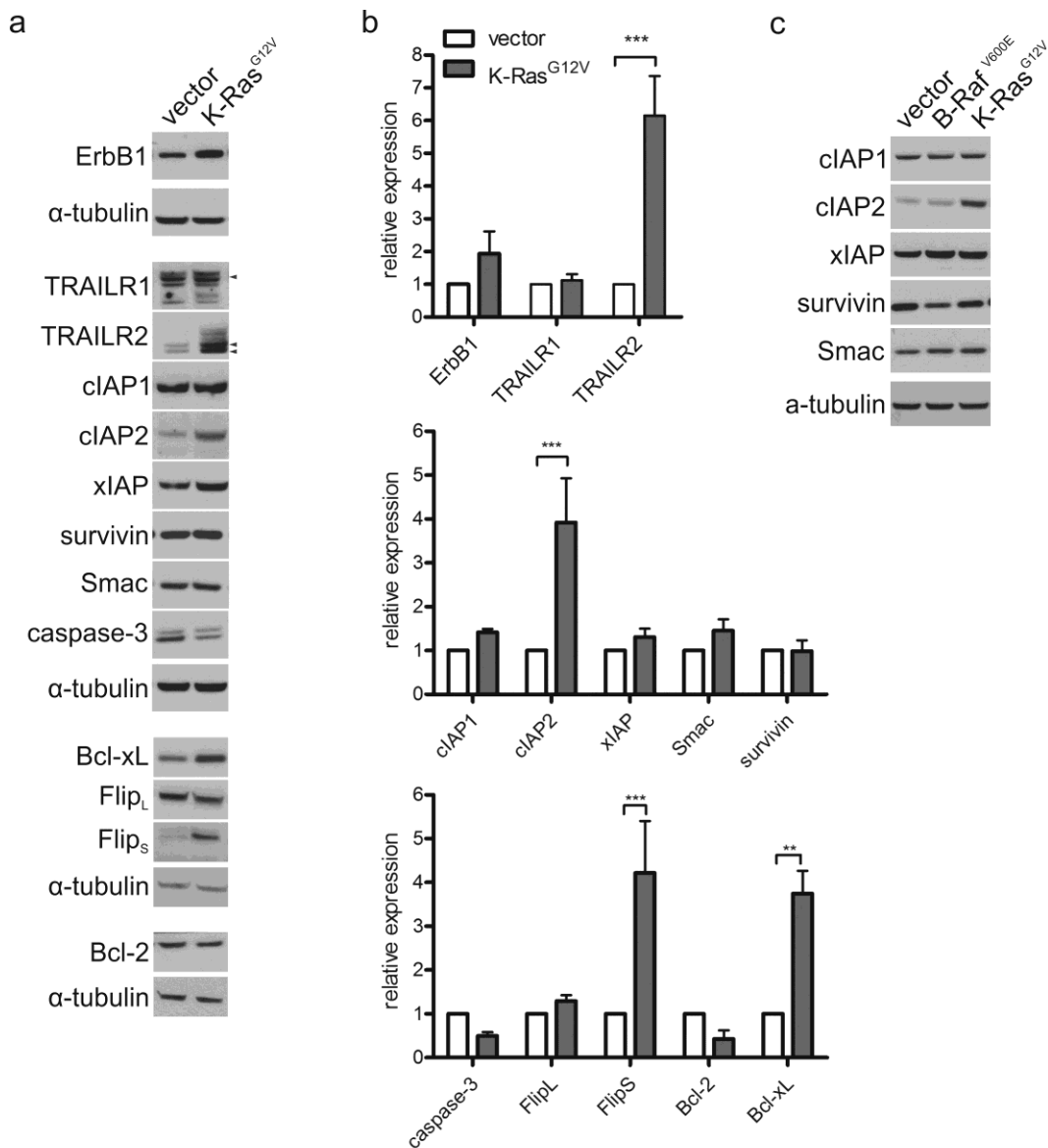


Figure III-21: Oncogenic K-Ras changes the pro- and anti-apoptotic protein balance. (a) Caco-2tet vector control and K-Ras^{G12V} cells were grown in 3D cultures in the presence of dox for 4 days. Cells were recovered from the 3D cultures and lysates were analyzed by immunoblotting. Shown is one representative blot of three independent experiments. Tubulin was detected as a loading control. Specific bands are marked by arrowheads. (b) Quantification of Western blots from (a). Protein levels were normalized to the corresponding tubulin control; levels in the vector control were set as 1 (N=3). (c) Immunoblotting of Caco-2tet vector control, B-Raf^{V600E} and K-Ras^{G12V} cells as described in (a). Shown is one representative blot of two independent experiments.

Indeed, co-treatment of Caco-2tet K-Ras^{G12V} cells with Db-scTRAIL and a previously developed highly efficient dimeric Smac mimetic, SM83 [115,116], decreased cell viability by 35% compared with the single treatments. This was efficiently blocked by Z-VAD, proving the involvement of caspase activation in the case of the combinatorial treatment (Fig. III-22a). TUNEL staining further confirmed the enhancement of apoptosis by SM83 (Fig. III-22b).

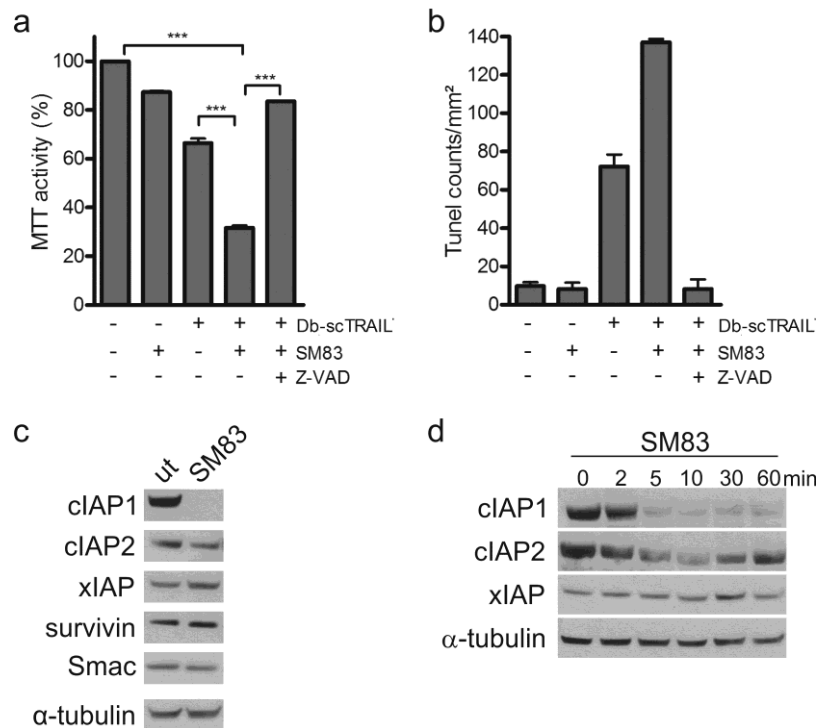


Figure III-22: The Smac mimetic SM83 overcomes the K-Ras^{G12V} induced Db-scTRAIL resistance. (a-c) Caco-2tet Ras^{G12V} cells were seeded into 3D cultures in the presence of dox. (a) Three days later, cultures were left untreated or treated with 5 μM SM83 or 20 μM Z-VAD for 1 h prior to addition of 1 nM Db-scTRAIL. Viability was measured 24 h later by MTT assay and normalized to the untreated control (N=3). (b) 24 h after treatment, cells were fixed and stained for DNA strand breaks. TUNEL-positive cells were counted (N=2). (c) Three days post seeding, cultures were left untreated (ut) or treated with 5 μM SM83. Cells were recovered from the cultures 24 h later and lysates were analyzed by immunoblotting. Shown is one representative blot of two independent experiments. Tubulin was detected as a loading control. (d) Caco-2tet Ras^{G12V} cells grown in 2D for 72 h in the presence of dox followed by treatment with 5 μM SM83 for the indicated time points prior to lysis. Proteins were analyzed by immunoblotting using the indicated antibodies. Tubulin was detected as a loading control.

Of note, the presence of SM83 also lowered the Db-scTRAIL concentration required to kill parental Caco-2 and Caco-2tet vector cells (data not shown). Analysis of cell lysates derived from Caco-2 3D cultures showed that SM83 incubation for 24 h led to the

complete loss of cIAP1, whereas cIAP2 levels were only slightly decreased and XIAP, survivin and Smac were not affected (Fig. III-22c). The presence of cIAP2 at this time point can be explained by its upregulation in response to cIAP1 loss in accordance with a previous report [123]. Indeed cIAP2 protein levels were initially downregulated, but come back to normal levels after 60 min of SM83 treatment (Fig. III-22d). Nevertheless, by regulating the overall IAP/Smac balance, SM83 appears to restore the apoptotic response in oncogenic Ras expressing Caco-2 cells.

Finally, to investigate whether our targeted combinatorial strategy could be transferred to CRC cell lines with endogenous K-Ras mutations, co-treatment of HCT-116 and LoVo cells with Db-scTRAIL and SM83 in 3D cultures was performed. These cell lines are ErbB1-positive (data not shown) and show moderate sensitivity to Db-scTRAIL, making them amenable to the combined action of Db-scTRAIL and Smac mimetics.

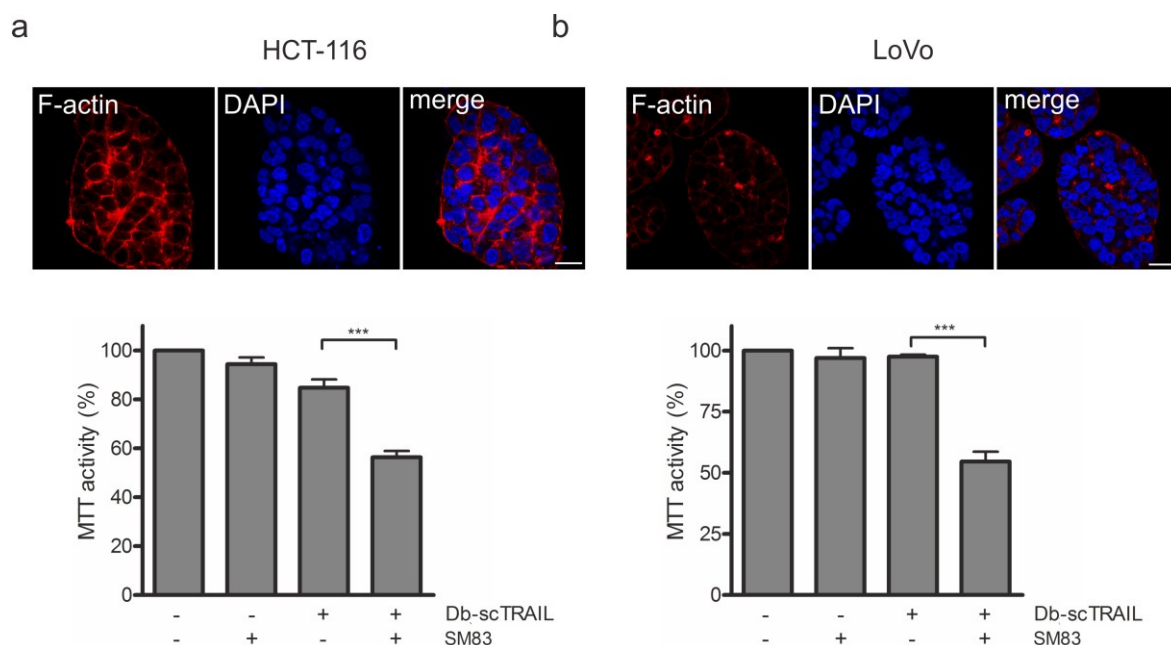


Figure III-23: The Smac mimetic SM83 sensitizes oncogenic K-Ras expressing CRC cells to Db-scTRAIL treatment. (a) HCT-116 and (b) LoVo cells were grown in 3D cultures for six days, and then fixed and stained for F-actin (red) and DNA (DAPI; blue) (scale: 20 μ m) (top panels). Three days post seeding cultures were left untreated or pretreated with 5 μ M SM83 prior to addition of 0.05 nM Db-scTRAIL. Viability was measured 24 h later by MTT assay and normalized to the untreated control (bottom panels) (N=3).

Reminiscent of the Caco-2tet K-Ras^{G12V} cells, HCT-116 and LoVo cells failed to form differentiated and polarized spheroids in 3D culture (Fig. III-23a,b; upper panel). Importantly, a synergistic cytotoxic effect of Db-scTRAIL and SM83 was observed for both cell lines when Db-scTRAIL was applied at a sublethal concentration (Fig. III-23a,b; lower panel). Thus, based on these data I propose that ErbB1-targeted scTRAIL molecules, together with apoptosis-sensitizing agents, may be an effective therapy for CRC independently of the K-Ras status.

In sum, using a 3D CRC cell culture model, in this thesis it was shown for the first time that K-Ras^{G12V} induced hyperproliferation, loss of polarized morphogenesis and escape from apoptosis, which are hallmarks of cancer cells, involve an ErbB3-dependent autocrine signaling loop on the one hand and the upregulation of anti-apoptotic proteins such as cIAPs on the other hand. Provided that the activation of these signaling pathways can also be observed in additional Ras-mutant CRC cell lines and in primary human CRC, these findings have important implications for the design of novel targeted treatment strategies of K-Ras mutant CRC.

IV. DISCUSSION

In this thesis, studies were performed in a matrix-dependent 3D model system of Caco-2 cells because this model mimics important features of polarized epithelial organization that are not recapitulated in conventional 2D cell cultures. In addition, the tetOn system allowed the investigation of the immediate effect of K-Ras^{G12V} expression in the Caco-2 model on cell proliferation and polarization. In the development of CRC, Ras mutations are preceded by mutations in APC associated with the activation of the WNT pathway and the formation of benign polyps [12]. Considering the frequent co-occurrence of APC and K-Ras mutations, Caco-2 cells are a suitable model for the analysis of the early molecular and cellular changes induced by Ras activation, as these cells harbor an inactivating mutation in APC, but they lack oncogenic alterations within the MAPK and PI3K pathway [88].

Because of the limitations in treatment of K-Ras mutated CRC patients with available blocking antibodies alone and the inevitable evolution of resistance during anti-proliferative treatment, induction of apoptosis in tumor cells via TRAIL seems to be an alternative strategy in treating CRC. Due to its selectivity for tumor cells, TRAIL is regarded as a promising anti-cancer therapeutic. Apoptosis induction by TRAIL moreover does not depend on p53, the frequent loss or mutation of which is a major cause of chemotherapy resistance. Despite these advantageous features of TRAIL, the molecular mechanisms that govern TRAIL sensitivity versus resistance still remain poorly understood. There is neither a clear correlation between total TRAILR1/2 levels nor the ratio of TRAILR1/2 and the decoy receptors DcR1, DcR2 and TRAIL sensitivity [124,125]; instead, activation of PI3K/AKT and NFκB signaling pathways, and the overexpression of anti-apoptotic proteins such as Bcl-2, IAPs and Flip have been implicated in TRAIL resistance [62,64,126].

A better understanding of tumor development and progression as well as of resistance mechanisms and the identification of effective drug combinations are thus essential for

the right choice of target patients and an optimized personalized treatment design. Therefore I explored the effect of oncogenic K-Ras on initial steps of tumor development like hyperproliferation and polarization defects and furthermore investigated potential mechanisms of action of a targeted single-chain TRAIL molecule (Db-scTRAIL) comprising an ErbB1 blocking and targeting moiety derived from cetuximab and three TRAIL monomers in the 3D model of CRC.

Impact of culture conditions on cell signaling

The comparison of Caco-2 cells grown in 2D versus 3D culture revealed that the cellular environment not only affected morphology but also profoundly altered important signaling pathways, and therefore the balance between proliferation, survival and death. The most apparent changes in these hallmarks of cancer included the expression and/or activation levels in AKT, ERK and cIAP2. In 3D cultures, Caco-2 cells displayed dramatically increased sensitivity to Db-scTRAIL-induced apoptosis, whereas 2D cultured Caco-2 cells were highly resistant against Db-scTRAIL (Fig. III-14). The increased apoptotic potency in 3D of this targeted TRAIL molecule can neither be explained by elevated levels of the target itself nor by elevated death receptor expression as no changes in ErbB1 or TRAIL1/2 receptor levels were observable in 3D compared to 2D cultured Caco-2 cells. Another mechanism that could enhance targeting efficiency and/or the signaling capacity of the death receptors could be clustering of the receptors. The basolateral localization of ErbB1 and the TRAIL receptors may create a more densely packed signaling platform that facilitates accumulation of Db-scTRAIL and therefore death receptor oligomerization and activation [47,127]. The subcellular localization of the ErbB receptors can play an important role as well. The regulation of ErbB2 signaling in polarized epithelia by relocation of the receptor to the apical surface after overexpression leads to changes in the signaling pattern towards survival via a Bcl-2 related pathway [128]. As all ErbB receptors are localized to the basolateral membrane in normal, differentiated tissues [129], the effect of relocation could be important for the other ErbB receptors as well and could be responsible for the signaling changes in the MAPK and PI3K cascades observed here. Unfortunately the ErbB receptors could not be detected by immunofluorescence staining in the 3D cultures to address their precise localization.

Polarized growth of Caco-2 cells in the presence of extracellular matrix components also altered the activation states of intracellular signaling pathways. In particular, the suppression of the PI3K pathway in Caco-2 3D cultures is likely to contribute to the enhanced TRAIL sensitivity, as activation of this pathway correlates with TRAIL resistance in several tumor cell lines and PI3K inhibition rendered cells more sensitive toward TRAIL treatment [48,130,131]. In addition to the changes in the PI3K pathway the downregulation of the anti-apoptotic protein cIAP2 probably adds to the observed Db-scTRAIL sensitivity in the Caco-2 3D cell culture model.

Regardless of the precise mechanism, the impact of the cell culture set-up seems to be tremendous and has to be considered in the translation of in vitro drug testing to in vivo studies.

K-Ras^{G12V} induced TRAIL resistance

In Caco-2tet cells inducibly expressing K-Ras^{G12V}, oncogenic K-Ras not only interfered with proper polarization but it also protected from death receptor-induced apoptosis in the 3D cultures (Fig. III-20). In CRC, ligand-independent activation of the ERK/MAPK and PI3K pathways by mutant K-Ras is associated with the loss of responsiveness to cetuximab [70] and additionally enhances cell proliferation and favors survival by interfering with the apoptotic machinery. Specifically, K-RAS mutations at codon 12 could be correlated with reduced apoptosis in vitro and lower apoptotic indices in colorectal tumors [132]. By contrast, K-Ras has also been reported to promote apoptosis through the upregulation of TRAILR2 [82,83]. Intriguingly, in the used doxycycline-treated Caco-2tet K-Ras^{G12V} cells TRAILR2 was also found to be upregulated, however, this was not sufficient to trigger apoptosis. It appears that the additional molecular changes in the apoptotic pathway downstream of TRAIL receptors, such as the elevation of FlipS, Bcl-xL and cIAP2, ultimately favor cell survival.

Especially alterations in IAPs are found in many types of human cancer and associated with chemoresistance, disease progression and poor prognosis [120,133]. In intestinal epithelial cells, mutated Ras was shown to cause cIAP2 upregulation via a TGF- α autocrine loop [80]. This observation is consistent with the results obtained with the K-Ras^{G12V} expressing Caco-2 cells used here and further supports the potential benefit of blocking

autocrine ErbB1 signaling in combination with death receptor stimulation. cIAP proteins bind, but do not inhibit caspases 3 and 7, promoting their ubiquitination and degradation [127]. This explains the reduced caspase 3 levels observed in Caco-2tet Ras^{G12V} cells, although this downregulation was not significant. IAPs can be targeted and inhibited by Smac mimicking molecules. These Smac mimetics were originally developed to block xIAP, but they are most effective in triggering the auto-ubiquitination and degradation of cIAP1 and cIAP2. In the 3D Caco-2 model, strongly reduced cIAP1 levels were detected 24 hours after SM83 treatment, whereas cIAP2 was only transiently downregulated, in accordance with the finding that cIAP1 downregulation causes cIAP2 upregulation by non-canonical NFκB activation [127]. Nevertheless, the potent downregulation of cIAP1 by SM83 appears to be sufficient to tip the balance and restore an apoptotic response to Db-scTRAIL treatment in three different CRC cell lines. Smac mimetics have further been reported to induce cytotoxicity as single agents, a feature linked to the induction of TNF-α synthesis and secretion [134,135]. However, in Caco-2, HCT-116 and LoVo cells, there was no cytotoxicity in response to SM83 alone, suggesting that the increased susceptibility to death receptor-induced apoptosis primarily stems from TRAIL receptor signaling.

ErbB1 targeting in the context of K-Ras^{G12V}

The efficient reduction of basal and ErbB1 ligand-induced proliferation of Caco-2 cells in 3D cultures by Db-scTRAIL in addition to efficiently inducing apoptosis of ErbB1-positive cells irrespective of the presence of the ErbB1 ligands EGF or TGF-α clearly showed the biological activity of the anti-ErbB1 targeting moiety. Indeed, in an ErbB2 tumor mouse model the combined treatment with an ErbB2 blocking antibody and a TRAILR2 agonistic antibody had synergistic effects [136]. And as oncogenic K-Ras has also been associated with the increased expression and/or shedding of ErbB1 ligands such as TGF-α, amphiregulin and HB-EGF the blocking of ErbB1 in the presence of mutated K-Ras may be useful [29,30,86]. ErbB1 ligands further have been reported to protect epithelial cells from TRAIL-induced apoptosis, mainly via the activation of PI3K signaling [119,137]. Treatment of CRC cells with recombinant TRAIL was further reported to lead to ErbB1 upregulation and shedding of TGF-α, resulting in the activation of autocrine and paracrine ErbB1/HER2 pro-survival signaling [86]. Additionally, ErbB1 ligand shedding may also be induced by

oncogenic Ras signaling [86] that could lead to paracrine activation of the surrounding cells, not necessarily carrying an active K-Ras mutation and therefore responding to ErbB1 inhibition. These findings provide a rationale for combining pharmacological ErbB1 blockade with TRAIL receptor agonists for treatment of K-Ras mutated CRC, although cetuximab itself is not recommended for K-Ras mutated tumors.

A very important aspect uncovered by this study is the requirement for tumor cell-specific targeting of recombinant TRAIL to elicit a potent cytotoxic response. Intriguingly, cells surviving Db-scTRAIL treatment in the 3D cultures expressed very low ErbB1 levels. Although the diabody moiety does not actively contribute to apoptosis and mainly has a growth inhibitory function in Caco-2 3D cultures, the ErbB1-directed targeting is important to increase the local TRAIL concentration and to trigger an efficient apoptotic response. It can thus be assumed that patients whose tumors express high ErbB1 levels should respond best to Db-scTRAIL. Directing recombinant single-chain TRAIL molecules to tumor-specific surface antigens using a diabody-based forced dimerization strategy is not limited to the ErbB1 and together with appropriate apoptosis sensitizing agents may be a powerful approach to efficiently kill a broad range of cancer cells.

ErbB receptor ligands and polarization in the context of K-Ras^{G12V}

Besides its impact on TRAIL sensitivity by upregulation of cIAP2 the expression of K-Ras^{G12V} also induced the transcriptional activation of HRG1/2, an ErbB3 specific ligand. The ablation of HRG1/2 in these cells restored both, normal proliferation and morphology of Caco-2 cells. By exogenous addition of HRG to Caco-2 and primary intestinal organoid cultures it was clearly shown that HRG-induced ErbB3 signaling is not compatible with intestinal epithelial organization. Apart from driving proliferation, HRG is a stimulator of cell migration and invasion as well as tumorigenicity and metastasis [19,24]. In the breast cancer cell line MCF-7, HRG leads to loss of cell-cell contacts by inducing breakdown of adherens and tight junctions dependent on the MAPK pathway [138]. By contrast, HRG-ErbB2/3 signaling is crucial for the proper establishment of normal barrier function in the airway epithelium [139], showing again the cell context dependence of the impact of growth factor induced activation of the ErbB receptor pathways. The HRG-ErbB3 induced secretion of the growth factor VEGF in CRC cell lines and the correlation of HRG mRNA

expression with VEGF mRNA expression in colon cancer biopsy samples further shows the importance of this signaling axis in tumor establishment and progression also in the context of angiogenesis [140]. In the different CRC subtypes, however, there is still little known about the expression of ErbB3 and the ErbB ligands. Irrespective of cancer-associated mutations in K-Ras, aberrant HRG production by the stromal compartment could also impact the integrity of the intestinal epithelium. In contrast to HRG, addition of ErbB1 ligands only enhanced the proliferation of Caco-2 and organoid cultures but did not interfere with polarized morphogenesis. This highlights the independent regulation of proliferation and polarity and the qualitatively distinct signaling characteristics of the different ErbB ligands.

Although Ras directly activates PI3K [31], I would suggest that the autocrine HRG-ErbB3 signaling loop is engaged to amplify PI3K activation and cooperates with constitutively active MAPK in cell transformation downstream of Ras. This is in line with Venkateswarlu et al. who found that in the colon cancer cell line GEO, growth factor independence and block of apoptosis generated by autocrine heregulin was based on AKT and not MAPK activation [141]. This idea is further corroborated by the observation that RTKs exert dominant control over PI3K signaling in K-Ras mutant CRC cells [142]. Although pan-ErbB inhibition did not lead to detectable suppression of pAKT levels in K-Ras^{G12V} expressing Caco-2 cells, the acute ectopic expression of mutated Ras in the 3D Caco-2 cell system may differ from the situation in established CRC cells harboring endogenous K-Ras mutations.

Downstream effector pathways of the polarization defect in K-Ras^{G12V} cells

Considering that AKT activation is strongly suppressed in Caco-2 3D cultures compared to 2D monolayers the elevation of pAKT levels downstream of ErbB3 may contribute to the HRG-induced proliferation and/or polarity loss. However, in a previous report, the stable expression of activated PI3K in Caco-2 cells did not perturb 3D morphogenesis and PI3K inhibition failed to rescue the morphology or size of Caco-2 spheroids stably expressing mutant Ras [88].

Of note, the Caco-2 cells used in the publications by Magudia et al., Drosopoulos et al. and Jaffe et al. [83,88,107] were all stably transfected with oncogenic K-Ras and could have

undergone pathway adaptations due to the selection process or the impact of the mutated KRAS gene itself. This might explain why elevated expression of c-myc after K-Ras^{G12V} expression, as described by Magudia et al., was not observed in the Caco-2tet K-Ras^{G12V} cells, suggesting also that the polarization defect observed here differs from the one described before [88]. This is also supported by the finding that the inducible expression of B-Raf^{V600E} did not lead to increased HRG or cIAP2 levels in the Caco-2 model system used here. As B-Raf^{V600E} expression in the Caco-2tet cells also results in polarization defects [143], the underlying molecular pathways triggered by constitutively active Ras and Raf appear to be distinct and suggest that further signaling pathways are required to stimulate proliferation and disrupt epithelial morphogenesis in Caco-2tet K-Ras^{G12V} cells.

For example, in pancreatic adenocarcinoma, both PI3K and Stat3 activation downstream of ErbB1 were found to be essential for Ras-induced transformation [144]. In further experiments it could also be shown, that long-term stimulation with HRG lead to the activation of the Stat3 pathway in the 3D cultured Caco-2 cells used here [112]. This supports the involvement of other pathways like c-Met (hepatocyte growth factor receptor) signaling, also a RTK, or ErbB4 activation. It has been shown that pairing of c-Met with ErbB3 plays an important role in CRC cell lines and c-Met overexpression is observed in various cancer types [95,145]. This signaling platform serves as an alternative pathway to ErbB2/ErbB3 signaling. In K-Ras mutated CRC cell lines c-Met signaling was also described as the main driver in resistance to MEK inhibition [87]. In addition, expression of c-Met correlates with cetuximab resistance in patient derived xenografts and inhibition of this RTK added to the anti-proliferative effect of cetuximab [146].

ErbB3, a promising target in CRC

Despite its impaired kinase activity, ErbB3 has attracted growing attention due to its emerging role in survival signaling and as a mediator of drug resistance by circumventing the targeted pathway [22,23] or, as ErbB3 is not targeted by common TKIs, by restoring the signaling pathways of the originally inhibited RTK by serving as an alternative dimerization partner [147]. At the molecular level this is primarily associated with the potent induction of the PI3K pathway. The important function in linking RTK and PI3K activation is best described in breast cancer, where the ErbB2-ErbB3 signaling dimer was

shown to be essential for tumor formation and maintenance [89,148,149]. Recently, somatic mutations in ErbB3 with transforming potential were reported in colon and gastric cancers, however, these variants were still functionally dependent on ErbB2 [25]. Although ErbB2-ErbB3 is regarded as the most potent ErbB dimer, ErbB3 also dimerizes with ErbB1 and non-ErbB family RTKs such as c-Met [145]. It is also discussed that ErbB3 homo-dimers can sufficiently transactivate the receptor upon ligand binding [150]. An intestinal-specific ErbB3 knockout mouse model showed that the loss of ErbB3 resulted in loss of the ErbB4 protein, indicative of the formation of active ErbB3/4 signaling units [151]. Interestingly, when crossed to *Apc*^{Min} mice, ErbB3 loss almost completely prevented colonic tumorigenesis, underscoring the important role of ErbB3 signaling in tumor establishment and progression [151]. The promiscuous pairing of ErbB3 with other RTKs like c-Met may explain why the single knockdown of ErbB1 or ErbB2 did not mirror the effects of ErbB3 depletion in the Caco-2tet K-Ras^{G12V} cells. As residual ErbB2 in siRNA-treated cells could be sufficient to transactivate ErbB3, it cannot be ruled out that ErbB2 is the heterodimerization partner in this setting, in line with a report showing, that disproportionate ErbB2 levels efficiently activate ErbB3 [152]. The fact that ErbB3 phosphorylation was below the detection limit upon K-Ras^{G12V} induction in Caco-2 cells further indicates that a low number of activated receptors suffices in the cooperative signaling with oncogenic Ras.

Expression of ErbB3 in CRC was found to correlate with poorer overall survival and disease stage [92,93] and as revealed with higher tumor grade [112]. Tumor de-differentiation is a major prognostic factor, correlating with the risk of developing metastasis. Currently, several ErbB3-directed antibodies targeting the extracellular domain of the receptor are in clinical development [153]. A subset of CRC patients with Ras wild-type tumors fail to show an initial response to anti-ErbB1 therapy, whereas those that do respond routinely develop resistance, often by selection of Ras mutant clones. In such patients elevated circulating HRG levels were associated with both de novo and acquired resistance to cetuximab therapy [90]. Several reports describe the upregulation of ErbB3 as an evasion strategy to RTK inhibition [147,154,155] and pharmacologic MEK inhibition downstream of mutant Ras also unleashes feedbacks at the level of RTKs, including ErbB3 [79,156]. Thus,

combinatorial treatments involving ErbB3 may be particularly effective for the treatment of Ras mutant CRC and may also prevent HRG-mediated resistance in Ras wild-type CRC.

Outlook

As the dimerization partner of ErbB3 involved in hyperproliferation and the observed polarization defects could not be defined, dual targeting strategies would be more insightful in future studies. A bi-specific antibody targeting ErbB1/3 or ErbB2/3 could be more efficient and could eventually help to answer who is the favorable dimerization partner of ErbB3 in this specific setting.

As the targeting and dimerization effect of the Db-scTRAIL seems to be the most important factor in efficient delivery and apoptosis induction, a new rational targeting strategy for K-Ras mutated CRC could be the targeting of ErbB3 receptor. Further combination with a sensitizing smac mimetic could lead to efficient induction of apoptosis in K-Ras mutated cancer and significant inhibition of hyperproliferation and transformation processes like depolarization.

In future studies it will be of great importance to not only analyze the mutational status of the tumor itself but also the signaling profiles and transcriptional programs in the surrounding tissue to evaluate the effect of paracrine signaling. Even if the inhibition of the induced growth factor signaling does not affect Ras mutated cells directly, blocking of proliferative signals in the surrounding tissue could efficiently contribute to treatment success. Additionally the effect of the observed HRG upregulation towards other tumor associated pathways like angiogenesis and metastasis could be blocked by an ErbB3 targeted approach. The expression levels of these ErbB related ligands could be of great importance concerning the right treatment decision. The ligands strongly impact the efficiency of the specific targeting subunit of combined strategies. In accordance with the principle of a modular construction system the targeting components must be adjusted to the molecular profile of the tumor and the microenvironment to efficiently interrupt the oncogenic signaling pathways in the heterogeneous setting of cancer.

V. REFERENCES

1. McGuire S. World Cancer Report 2014. Geneva, Switzerland: World Health Organization, International Agency for Research on Cancer, WHO Press, 2015. *Adv Nutr.* 2016; 7:418–419.
2. Hanahan D and Weinberg RA. Hallmarks of cancer: the next generation. *Cell.* 2011; 144:646–674.
3. Hanahan D and Weinberg RA. The Hallmarks of Cancer. *Cell.* 2000; 100:57–70.
4. Deep G and Agarwal R. Targeting tumor microenvironment with silibinin: promise and potential for a translational cancer chemopreventive strategy. *Curr Cancer Drug Targets.* 2013; 13:486–499.
5. Sun Y and Nelson PS. Molecular pathways: involving microenvironment damage responses in cancer therapy resistance. *Clin Cancer Res.* 2012; 18:4019–4025.
6. Gelband H, Jha P, Sankaranarayanan R and Horton S, eds. *Cancer: Disease Control Priorities, Third Edition (Volume 3).* Washington (DC). 2015.
7. Chan AT and Giovannucci EL. Primary prevention of colorectal cancer. *Gastroenterology.* 2010; 138:2029–2043.e10.
8. Brand TM and Wheeler DL. KRAS mutant colorectal tumors: Past and present. *smallgtpases.* 2012; 3:34–39.
9. Kerr D. Clinical development of gene therapy for colorectal cancer. *Nat Rev Cancer.* 2003; 3:615–622.
10. Fearon ER and Vogelstein B. A genetic model for colorectal tumorigenesis. *Cell.* 1990; 61:759–767.
11. Potter JD and Lindor. NM, eds. *Genetics of Colorectal Cancer.* s.l. 2009.
12. Armaghany T, Wilson JD, Chu Q, Mills G. Genetic alterations in colorectal cancer. *Gastrointest Cancer Res.* 2012; 5:19–27.
13. Markowitz SD and Bertagnolli MM. Molecular origins of cancer: Molecular basis of colorectal cancer. *N Engl J Med.* 2009; 361:2449–2460.
14. Xu Y and Pasche B. TGF-beta signaling alterations and susceptibility to colorectal cancer. *Hum Mol Genet.* 2007; 16 Spec No 1:R14–20.
15. Dhillon AS, Hagan S, Rath O, Kolch W. MAP kinase signalling pathways in cancer. *Oncogene.* 2007; 26:3279–3290.
16. Lurje G and Lenz H. EGFR signaling and drug discovery. *Oncology.* 2009; 77:400–410.

17. Hynes NE and MacDonald G. ErbB receptors and signaling pathways in cancer. *Curr Opin Cell Biol.* 2009; 21:177–184.
18. Yarden Y and Sliwkowski MX. Untangling the ErbB signalling network. *Nat Rev Mol Cell Biol.* 2001; 2:127–137.
19. Breuleux M. Role of heregulin in human cancer. *Cell Mol Life Sci.* 2007; 64:2358–2377.
20. Garrett TPJ, McKern NM, Lou M, Elleman TC, Adams TE, et al. Ward CW. The crystal structure of a truncated ErbB2 ectodomain reveals an active conformation, poised to interact with other ErbB receptors. *Mol Cell.* 2003; 11:495–505.
21. Guy PM, Platko JV, Cantley LC, Cerione RA, Carraway KL. Insect cell-expressed p180erbB3 possesses an impaired tyrosine kinase activity. *Proc Natl Acad Sci USA.* 1994; 91:8132–8136.
22. Amin DN, Campbell MR, Moasser MM. The role of HER3, the unpretentious member of the HER family, in cancer biology and cancer therapeutics. *Semin Cell Dev Biol.* 2010; 21:944–950.
23. Baselga J and Swain SM. Novel anticancer targets: revisiting ERBB2 and discovering ERBB3. *Nat Rev Cancer.* 2009; 9:463–475.
24. Montero JC, Rodríguez-Barrueco R, Ocaña A, Díaz-Rodríguez E, Esparís-Ogando A, et al. Pandiella A. Neuregulins and cancer. *Clin Cancer Res.* 2008; 14:3237–3241.
25. Jaiswal BS, Kljavin NM, Stawiski EW, Chan E, Parikh C, et al. Seshagiri S. Oncogenic ERBB3 mutations in human cancers. *Cancer Cell.* 2013; 23:603–617.
26. Ciardiello F, Kim N, Saeki T, Dono R, Persico MG, et al. Salomon DS. Differential expression of epidermal growth factor-related proteins in human colorectal tumors. *Proc Natl Acad Sci USA.* 1991; 88:7792–7796.
27. Arteaga CL and Engelman JA. ERBB receptors: from oncogene discovery to basic science to mechanism-based cancer therapeutics. *Cancer Cell.* 2014; 25:282–303.
28. Valastyan S and Weinberg RA. Tumor metastasis: molecular insights and evolving paradigms. *Cell.* 2011; 147:275–292.
29. Toulany M, Baumann M, Rodemann HP. Stimulated PI3K-AKT signaling mediated through ligand or radiation-induced EGFR depends indirectly, but not directly, on constitutive K-Ras activity. *Mol Cancer Res.* 2007; 5:863–872.
30. Gangarosa LM, Sizemore N, Graves-Deal R, Oldham SM, Der CJ, et al. Coffey RJ. A raf-independent epidermal growth factor receptor autocrine loop is necessary for Ras transformation of rat intestinal epithelial cells. *J Biol Chem.* 1997; 272:18926–18931.

31. Castellano E and Downward J. Role of RAS in the regulation of PI3-kinase. *Curr Top Microbiol Immunol*. 2010; 346:143–169.
32. Nelson WJ. Adaptation of core mechanisms to generate cell polarity. *Nature*. 2003; 422:766–774.
33. Downward J. Targeting RAS signalling pathways in cancer therapy. *Nat Rev Cancer*. 2003; 3:11–22.
34. Prior IA, Lewis PD, Mattos C. A comprehensive survey of Ras mutations in cancer. *Cancer Research*. 2012; 72:2457–2467.
35. Walther A, Johnstone E, Swanton C, Midgley R, Tomlinson I, et al. Kerr D. Genetic prognostic and predictive markers in colorectal cancer. *Nat Rev Cancer*. 2009; 9:489–499.
36. Barbacid M. ras genes. *Annu Rev Biochem*. 1987; 56:779–827.
37. Oikonomou E, Koustas E, Goulielmaki M, Pintzas A. BRAF vs RAS oncogenes: are mutations of the same pathway equal? Differential signalling and therapeutic implications. *Oncotarget*. 2014; 5:11752–11777.
38. Ellenbroek SIJ, Iden S, Collard JG. Cell polarity proteins and cancer. *Semin Cancer Biol*. 2012; 22:208–215.
39. Braun AC, Hendrick J, Eisler SA, Schmid S, Hausser A, et al. Olayioye MA. The Rho-specific GAP protein DLC3 coordinates endocytic membrane trafficking. *J Cell Sci*. 2015; 128:1386–1399.
40. Vermeer PD, Einwalter LA, Moninger TO, Rokhlina T, Kern JA, et al. Welsh MJ. Segregation of receptor and ligand regulates activation of epithelial growth factor receptor. *Nature*. 2003; 422:322–326.
41. Aranda V, Haire T, Nolan ME, Calarco JP, Rosenberg AZ, et al. Muthuswamy SK. Par6-aPKC uncouples ErbB2 induced disruption of polarized epithelial organization from proliferation control. *Nat Cell Biol*. 2006; 8:1235–1245.
42. Linch M, Sanz-Garcia M, Rosse C, Riou P, Peel N, et al. Parker PJ. Regulation of polarized morphogenesis by protein kinase C iota in oncogenic epithelial spheroids. *Carcinogenesis*. 2014; 35:396–406.
43. Hendrick J, Franz-Wachtel M, Möller Y, Schmid S, Macek B, et al. Olayioye MA. The polarity protein Scribble positions DLC3 at adherens junctions to regulate Rho signaling. *J Cell Sci*. 2016; 129:3583–3596.
44. Chatterjee S, Seifried L, Feigin ME, Gibbons DL, Scuoppo C, et al. Muthuswamy SK. Dysregulation of cell polarity proteins synergize with oncogenes or the microenvironment to induce invasive behavior in epithelial cells. *PLoS ONE*. 2012; 7:e34343.
45. Sato T and Clevers H. Growing self-organizing mini-guts from a single intestinal stem cell: mechanism and applications. *Science*. 2013; 340:1190–1194.

46. Abreu MT. Toll-like receptor signalling in the intestinal epithelium: how bacterial recognition shapes intestinal function. *Nat Rev Immunol.* 2010; 10:131–144.
47. Koff JL, Ramachandiran S, Bernal-Mizrachi L. A time to kill: targeting apoptosis in cancer. *Int J Mol Sci.* 2015; 16:2942–2955.
48. Johnstone RW, Frew AJ, Smyth MJ. The TRAIL apoptotic pathway in cancer onset, progression and therapy. *Nat Rev Cancer.* 2008; 8:782–798.
49. Falschlehner C, Emmerich CH, Gerlach B, Walczak H. TRAIL signalling: Decisions between life and death. *The International Journal of Biochemistry & Cell Biology.* 2007; 39:1462–1475.
50. Debatin K and Krammer PH. Death receptors in chemotherapy and cancer. *Oncogene.* 2004; 23:2950–2966.
51. Wang S and El-Deiry WS. TRAIL and apoptosis induction by TNF-family death receptors. *Oncogene.* 2003; 22:8628–8633.
52. Ghavami S, Hashemi M, Ande SR, Yeganeh B, Xiao W, et al. Los M. Apoptosis and cancer: mutations within caspase genes. *J Med Genet.* 2009; 46:497–510.
53. Pandey MK, Prasad S, Tyagi AK, Deb L, Huang J, et al. Aggarwal BB. Targeting Cell Survival Proteins for Cancer Cell Death. *Pharmaceuticals (Basel).* 2016; 9.
54. LaCasse EC, Mahoney DJ, Cheung HH, Plenchette S, Baird S, et al. Korneluk RG. IAP-targeted therapies for cancer. *Oncogene.* 2008; 27:6252–6275.
55. Goldstein M and Kastan MB. The DNA damage response: implications for tumor responses to radiation and chemotherapy. *Annu Rev Med.* 2015; 66:129–143.
56. Vanneman M and Dranoff G. Combining immunotherapy and targeted therapies in cancer treatment. *Nat Rev Cancer.* 2012; 12:237–251.
57. Pardoll DM. The blockade of immune checkpoints in cancer immunotherapy. *Nat Rev Cancer.* 2012; 12:252–264.
58. Drake JM, Lee JK, Witte ON. Clinical targeting of mutated and wild-type protein tyrosine kinases in cancer. *Mol Cell Biol.* 2014; 34:1722–1732.
59. Gaumann AKA, Kiefer F, Alfer J, Lang SA, Geissler EK, et al. Breier G. Receptor tyrosine kinase inhibitors: Are they real tumor killers? *Int J Cancer.* 2016; 138:540–554.
60. Weiner GJ. Building better monoclonal antibody-based therapeutics. *Nat Rev Cancer.* 2015; 15:361–370.
61. Galizia G, Lieto E, Vita F de, Orditura M, Castellano P, et al. Ciardiello F. Cetuximab, a chimeric human mouse anti-epidermal growth factor receptor monoclonal antibody, in the treatment of human colorectal cancer. *Oncogene.* 2007; 26:3654–3660.

62. Oikonomou E and Pintzas A. The TRAIL of oncogenes to apoptosis. *Biofactors*. 2013; 39:343–354.
63. Soria J, Mark Z, Zatloukal P, Szima B, Albert I, et al. Blackhall F. Randomized phase II study of dulanermin in combination with paclitaxel, carboplatin, and bevacizumab in advanced non-small-cell lung cancer. *J Clin Oncol*. 2011; 29:4442–4451.
64. Dimberg LY, Anderson CK, Camidge R, Behbakht K, Thorburn A, et al. Ford HL. On the TRAIL to successful cancer therapy? Predicting and counteracting resistance against TRAIL-based therapeutics. *Oncogene*. 2012; 32:1341–1350.
65. Schneider B, Münkel S, Krippner-Heidenreich A, Grunwald I, Wels WS, et al. Gerspach J. Potent antitumoral activity of TRAIL through generation of tumor-targeted single-chain fusion proteins. *Cell Death Dis*. 2010; 1:e68.
66. Siegemund M, Pollak N, Seifert O, Wahl K, Hanak K, et al. Pfizenmaier K. Superior antitumoral activity of dimerized targeted single-chain TRAIL fusion proteins under retention of tumor selectivity. *Cell Death Dis*. 2012; 3:e295.
67. Amado RG, Wolf M, Peeters M, van Cutsem E, Siena S, et al. Chang DD. Wild-type KRAS is required for panitumumab efficacy in patients with metastatic colorectal cancer. *J Clin Oncol*. 2008; 26:1626–1634.
68. Khambata-Ford S, Garrett CR, Meropol NJ, Basik M, Harbison CT, et al. Mauro DJ. Expression of epiregulin and amphiregulin and K-ras mutation status predict disease control in metastatic colorectal cancer patients treated with cetuximab. *J Clin Oncol*. 2007; 25:3230–3237.
69. Normanno N, Tejpar S, Morgillo F, Luca A de, van Cutsem E, et al. Ciardiello F. Implications for KRAS status and EGFR-targeted therapies in metastatic CRC. *Nat Rev Clin Oncol*. 2009; 6:519–527.
70. Lièvre A, Bachet J, Boige V, Cayre A, Le Corre D, et al. Laurent-Puig P. KRAS mutations as an independent prognostic factor in patients with advanced colorectal cancer treated with cetuximab. *J Clin Oncol*. 2008; 26:374–379.
71. Tejpar S, Celik I, Schlichting M, Sartorius U, Bokemeyer C, et al. van Cutsem E. Association of KRAS G13D Tumor Mutations With Outcome in Patients With Metastatic Colorectal Cancer Treated With First-Line Chemotherapy With or Without Cetuximab. *Journal of Clinical Oncology*. 2012; 30:3570–3577.
72. Rook W de, Jonker DJ, Di Nicolantonio F, Sartore-Bianchi A, Tu D, et al. Tejpar S. Association of KRAS p.G13D mutation with outcome in patients with chemotherapy-refractory metastatic colorectal cancer treated with cetuximab. *JAMA*. 2010; 304:1812–1820.
73. Asati V, Mahapatra DK and Bharti SK, eds. K-Ras and its inhibitors towards personalized cancer treatment: Pharmacological and structural perspectives. 2016.

74. Spiegel J, Cromm PM, Zimmermann G, Grossmann TN, Waldmann H. Small-molecule modulation of Ras signaling. *Nat Chem Biol.* 2014; 10:613–622.
75. Brand TM, Iida M, Wheeler DL. Molecular mechanisms of resistance to the EGFR monoclonal antibody cetuximab. *Cancer Biol Ther.* 2011; 11:777–792.
76. Temraz S, Mukherji D, Shamseddine A. Dual Inhibition of MEK and PI3K Pathway in KRAS and BRAF Mutated Colorectal Cancers. *Int J Mol Sci.* 2015; 16:22976–22988.
77. Holderfield M, Deuker MM, McCormick F, McMahon M. Targeting RAF kinases for cancer therapy: BRAF-mutated melanoma and beyond. *Nat Rev Cancer.* 2014; 14:455–467.
78. Grimaldi AM, Simeone E, Ascierto PA. The role of MEK inhibitors in the treatment of metastatic melanoma. *Curr Opin Oncol.* 2014; 26:196–203.
79. Turke AB, Song Y, Costa C, Cook R, Arteaga CL, et al. Engelman JA. MEK inhibition leads to PI3K/AKT activation by relieving a negative feedback on ERBB receptors. *Cancer Research.* 2012; 72:3228–3237.
80. Liu Z, Li H, Derouet M, Filmus J, LaCasse EC, et al. Rosen KV. ras Oncogene Triggers Up-regulation of cIAP2 and XIAP in Intestinal Epithelial Cells: Epidermal Growth Factor Receptor-Dependent and -Independent Mechanisms of RAS-Induced Transformation. *Journal of Biological Chemistry.* 2005; 280:37383–37392.
81. Cox AD and Der CJ. The dark side of Ras: regulation of apoptosis. *Oncogene.* 2003; 22:8999–9006.
82. Overmeyer JH and Maltese WA. Death pathways triggered by activated Ras in cancer cells. *Front Biosci (Landmark Ed).* 2011; 16:1693–1713.
83. Drosopoulos KG, Roberts ML, Cermak L, Sasazuki T, Shirasawa S, et al. Pintzas A. Transformation by Oncogenic RAS Sensitizes Human Colon Cells to TRAIL-induced Apoptosis by Up-regulating Death Receptor 4 and Death Receptor 5 through a MEK-dependent Pathway. *Journal of Biological Chemistry.* 2005; 280:22856–22867.
84. Huang S, Ren X, Wang L, Zhang L, Wu X. Lung-Cancer Chemoprevention by Induction of Synthetic Lethality in Mutant KRAS Premalignant Cells In Vitro and In Vivo. *Cancer Prevention Research.* 2011; 4:666–673.
85. McCarthy SA, Samuels ML, Pritchard CA, Abraham JA, McMahon M. Rapid induction of heparin-binding epidermal growth factor/diphtheria toxin receptor expression by Raf and Ras oncogenes. *Genes Dev.* 1995; 9:1953–1964.
86. van Schaeybroeck S, Kyula JN, Fenton A, Fenning CS, Sasazuki T, et al. Johnston PG. Oncogenic Kras Promotes Chemotherapy-Induced Growth Factor Shedding via ADAM17. *Cancer Research.* 2011; 71:1071–1080.

87. van Schaeybroeck S, Kalimutho M, Dunne PD, Carson R, Allen W, et al. Johnston PG. ADAM17-dependent c-MET-STAT3 signaling mediates resistance to MEK inhibitors in KRAS mutant colorectal cancer. *Cell Rep.* 2014; 7:1940–1955.
88. Magudia K, Lahoz A, Hall A. K-Ras and B-Raf oncogenes inhibit colon epithelial polarity establishment through up-regulation of c-myc. *The Journal of Cell Biology.* 2012; 198:185–194.
89. Lee-Hoeflich ST, Crocker L, Yao E, Pham T, Munroe X, et al. Stern HM. A central role for HER3 in HER2-amplified breast cancer: implications for targeted therapy. *Cancer Research.* 2008; 68:5878–5887.
90. Yonesaka K, Zejnullahu K, Okamoto I, Satoh T, Cappuzzo F, et al. Jänne PA. Activation of ERBB2 signaling causes resistance to the EGFR-directed therapeutic antibody cetuximab. *Sci Transl Med.* 2011; 3:99ra86.
91. Grivas PD, Antonacopoulou A, Tzelepi V, Sotiropoulou-Bonikou G, Kefalopoulou Z, et al. Kalofonos H. HER-3 in colorectal tumourigenesis: from mRNA levels through protein status to clinicopathologic relationships. *Eur J Cancer.* 2007; 43:2602–2611.
92. Gespach C. Increasing potential of HER3 signaling in colon cancer progression and therapy. *Clin Cancer Res.* 2012; 18:917–919.
93. Beji A, Horst D, Engel J, Kirchner T, Ullrich A. Toward the prognostic significance and therapeutic potential of HER3 receptor tyrosine kinase in human colon cancer. *Clin Cancer Res.* 2012; 18:956–968.
94. Krumbach R, Schuler J, Hofmann M, Giesemann T, Fiebig H, et al. Beckers T. Primary resistance to cetuximab in a panel of patient-derived tumour xenograft models: activation of MET as one mechanism for drug resistance. *Eur J Cancer.* 2011; 47:1231–1243.
95. Yao Y, Shao J, Zhang C, Wu J, Zhang Q, et al. Zhu W. Proliferation of colorectal cancer is promoted by two signaling transduction expression patterns: ErbB2/ErbB3/AKT and MET/ErbB3/MAPK. *PLoS ONE.* 2013; 8:e78086.
96. Yonesaka K, Takegawa N, Satoh T, Ueda H, Yoshida T, et al. Nakagawa K. Combined analysis of plasma amphiregulin and heregulin predicts response to cetuximab in metastatic colorectal cancer. *PLoS ONE.* 2015; 10:e0143132.
97. Prasetyanti PR, Capone E, Barcaroli D, D'Agostino D, Volpe S, et al. Sala G. ErbB-3 activation by NRG-1beta sustains growth and promotes vemurafenib resistance in BRAF-V600E colon cancer stem cells (CSCs). *Oncotarget.* 2015; 6:16902–16911.
98. Lee GY, Kenny PA, Lee EH, Bissell MJ. Three-dimensional culture models of normal and malignant breast epithelial cells. *Nat Methods.* 2007; 4:359–365.
99. Debnath J and Brugge JS. Modelling glandular epithelial cancers in three-dimensional cultures. *Nat Rev Cancer.* 2005; 5:675–688.

100. Shamir ER and Ewald AJ. Three-dimensional organotypic culture: experimental models of mammalian biology and disease. *Nat Rev Mol Cell Biol.* 2014; 15:647–664.
101. Pereira JFS, Awatade NT, Loureiro CA, Matos P, Amaral MD, et al. Jordan P. The third dimension: new developments in cell culture models for colorectal research. *Cell Mol Life Sci.* 2016.
102. Debnath J, Walker SJ, Brugge JS. Akt activation disrupts mammary acinar architecture and enhances proliferation in an mTOR-dependent manner. *The Journal of Cell Biology.* 2003; 163:315–326.
103. Yang T, Barbone D, Fennell DA, Broaddus VC. Bcl-2 family proteins contribute to apoptotic resistance in lung cancer multicellular spheroids. *Am J Respir Cell Mol Biol.* 2009; 41:14–23.
104. Möller Y, Siegemund M, Beyes S, Herr R, Lecis D, et al. Olayioye MA. EGFR-targeted TRAIL and a Smac mimetic synergize to overcome apoptosis resistance in KRAS mutant colorectal cancer cells. *PLoS ONE.* 2014; 9:e107165.
105. Longati P, Jia X, Eimer J, Wagman A, Witt M, et al. Heuchel RL. 3D pancreatic carcinoma spheroids induce a matrix-rich, chemoresistant phenotype offering a better model for drug testing. *BMC Cancer.* 2013; 13:95.
106. Thoma CR, Zimmermann M, Agarkova I, Kelm JM, Krek W. 3D cell culture systems modeling tumor growth determinants in cancer target discovery. *Adv Drug Deliv Rev.* 2014; 69-70:29–41.
107. Jaffe AB, Kaji N, Durgan J, Hall A. Cdc42 controls spindle orientation to position the apical surface during epithelial morphogenesis. *The Journal of Cell Biology.* 2008; 183:625–633.
108. Ohta Y and Sato T. Intestinal tumor in a dish. *Front Med (Lausanne).* 2014; 1:14.
109. Fujii M, Matano M, Nanki K, Sato T. Efficient genetic engineering of human intestinal organoids using electroporation. *Nat Protoc.* 2015; 10:1474–1485.
110. Fujii M, Shimokawa M, Date S, Takano A, Matano M, et al. Sato T. A Colorectal Tumor Organoid Library Demonstrates Progressive Loss of Niche Factor Requirements during Tumorigenesis. *Cell Stem Cell.* 2016; 18:827–838.
111. van de Wetering M, Francies HE, Francis JM, Bounova G, Iorio F, et al. Clevers H. Prospective derivation of a living organoid biobank of colorectal cancer patients. *Cell.* 2015; 161:933–945.
112. Möller Y, Morkel M, Schmid J, Beyes S, Hendrick J, et al. Olayioye MA. Oncogenic Ras triggers hyperproliferation and impairs polarized colonic morphogenesis by autocrine ErbB3 signaling. *Oncotarget.* 2016.

113. Röring M, Herr R, Fiala GJ, Heilmann K, Braun S, et al. Brummer T. Distinct requirement for an intact dimer interface in wild-type, V600E and kinase-dead B-Raf signalling. *EMBO J.* 2012; 31:2629–2647.
114. Herr R, Wöhrle FU, Danke C, Berens C, Brummer T. A novel MCF-10A line allowing conditional oncogene expression in 3D culture. *Cell Commun. Signal.* 2011; 9:17.
115. Manzoni L, Belvisi L, Bianchi A, Conti A, Drago C, et al. Seneci P. Homo- and heterodimeric Smac mimetics/IAP inhibitors as in vivo-active pro-apoptotic agents. Part I: Synthesis. *Bioorganic & Medicinal Chemistry.* 2012; 20:6687–6708.
116. Lecis D, Mastrangelo E, Belvisi L, Bolognesi M, Civera M, et al. Seneci P. Dimeric Smac mimetics/IAP inhibitors as in vivo-active pro-apoptotic agents. Part II: Structural and biological characterization. *Bioorganic & Medicinal Chemistry.* 2012; 20:6709–6723.
117. Mendelsohn J. Blockade of Receptors for Growth Factors: An Anticancer Therapy. The Fourth Annual Joseph H. Burchenal American Association for Cancer Research Clinical Research Award Lecture. *Clinical Cancer Research.* 2000; 6:747–753.
118. van Geelen, C. M., Vries EG de, Le TK, van Weeghel RP, Jong S. Differential modulation of the TRAIL receptors and the CD95 receptor in colon carcinoma cell lines. *Br J Cancer.* 2003; 89:363–373.
119. Gibson EM, Henson ES, Haney N, Villanueva J, Gibson SB. Epidermal growth factor protects epithelial-derived cells from tumor necrosis factor-related apoptosis-inducing ligand-induced apoptosis by inhibiting cytochrome c release. *Cancer Res.* 2002; 62:488–496.
120. Gyrd-Hansen M and Meier P. IAPs: from caspase inhibitors to modulators of NF- κ B, inflammation and cancer. *Nat Rev Cancer.* 2010; 10:561–574.
121. Fulda S, Wick W, Weller M, Debatin K. Smac agonists sensitize for Apo2L/TRAIL- or anticancer drug-induced apoptosis and induce regression of malignant glioma in vivo. *Nat. Med.* 2002.
122. Lecis D, Drago C, Manzoni L, Seneci P, Scolastico C, et al. Clark S. Novel SMAC-mimetics synergistically stimulate melanoma cell death in combination with TRAIL and Bortezomib. *Br J Cancer.* 2010; 102:1707–1716.
123. Darding M, Feltham R, Tenev T, Bianchi K, Benetatos C, et al. Meier P. Molecular determinants of Smac mimetic induced degradation of cIAP1 and cIAP2. *Cell Death Differ.* 2011; 18:1376–1386.
124. Sträter J, Hinz U, Walczak H, Mechttersheimer G, Koretz K, et al. Lehnert T. Expression of TRAIL and TRAIL receptors in colon carcinoma: TRAIL-R1 is an independent prognostic parameter. *Clin. Cancer Res.* 2002; 8:3734–3740.

125. Kriegl L, Jung A, Horst D, Rizzani A, Jackstadt R, et al. Srivastava RK. Microsatellite Instability, KRAS Mutations and Cellular Distribution of TRAIL-Receptors in Early Stage Colorectal Cancer. *PLoS ONE*. 2012; 7:e51654.
126. Fulda S, Meyer E, Debatin K. Inhibition of TRAIL-induced apoptosis by Bcl-2 overexpression. *Oncogene*. 2002; 21:2283–2294.
127. Bishop WP and Wen JT. Regulation of Caco-2 cell proliferation by basolateral membrane epidermal growth factor receptors. *Am J Physiol*. 1994; 267:G892-900.
128. Pfister AB, Wood RC, Salas PJI, Zea DL, Ramsauer VP. Early response to ErbB2 over-expression in polarized Caco-2 cells involves partial segregation from ErbB3 by relocalization to the apical surface and initiation of survival signaling. *J Cell Biochem*. 2010; 111:643–652.
129. Shelly M, Mosesson Y, Citri A, Lavi S, Zwang Y, et al. Yarden Y. Polar expression of ErbB-2/HER2 in epithelia. Bimodal regulation by Lin-7. *Dev Cell*. 2003; 5:475–486.
130. Chen X, Thakkar H, Tyan F, Gim S, Robinson H, et al. Srivastava RK. Constitutively active Akt is an important regulator of TRAIL sensitivity in prostate cancer. *Oncogene*. 2001; 20:6073–6083.
131. Vaculová A, Hofmanová J, Soucek K, Kozubík A. Different modulation of TRAIL-induced apoptosis by inhibition of pro-survival pathways in TRAIL-sensitive and TRAIL-resistant colon cancer cells. *FEBS Lett*. 2006; 580:6565–6569.
132. Guerrero S, Casanova I, Farré L, Mazo A, Capellà G, et al. Mangués R. K-ras codon 12 mutation induces higher level of resistance to apoptosis and predisposition to anchorage-independent growth than codon 13 mutation or proto-oncogene overexpression. *Cancer Res*. 2000; 60:6750–6756.
133. Miura K, Karasawa H, Sasaki I. cIAP2 as a therapeutic target in colorectal cancer and other malignancies. *Expert Opin. Ther. Targets*. 2009; 13:1333–1345.
134. Vince JE, Wong WW, Khan N, Feltham R, Chau D, et al. Silke J. IAP Antagonists Target cIAP1 to Induce TNF α -Dependent Apoptosis. *Cell*. 2007; 131:682–693.
135. Varfolomeev E, Blankenship JW, Wayson SM, Fedorova AV, Kayagaki N, et al. Vucic D. IAP Antagonists Induce Autoubiquitination of c-IAPs, NF- κ B Activation, and TNF α -Dependent Apoptosis. *Cell*. 2007; 131:669–681.
136. Stagg J, Sharkey J, Pommey S, Young R, Takeda K, et al. Smyth MJ. Antibodies targeted to TRAIL receptor-2 and ErbB-2 synergize in vivo and induce an antitumor immune response. *Proc Natl Acad Sci USA*. 2008; 105:16254–16259.

137. Henson ES and Gibson SB. Surviving cell death through epidermal growth factor (EGF) signal transduction pathways: Implications for cancer therapy. *Cellular Signalling*. 2006; 18:2089–2097.
138. Okoshi R, Shu C, Ihara S, Fukui Y. Scattering of MCF7 cells by heregulin ss-1 depends on the MEK and p38 MAP kinase pathway. *PLoS ONE*. 2013; 8:e53298.
139. Gon Y, Matsumoto K, Terakado M, Sekiyama A, Maruoka S, et al. Hashimoto S. Heregulin activation of ErbB2/ErbB3 signaling potentiates the integrity of airway epithelial barrier. *Exp Cell Res*. 2011; 317:1947–1953.
140. Yonezawa M, Wada K, Tatsuguchi A, Akamatsu T, Gudis K, et al. Sakamoto C. Heregulin-induced VEGF expression via the ErbB3 signaling pathway in colon cancer. *Digestion*. 2009; 80:215–225.
141. Venkateswarlu S, Dawson DM, St Clair P, Gupta A, Willson JKV, et al. Brattain MG. Autocrine heregulin generates growth factor independence and blocks apoptosis in colon cancer cells. *Oncogene*. 2002; 21:78–86.
142. Ebi H, Corcoran RB, Singh A, Chen Z, Song Y, et al. Engelman JA. Receptor tyrosine kinases exert dominant control over PI3K signaling in human KRAS mutant colorectal cancers. *J Clin Invest*. 2011; 121:4311–4321.
143. Herr R, Köhler M, Andrlova H, Weinberg F, Möller Y, et al. Brummer T. B-Raf inhibitors induce epithelial differentiation in BRAF-mutant colorectal cancer cells. *Cancer Research*. 2015; 75:216–229.
144. Navas C, Hernández-Porras I, Schuhmacher AJ, Sibilia M, Guerra C, et al. Barbacid M. EGF receptor signaling is essential for k-ras oncogene-driven pancreatic ductal adenocarcinoma. *Cancer Cell*. 2012; 22:318–330.
145. Engelman JA, Zejnullahu K, Mitsudomi T, Song Y, Hyland C, et al. Jänne PA. MET amplification leads to gefitinib resistance in lung cancer by activating ERBB3 signaling. *Science*. 2007; 316:1039–1043.
146. Wadlow RC, Hezel AF, Abrams TA, Blaszkowsky LS, Fuchs CS, et al. Clark JW. Panitumumab in patients with KRAS wild-type colorectal cancer after progression on cetuximab. *Oncologist*. 2012; 17:14.
147. Sergina NV, Rausch M, Wang D, Blair J, Hann B, et al. Moasser MM. Escape from HER-family tyrosine kinase inhibitor therapy by the kinase-inactive HER3. *Nature*. 2007; 445:437–441.
148. Vaught DB, Stanford JC, Young C, Hicks DJ, Wheeler F, et al. Cook RS. HER3 is required for HER2-induced preneoplastic changes to the breast epithelium and tumor formation. *Cancer Research*. 2012; 72:2672–2682.
149. Holbro T, Beerli RR, Maurer F, Koziczak M, Barbas CF, et al. Hynes NE. The ErbB2/ErbB3 heterodimer functions as an oncogenic unit: ErbB2 requires ErbB3 to drive breast tumor cell proliferation. *Proc Natl Acad Sci USA*. 2003; 100:8933–8938.

150. Shi F, Telesco SE, Liu Y, Radhakrishnan R, Lemmon MA. ErbB3/HER3 intracellular domain is competent to bind ATP and catalyze autophosphorylation. *Proc Natl Acad Sci USA*. 2010; 107:7692–7697.
151. Lee D, Yu M, Lee E, Kim H, Yang Y, et al. Threadgill DW. Tumor-specific apoptosis caused by deletion of the ERBB3 pseudo-kinase in mouse intestinal epithelium. *J Clin Invest*. 2009; 119:2702–2713.
152. Steinkamp MP, Low-Nam ST, Yang S, Lidke KA, Lidke DS, et al. Wilson BS. erbB3 is an active tyrosine kinase capable of homo- and heterointeractions. *Mol Cell Biol*. 2014; 34:965–977.
153. Gala K and Chandarlapaty S. Molecular pathways: HER3 targeted therapy. *Clin Cancer Res*. 2014; 20:1410–1416.
154. Wheeler DL, Huang S, Kruser TJ, Nechrebecki MM, Armstrong EA, et al. Harari PM. Mechanisms of acquired resistance to cetuximab: role of HER (ErbB) family members. *Oncogene*. 2008; 27:3944–3956.
155. Garrett JT, Olivares MG, Rinehart C, Granja-Ingram ND, Sánchez V, et al. Arteaga CL. Transcriptional and posttranslational up-regulation of HER3 (ErbB3) compensates for inhibition of the HER2 tyrosine kinase. *Proc Natl Acad Sci USA*. 2011; 108:5021–5026.
156. Sun C, Hobor S, Bertotti A, Zecchin D, Huang S, et al. Bernards R. Intrinsic resistance to MEK inhibition in KRAS mutant lung and colon cancer through transcriptional induction of ERBB3. *Cell Rep*. 2014; 7:86–93.

VI. APPENDIX

Publications

Acknowledgments

Curriculum vitae

Declaration

Publications

This work was published in part in the following publications:

Möller Y, Morkel M, Schmid J, Beyes S, Hendrick J, Strotbek M, Riemer P, Schmid S, Schmitt LC, Kontermann R, Murdter T, Schwab M, Sers C, Olayioye MA. Oncogenic Ras triggers hyperproliferation and impairs polarized colonic morphogenesis by autocrine ErbB3 signaling. *Oncotarget*. 2016.

Möller Y, Siegemund M, Beyes S, Herr R, Lecis D, Delia D, Kontermann R, Brummer T, Pfizenmaier K, Olayioye MA. EGFR-targeted TRAIL and a Smac mimetic synergize to overcome apoptosis resistance in KRAS mutant colorectal cancer cells. *PLoS ONE*. 2014

Further publications:

Lakner PH, Monaghan MG, **Möller Y**, Olayioye MA, Schenke-Layland K. Applying a phasor approach analysis of multiphoton fluorescence lifetime imaging microscopy measurements to probe the metabolic activity of three-dimensional in vitro cell culture models. *Scientific Reports*. 2017.

Hendrick J, Franz-Wachtel M, **Möller Y**, Schmid S, Macek B, Olayioye MA. The polarity protein Scribble positions DLC3 at adherens junctions to regulate Rho signaling. *Cell Sci*. 2016

Herr R, Köhler M, Andrlova H, Weinberg F, **Möller Y**, Halbach S, Lutz L, Mastroianni J, Klose M, Bittermann N, Kowar S, Zeiser R, Olayioye MA, Lassmann S, Busch H, Boerries M, Brummer T. B-Raf inhibitors induce epithelial differentiation in BRAF-mutant colorectal cancer cells. *Cancer Research*. 2015.

Abstracts and conference participation

Lakner PH, **Möller Y**, Olayioye MA, Brucker SY, Schenke-Layland K and Monaghan MG. A phasor approach analysis of multiphoton FLIM measurements of three-dimensional cell culture models. *Proc. SPIE*; 2016; Conference Volume 9712.

Möller Y, Siegemund M, Beyes S, Kontermann R, Olayioye MA. Targeted single-chain TRAIL is a potent cytotoxic agent in a 3D model of colorectal cancer. *3D Cell Culture 2014 - Advanced Model Systems*; Freiburg 2014

Möller Y, Kiepfner K, Noll M. Development of an autologous full skin transplant. *World Conference on Regenerative Medicine*; Leipzig 2011

Acknowledgments

Danksagung

An dieser Stelle ist nun Zeit sich bei all denjenigen zu bedanken, die wesentlich dazu beigetragen haben, dass ich an diesem Punkt angekommen bin und ein wichtiges Kapitel abschließen kann.

An erster Stelle möchte ich mich bei Prof. Monilola Olayioye bedanken. Vielen Dank Moni, dass ich Teil des MoLabs sein durfte, für die herausfordernde Aufgabenstellung, die Freiheit experimentieren zu dürfen und meinen Weg zu versuchen. Danke für Dein Vertrauen, für Deine Unterstützung und Deinen unermüdlichen Enthusiasmus und Antrieb für mein Projekt, danke dafür, dass Dir nie die Ideen ausgegangen sind, auch wenn ich schon am Verzweifeln war. Danke für die in jeder Hinsicht lehrreiche und wunderbare Zeit.

Mein herzlicher Dank gilt auch Prof. Klaus Pfizenmaier, der mich an seinem Institut aufgenommen und einen Teil meiner wissenschaftlichen Arbeit begleitet hat. Ebenso bedanken möchte ich mich bei Prof. Roland Kontermann für die Unterstützung und die Zusammenarbeit im Rahmen meiner Dissertation sowie für die Übernahme des Prüfungsvorsitzes. Für die Beurteilung meiner Arbeit als Mitberichter möchte ich herzlichst Prof. Nisar Malek danken.

Ohne Euch liebes MoLab wäre diese Arbeit niemals so zu Stande gekommen, daher gilt Euch mein wärmster Dank; von Herzen danke für die unvergessliche Zeit, für die vielen schönen Stunden, für Euer Mitgefühl in den weniger schönen, für Eure Verlässlichkeit und Eure Unterstützung. Besonders möchte ich mich bei Sven für seine Begeisterung und seine wertvolle Arbeit während seiner Diplomarbeit bedanken sowie bei Janina und Michaela und Simone, die neben ihrer eigenen Arbeit viel von dem beendet haben, was ich nicht mehr geschafft habe, ohne Euch wäre so viel unerledigt und unentdeckt geblieben.

Mein tiefster Dank gilt meiner Familie, besonders meinen Eltern und meinen Schwestern; danke, für den bedingungslosen Rückhalt und die wichtigen Dinge im Leben.

Und Dir Thomas, dass Du all das mit mir teilst und damit alles Missglückte nur halb so schlimm und alles Gelungene doppelt so schön ist.

Curriculum vitae

Name	Yvonne Möller
Place of birth	Bad Hersfeld
Nationality	German

**Professional Occupation**

since	03/2015	Scientific coordinator of the Center for Personalized Medicine at the University Hospital Tübingen
	08/2010 - 12/2011	Research associate at AgenoLAB GmbH & Co.KG, Stuttgart BMBF project "Development of an autologous full skin transplant"
	11/2007 - 03/2010	Research assistant at Fraunhofer IGB, Stuttgart

Ph. D. Studies

01/2012	02/2015	Ph.D. in molecular tumor biology at University of Stuttgart, Institute of Cell Biology and Immunology "Targeting ErbB receptors in a three-dimensional cell culture model of K-Ras mutant colorectal cancer"
---------	---------	--

Education

07/2006 - 03/2010	Main study „technical biology“ at the University of Stuttgart Diploma degree, grade: 1.1
04/2009 - 01/2010	Diploma thesis at Fraunhofer IGB, Stuttgart „Establishment of a cell based reporter gene assay to detect microorganisms“
04/2008 - 07/2008	Student research project at Fraunhofer IGB, Stuttgart „Extension of a mammalian expression vector system with additional selection markers“
10/2004 - 07/2006	Basic study „technical biology“ at the University of Stuttgart Grade: 1.6
07/2004	Werratalsschule Heringen Abitur, grade: 1.4

Declaration

I hereby assure that I performed this work independently without further help or other materials than stated. Passages and ideas from other sources have been clearly indicated.

Eidesstattliche Erklärung

Hiermit erkläre ich, dass ich die vorliegende Arbeit selbständig verfasst und keine anderen, als die angegebenen, Quellen und Hilfsmittel benutzt habe. Wörtlich oder sinngemäß übernommenes Gedankengut habe ich als solches kenntlich gemacht.

Name/Name: Yvonne Möller

Signature/Unterschrift: _____

Date/Datum: _____